UNIVERSITÀ
DEGLI STUDI
DI PADOVA

Dipartimento di Pediatria

SCUOLA DI DOTTORATO DI RICERCA IN MEDICINA DELLO SVILUPPO E SCIENZE DELLA PROGRAMMAZIONE
INDIRIZZO EMATOONCOLOGIA E IMMUNOLOGIA
XXII CICLO

Skeletal muscle reconstruction through *in vivo* tissue engineering and characterization of satellite cell heterogeneity

Direttore della Scuola e coordinatore di indirizzo:
Ch.mo Prof. Giuseppe Basso

Supervisore: Ch.ma Prof.ssa Chiara Messina

Dottorando: Carlo Alberto Rossi

UNIVERSITÀ
DEGLI STUDI
DI PADOVA

Dipartimento di Pediatria

SCUOLA DI DOTTORATO DI RICERCA IN MEDICINA DELLO SVILUPPO E SCIENZE DELLA PROGRAMMAZIONE
INDIRIZZO EMATOONCOLOGIA E IMMUNOLOGIA
XXII CICLO

Ricostruzione del muscolo scheletrico attraverso ingegneria tissutale *in vivo* e caratterizzazione dell'eterogeneità delle cellule satelliti

Direttore della Scuola e coordinatore di indirizzo:
Ch.mo Prof. Giuseppe Basso

Supervisore: Ch.ma Prof.ssa Chiara Messina

Dottorando: Carlo Alberto Rossi

ABSTRACT

One of the most exciting challenges in tissue engineering is the complete reconstruction of an organ, with all its components. This depends on finding the most effective combination of stem cells and a biocompatible scaffold, able to support cell proliferation and differentiation, other than a physical structure. During my PhD study, I investigated about the possibility to reconstruct a muscle after severe ablation, and I designed and developed an experimental protocol for the delivery of either muscle progenitor cells (MPCs) or SCs *via* an injectable and *in situ* photo-crosslinkable hyaluronan-based hydrogel (HA-PI). Engrafting partially ablated *tibialis anterioris* (TA) muscles of C57BL/6J mice with freshly isolated GFP^+ SCs embedded in hydrogel, I found a huge recovery of muscle mass, when compared to TAs receiving hydrogel+MPCs or hydrogel alone. Moreover, freshly isolated SCs embedded in HA-PI were also able to promote functional recovery, as monitored by contractile force measurements. The latter was associated with generation of both neural and vascular networks and the reconstitution of a functional satellite cell niche. This work constitutes the first realization of an *in vivo* tissue engineering approach, that hopefully would overcome previous limitations in skeletal muscle tissue engineering.

Following these results, I also focused on finding a subpopulation of SCs, endowed with great capacity of proliferation and migration in the host muscle, and able to promote the best regeneration after damage. SCs were initially considered unipotent stem cells with the ability of generating a unique specialized phenotype. Subsequently, it was demonstrated in mice that opposite differentiation towards osteogenic and adipogenic pathways was also possible. Even though the pool of SCs has been accepted as the major, and possibly the only, source of myonuclei in postnatal muscle, it is likely that SCs are not all multipotent stem cells and evidences for diversities within the myogenic compartment have been described both *in vitro* and *in vivo*. In my study, by isolating single fibers from rat *flexor digitorum brevis* (FDB) muscle, I was able to identify and clonally characterize two main subpopulations of SCs: the low proliferative clones (LPC) present in major proportion (~75%) and the high proliferative clones (HPC), present instead in minor amount (~25%). LPC spontaneously generated myotubes whilst HPC differentiated into adipocytes even

though might skip the adipogenic program if co-cultured with LPC. LPC and HPC differed also for mitochondrial membrane potential ($\Delta\Psi_m$), ATP balance and Reactive Oxygen Species (ROS) generation underlying diversities in metabolism that preceded differentiation. Notably, SCs heterogeneity was retained *in vivo*. I could conclude that SCs may therefore comprise of two distinct, though not irreversibly committed, populations of cells distinguishable for prominent differences in basal biological features such as proliferation, metabolism and differentiation.

SOMMARIO

Una delle sfide più intriganti nell'ambito dell'ingegneria tissutale è la ricostruzione completa di un organo. Questa dipende dal trovare la combinazione più efficace tra cellule staminali e uno scaffold biocompatibile, in grado di fornire supporto per la proliferazione e la migrazione cellulare, oltre ad una struttura fisica. Durante i miei studi per il dottorato di ricerca mi sono concentrato specificamente nella ricostruzione del muscolo in seguito ad una consistente rimozione di tessuto, e ho disegnato e sviluppato un protocollo sperimentale sia per l'impianto di cellule precursori muscolari (MPCs) che di cellule satelliti (SCs) attraverso un idrogel a base di acido ialuronico iniettabile e fotopolimerizzabile *in situ*. Impiantando muscoli *tibialis anterioris* (TA), parzialmente ablati, di topi C57BL/6J con SCs isolate a fresco e GFP-positive, inserite in idrogel, ho potuto documentare un consistente recupero di massa muscolare, se paragonato a TAs che avevano ricevuto idrogel+MPCs o il solo idrogel. Inoltre le SCs isolate a fresco e inserite in idrogel hanno portato ad un recupero funzionale, monitorato attraverso misurazione della forza contrattile. Questo recupero è stato associato alla generazione sia di un network neurale che vascolare e alla ricostituzione di una nicchia di SCs funzionale. Questo lavoro costituisce la prima realizzazione di un approccio di ingegneria tissutale *in vivo*, con le potenzialità per superare le limitazioni incontrate in precedenza nell'ingegnerizzazione del tessuto muscolare.
In seguito a questi risultati mi sono focalizzato nella caratterizzazione di una sottopopolazione di SCs, con elevata capacità proliferativa e di migrazione nel muscolo ricevente, nonché in grado di promuovere una efficace rigenerazione in seguito a danno. Le SCs sono state inizialmente considerate cellule staminali unipotenti, in grado cioé di dare origine ad un unico fenotipo specializzato. In seguito è stato dimostrato in topo come anche il differenziamento in senso alternativo verso le pathways osteogenica e adipogenica fosse possibile. Anche se si conviene che la popolazione delle SCs sia la maggiore, e probabilmente l'unica fonte di mionuclei per il muscolo, è verosimile che le cellule satelliti non siano tutte cellule staminali multipotenti, in quanto evidenze di diversità all'interno del compartimento miogenico sono state descritte sia *in vitro* che *in vivo*. Nel mio studio, attraverso l'isolamento di singole fibre da muscolo *flexor digitorum brevis* (FDB) di ratto, ho potuto identificare e caratterizzare clonalmente due principali

sottopopolazioni di SCs: i cloni a bassa proliferazione (LPC), presenti in proporzione maggiore (~75%), e i cloni ad alta proliferazione (HPC), presenti invece in minor quantità (~25%). I LPC generano spontaneamente miotubi mentre i HPC differenziano in adipociti, con la proprietà di skippare il programma adipogenico se messi in co-coltura con LPC. LPC e HPC differiscono anche per il potenziale di membrana ($\Delta\Psi_m$), il bilancio dell'ATP e la generazione di specie reattive dell'ossigeno (ROS), mettendo in evidenza diversità nel metabolismo che precedono il differenziamento. Inoltre l'eterogeneità delle SCs è mantenuta anche *in vivo*. Posso così concludere che il pool delle SCs sembra comprendere due popolazioni cellulari distinte, anche se non irreversibilmente determinate, distinguibili in base a notevoli differenze riguardo a parametri biologici basali, come proliferazione, metabolismo e differenziamento.

INTRODUCTION

Tissue engineering

Tissue engineering represents a scientific approach that attempts to mimic neoorganogenesis (Mooney & Mikos, 1999). In contrast to the transplantation of donor organs, tissue engineering starts with cultured proliferating cells and aims to reconstitute a tissue-like structure in culture. The aim of the process is to regenerate and engineer new tissues for the replacement of lost, damaged or failing tissues and organs (Bonassar & Vacanti, 1998). Many investigations, that have been developed and attempted to regenerate human tissues, have recently entered into clinical practice in the case of tissues such as skin, bone and cartilage (Horch et al., 2000; Vangsness et al., 2004; Kopp et al., 2004). The creation of skeletal muscle tissue using a tissue angineering approach is promising for the treatment of a variety of muscle diseases, including skeletal myopathies such as muscular dystrophy or spinal muscular atrophy (Law et al., 1993; Guettier-Sigrist et al., 1998); in addition, traumatic injury, aggressive tumour ablation and prolongued denervation are common clinical situations that often result in significant loss of muscle tissue and require subsequent surgical reconstruction. Engineering skeletal muscle tissue remains still a challenge, and many studies have indicated that it will be of great importance in medicine in the near future (Bach et al., 2003).

Engineering skeletal muscle tissue

The requirements for an engineered muscle are: a parallel alignment of myofibrils with myosin/actin filaments, intracellular calcium storage and acetylcholine receptors. Moreover, the neotissue must be biocompatible, must integrate and regenerate lost muscle tissue, and needs to be vascularized and innervated (Vandenburgh, 2002). Khodabukus et al. (2007) pointed out that engineered muscle needed to satisfy some criteria: the technique should be fast, easy and standardized, it should be preferable the use of transformed skeletal muscle cells in order to decrease the variability of primary cell isolation, and physiology and function need to be readily testable.

There are two general approaches to engineer artificial skeletal muscle tissue. One way is to generate autologous myogenic cells from biopsy, expand and differentiate them in a 3D defined environment *in vitro* in an artificial bioreactor, and reimplant the neotissue (*in vitro* tissue engineering, see Powell et al., 1999). The second approach involves the generation of myogenic cells, their expansion *in vitro* and the reimplantation using a transport matrix, which allows differentiation into myotubes *in vivo*. Implanted myoblasts might serve as vehicles for the delivery of recombinant proteins (*in vivo* tissue engineering, see Barr & Leiden, 1991).

Stem cells in muscle tissue engineering

Stem cells play a crucial role in the development and regeneration of human tissues. They are defined as cells that continuously renew themselves, while maintaining the ability to differentiate into various cell types (Thomson et al., 1998). Stem cells are found at all developmental stages, from embryonic stem cells that differentiate into all cell types found in the body to adult stem cells that have a more limited differentiation capacity, albeit being responsible for tissue regeneration. Controlling stem cell self-renewal, differentiation and maintaining stable cell lineage commitment is crucial to the success of utilizing stem cells clinically.

Embryonic stem (ES) cells derive from the inner cell mass of embryonic blastocyst. They have the ability to self-renew and they are pluripotent, meaning that they have the ability to become any cell type in the primary germ layers (ectoderm, mesoderm and endoderm). The controversies sorrounding the use of ES cells for research are complicated by the ethical issue of using human embryos. Moreover, caution must be taken in therapeutic applications when using ES cells because of the evidence that they can cause the formation of teratomas, and share genetic programs with cancer stem cells (Wong et al., 2008).

Adult stem cells are multipotent stem cells, i.e. with the ability of differentiating into bone, cartilage, muscle, fat and fibroblasts. This multidifferentiation ability allows adult stem cells to maintain tissue homeostasis, and to repair damaged tissue when the repair is needed. An example of adult stem cells are MSCs, that can be isolated from various adult tissues, and efforts to utilize the MSC population for treatment of degenerative musculoskeletal diseases are underway.

The bone marrow is the most common place to isolate MSCs (Pittenger et al., 1999). The most studied cell type for muscle tissue engineering is constituted by skeletal muscle satellite cells (SCs).

Skeletal muscle satellite cells

Skeletal muscle satellite cells (SCs) were first described in frog muscle by Mauro (1961). They were characterized for their morphology and position relative to mature myofibers, and were later identified in adult avian and mammalian muscle (Schultz, 1976; Armand et al., 1983). During muscle development, SCs adhere to the surface of myotubes prior to the formation of the basal lamina, such that the basal lamina sorrounding the myofiber is a continuous (Armand et al., 1983; Bischoff, 1990). The role of SCs is to mediate the postnatal growth of muscle and they constitute the primary means by which the mass of adult muscle is formed (Schultz, 1989). As happens in other stem cell populations, the number of SCs decreases with increasing age in rodents (Gibson & Schultz, 1983; Grounds, 1998). At birth SCs constitute about 32% of muscle nuclei, while in the adult there is a drop to less than 5% (2 months for mice, see Bischoff, 1994). This decline in SC nuclei as the postnatal muscle develops is a direct reflection of SC fusion into new or preexisting myofibers.

SCs in adult skeletal muscle are normally mitotically quiescent, but are activated (i.e. they begin multiple rounds of proliferation) in response to stress induced by weight-bearing or trauma (Appell et al., 1988; Rosenblatt et al., 1994). The descendants of activated SCs, called myogenic precursor cells (MPCs), undergo multiple rounds of division prior to fusing with existing or new myofibers (Appell et al., 1988; Grounds & Yablonka-Reuveni, 1993). SCs form a population of stem cells that are distinct from their daughter MPCs, concerning biological and biochemical criteria (Grounds & Yablonka-Reuveni, 1993; Bischoff, 1994). The number of SCs in adult muscle, in normal physiological conditions, remains relatively constant, over multiple cycles of degeneration/regeneration, .demonstrating a capacity for self-renewal (Gibson & Schultz, 1983). In pathological conditions, such as Duchenne Muscular Dystrophy, the number and the doubling potential of SCs become severely reduced, presumably due to high levels of ongoing regeneration (Bulfield et al., 1984; Schultz & Jaryszak, 1985; Webster & Blau, 1990; Emery, 1998).

SCs have an essential role in muscle regeneration, muscle hypertrophy and postnatal muscle growth (Darr & Schultz, 1987; Grounds & Yablonka-Reuveni, 1993; Rosenblatt et al., 1994; Schultz, 1996; Grounds, 1998).

Myogenic regulatory factors in satellite cell activation and differentiation

There are many factors involved in SC commitment and differentiation. The primary myogenic regulatory factors (MRFs) are Myf5 and MyoD, and are required for the determination of myoblasts, whereas the secondary MRFs, myogenin and MRF4, are involved in the regulation of terminal differentiation (Megeney & Rudnicki, 1995).

The MRF expression program during satellite cell activation, proliferation and differentiation recapitulates the embryonic development of skeletal muscle. While quiescent SCs do not express detectable levels of MRFs, MyoD is rapidly upregulated 12 hours after damage. Myogenin is expressed last during the time associated with fusion and differentiation (Smith et al., 1994; Yablonka-Reuveni & Rivera, 1994). SCs, after activation, express either Myf5 or MyoD, followed soon by coexpression of Myf5 and MyoD. Following proliferation, myogenin and MRF4 are expressed in cells beginning their differentiation program. The absence of MRF mRNA in satellite cells prior to activation is consistent with the hypothesis that SCs represent a stem cell type with an identity distinct from that of myoblasts. The inductive signals that activate Myf5 and MyoD transcription are analogous to those that occur during the specification of the myogenic lineage during embryonic development.

Developmental origin of satellite cells

SCs constitute a myogenic cell lineage that is distinct from the embryonic lineages, and they first appear in the limbs of mouse embryos at about 15.7 days postcoitum (Cossu et al., 1985; Feldman & Stockdale, 1991; Hartley et al., 1992). Adult SCs may also be further divided into subclasses on the basis on the fiber type. It is clear that SCs form fibers genetically similar to the muscle from which they originate (Matsuda et al., 1983; Feldman & Stockdale, 1991; Hoh & Hughes, 1991; Rosenblatt et al., 1996).

Quiescent SCs adjacent to mature fibers express c-Met and M-cadherin proteins but do not express markers of committed myoblasts, such as Myf5, MyoD or desmin (Irintchev et al., 1994; Cornelison & Wold, 1997). This observation is consistent with the possibility that SCs represent a pluripotential stem cell population. Committed myoblasts would therefore be generated as a function of their microenvironment and available growth factors. Such a model is also consistent with the observed ability of adult muscle-derived stem cells to repopulate the haematopoietic compartment as well as to give rise to skeletal myocytes following intravenus injection into irradiated mice (Ferrari et al., 1998; Bittner et al., 1999; Gussoni et al., 1999).

The pluripotentiality of muscle-derived stem cells has important implications for the role of the MRFs in the ontogeny of SCs. Muscle SCs are commonly considered as a distinct, yet committed population of myogenic cells. Accordingly, the immediate progenitors to SCs would down-regulate MRF expression prior to entering quiescence. The pluripotentiality of muscle-derived stem cells, however, raises the possibility of a MRF-independent mechanism for SC development.

Satellite cell self-renewal

The mechanism by which SCs undergo self-renewal in adult skeletal muscle is poorly understood. If SCs are identical to muscle-derived stem cells isolated by Gussoni and colleagues (1999), self-renewal of the stem cell compartment may occur prior to and completely independent of MRF expression.

Expression of Myf5 alone may facilitate stem cell self-renewal within the context of skeletal muscle. RT-PCR analyses revealed that activated SCs first express either Myf5 alone or MyoD alone, prior to coexpressing Myf5 ad MyoD and subsequently progressing through the myogenic program (Cornelison & Wold, 1997). Together these data suggest that expression of Myf5 alone may define a developmental stage during which SCs undergo self-renewal.

Another possibility which requires consideration is that “dedifferentiation” of previously committed MPCs could give rise to quiescent SCs. The existence of mechanisms for homing of SCs to discrete locations along muscle fibers, possibly involving cell adhesion molecules, such as M-cadherin (Irintchev et al., 1994; Zeschnigk et al., 1995; Kaufmann et al., 1999), supports the notion that the

immediate progenitors of SCs express tissue-specific molecules normally expressed in committed MPCs. Importantly, none of the above models are mutually exclusive and all could coexist to maintain the steady-state numbers of SCs.

Muscle regeneration

Satellite cells are activated in response to diverse stimuli, for example injury, denervation, exercise, or stretching (Schultz & Jaritzak, 1985; Darr & Schultz, 1987; Appell et al., 1988; Grounds & Yablonka-Reuveni, 1993). However, the molecular mechanisms that regulate the activation of SCs leading to their entry into the cell cycle remain to be elucidated. The major mechanisms involved, according to various studies, are the inflammatory response and the release of critical growth factors.

A role for leukocytes in SCs activation has been proposed on the basis of the observation that quiescent SCs express vascular adhesion molecule-1 (VCAM1, a cell surface integrin molecule), whereas infiltrating leukocytes express the specific coreceptor VLA-4 (integrin $\alpha 4\beta 1$; see Rosen et al., 1992; Jesse et al., 1998). The interaction between VCAM1 and VLA-4 may initiate genetic responses within SCs and immune cells to promote regeneration (Jesse et al., 1998).

Lymphocytes and macrophages (activated monocytes) migrate to sites of tissue damage within a few hours after trauma to muscle. Macrophages, however, are the dominant immune cells present within regenerating muscle at 48 hours post-injury (Orimo et al., 1991; Tidball, 1995). During the muscle regeneration process, macrophages phagocytize necrotic cells debris as well as they secrete a soluble growth factor, which exerts a specific mitogenic effect on myoblasts (Cantini & Carraro, 1995). Moreover, myogenesis is markedly impaired in the absence of macrophage infiltration (Lescaudron et al., 1999).

The cytokines IL-6 (interleukin-6) and LIF (leukemia inhibitory factor) stimulate the proliferation of MPCs in culture (Austin et al., 1992). LIF expression is markedly increased 3 hours after muscle injury (Kurek et al., 1996), suggesting that damaged muscle secretes LIF prior to infiltration of immune cells.

Biomaterials for musculoskeletal regeneration

The ability to direct adult stem cell differentiation using biomaterial systems offers a minimally invasive therapeutic option for diseases of the musculoskeletal system (e.g. bone, cartilage, joint, muscle) and tissue repair. *In vivo* stem cells reside and differentiate within a three-dimensional environment. A variety of biomaterials (alginate, collagen, hyaluronan, hydroxyapatite and PEG) are currently being explored as three-dimensional scaffolds to study the effects of stem cell proliferation, migration, self-renewal and differentiation (Radice et al., 2000; Nuttelman et al., 2004). Each material offers unique biological, chemical and physical signals that can be used to either maintain stem cell pluripotency, or to direct stem cell differentiation into more specialized lineages that ultimately guide and support new tissue formation. It is well established that many of these biomaterials are capable of encapsulating multiple cell types (Elisseeff, 2008). Notably, adult stem cells can be encapsulated into biomaterials to be implanted directly at the sight of a wound or diseased tissue. They are capable of sending and receiving signals that can eventually replace the injured tissue.

Methods for differentiating adult stem cells to specific lineages *in vitro* are widely accepted as being influenced by culture conditions with the presence of growth factors in the media (Liu et al., 2009), while controlling their differentiation *in vivo* remains a challenge. From the mechanistic perspective, understanding the relationship between adult stem cells and their environment is essential to gain a better idea of their *in vivo* cell behaviour. From the therapeutic perspective, building scaffolds that mimic the cells' natural environment has a great potential for developing better therapeutic modalities in tissue repair and regenerative medicine. *In vivo* the fate of many cells is regulated by the cues that reside in the local microenvironment that include the extracellular matrix (ECM) and signals from neighbouring cells (globally defined as niche).

The niche of muscle satellite cells

SCs are localized along the surface of muscle fibers under the basal lamina. As such, one important component of the SC niche is the host muscle fiber. Mechanical, electrical and chemical signals from the host fiber have all been shown to be involved in the regulation of SC function (Charge & Rudnicki, 2004). Equally important is the basal lamina as a component of the extracellular matrix

(ECM), and consists mainly of laminin, collagen, and proteoglycans. Anchoring to the basal lamina is vital for the maintenance of stem cell identity in several other systems (Fuchs et al., 2004). A third component of the SC niche is the microvasculature that nourishes, and interstitial cells that interact with, SCs. In human and mice, 68% and 82% of SCs, respectively, are found to be localized within 5 μm from neighbouring capillaries or vascular endothelial cells, under both quiescence and proliferation states (Christov et al., 2007). Extrinsic signals from the circulatory system and interstitial cells, such as macrophages, fibroblasts, and muscle-resident stem cells, are relayed to SCs through the basal lamina. These anatomical features of SC niche therefore suggest that a combination of signals from the host muscle fiber, curculation system, and ECM govern quiescence, activation and proliferation of SCs.

Regulation of satellite cell function by signals within the niche

Accumulating evidence indicates that the function of stem cells is regulated by signals from the niche. For instance, although the number of SCs is decreased in aged muscle, their intrinsic myogenic potential and self-renewal capacity remains unaltered (Shefer et al., 2006). Old muscle grafted to a young host resulted in robust activation and regeneration of grafted cells, whereas young SCs perform poorly in an old host (Carlson & Faulkner, 1989). Similar results were observed in parabiosis systems where young and aged systematic environment (circulation) were joined (Conboy et al., 2005). A key question is to address the identity of molecular signals within the SC niche that play a key role in regulating SC function.

The intense focus of several recent studies was to identify signals that regulate the quiescence of SCs. Caveolin-1 and sphingomyelin are specifically expressed in the caveolae (membrane invaginations/lipid rafts) of quiescent SCs (Nagata et al., 2006). Caveolin-1 has been shown to regulate the internalization of caveolae and may thus trigger sphingomyelin signaling. Notably, caveolin-1-mediated internalization of caveolae occurs concomitantly with cell detachment from the ECM, and regulates integrin-mediated downstream activation of the Erk MAP kinase, PI3K, and Rac signaling pathways (Del Pozo et al., 2005). It is plausible to hypothesize that laminin-integrin adhesion regulates satellite cell quiescence through inhibition of caveolin-1-dependent endocytosis of sphingomyelin

signaling. In addition, calcitonin receptors (CTR) have been shown to be exclusively expressed in the quiescent satellite cells, suggesting that calcitonin signalling is also involved in maintaining quiescence (Fukada et al., 2007). However, it is currently unknown how these signaling molecules trigger intracellular machinery that leads to quiescence.

It has been established that activation of quiescent satellite cells depends on HGF that is released from damaged myofibers. Recent studies indicate that nitric oxide (NO) signaling may act upstream of HGF to modulate the activation of satellite cells (Tatsumi et al., 2006; Wozniak and Anderson, 2007). In addition, although it is present in quiescent satellite cells, sphingomyelin signaling has been implicated in the cell-cycle entry of activated satellite cells (Nagata et al., 2006). In contrast, myostatin, a negative regulator of muscle growth, has been shown to inhibit the activation of satellite cells through an unknown mechanism (McCroskery et al., 2003).

Activated satellite cells face cell fate choices between self-renewal and differentiation. Wnt and Notch signaling are both involved in the cell fate regulation of satellite cells. Wnt signaling seems to act as a double-edged sword: on one hand, it has been shown to induce myogenic specification of muscle stem cells during regeneration; on the other hand, it has been shown to repress the myogenic lineage and force satellite cells to an alternative lineage, leading to fibrosis in aged muscle (Brack et al., 2007; Polesskaya et al., 2003). Intriguingly, differentiation of myoblasts *in vitro* and *in vivo* is correlated with an upregulation of canonical Wnt signaling. Furthermore, ectopic Wnt induces premature muscle differentiation whereas inhibition of Wnt signaling interferes with muscle differentiation (Brack et al., 2008). Perhaps these results are not so surprising given the variety of Wnts and the diversity of Wnt signaling pathways (Gordon & Nusse, 2006). Therefore, the source of Wnt proteins in the muscle and their specific function in satellite cells are important avenues of future investigations.

Notch signaling has been emerging as a major regulator of satellite cell proliferation and self-renewal. Knockout of Delta-1, a Notch ligand, or RBP/J, a nuclear mediator of Notch signaling, results in similar deficits in embryonic myogenic cells and ablation of satellite cells (Schuster-Gossler et al., 2007; Vasyutina et al., 2007). Likewise, pharmacological blockage of Notch signaling inhibits satellite cell proliferation and self-renewal, whereas enhancement of

Notch signaling promotes muscle regeneration in aged muscle (Conboy et al., 2003; Kuang et al., 2007). In asymmetrically divided myoblasts, the differentiating daughter expresses higher levels of Delta-1 that presumably initiates Notch signaling to promote self-renewal of the neighboring sister cell (Kuang et al., 2007). It remains unclear how the differential expression of Delta-1 and Notch in newly divided myoblasts and different subpopulations of quiescent satellite cells is established, and what are the Notch target genes that are involved in satellite cell self-renewal.

Proliferation and differentiation of satellite cells are also regulated by different growth factors and cytokines, including bFGF, IGF, EGF, VEGF, PDGF, TWEAK, IL-6, and LIF. Surprisingly, p38 MAP kinase, whose role in promoting differentiation has been well documented, also functions downstream of bFGF to stimulate activated satellite cell proliferation (Jones et al., 2005; Palacios & Puri, 2006). This finding suggests that p38 regulates distinct targets depending on its temporal kinetics, resulting in separate functions during myogenesis. It will also be interesting to determine whether p38 signaling regulates Myf5 expression following asymmetric cell division, as it has been reported to be necessary for Xmyf5 expression in Xenopus (Keren et al., 2005). An intriguing hypothesis would be the differential expression of Notch and p38 in the self-renewal ($Pax7^{+}Myf5^{-}$) and committed ($Pax7^{+}Myf5^{+}$) daughter cells, respectively.

It is worthwhile to emphasize that the ECM, particularly the heparan sulfate proteoglycans, play important roles in the regulation of many cell surface signaling pathways (Jenniskens et al., 2006). For instance, Syndecans-3/4 each regulate different aspects of satellite cell activation and differentiation (Cornelison et al., 2004). Moreover, variations in the sulfation patterns of the heparan sulfate side chains can influence the biological activity and accessibility of signaling molecules such as growth factors, chemokines, morphogens, and Wnts (Langsdorf et al., 2007; Olwin & Rapraeger, 1992). In fact, inhibition of protein sulfation on muscle fibers in culture retards satellite cell proliferation (Cornelison et al., 2001). It will be a challenging task to define the specific ECM components enriched at the satellite cell niche and how they regulate the various extracellular signals involved in the self-renewal, proliferation, and differentiation of satellite cells.

Material based ECM that mimics natural ECM

Biomaterials can be used as a tool to recreate the ECM niche in a controlled and functional manner. Understanding the interactions of the ECM on cell fate will provide the framework for designing and engineering synthetic ECMs to control cell behavior that can be used to direct stem cell differentiation. *In vivo*, SCs receive and integrate signals at various stages that induce differentiation into more specialized cells. Increasing evidence suggests that the ECM provides the signals to make up the highly defined specialized cell microenvironment that is essential for correct tissue development and function (Elisseeff, 2008). Although ECM assembly is poorly understood, efforts are currently underway to engineer synthetic ECMs to replace damaged tissues.

Scaffolds that possess various natural ECM components to mimic the natural ECM have been engineered and are showing promising results. Chondroitin sulfate (CS) is an important structural component in the cartilage ECM (Daley et al., 2008), which provides mechanical support for cells and regulates intracellular communication. CS is also one of the major molecules present during pre-cartilage condensation of MSCs, suggesting that it plays a significant role during chondrogenesis (Nehrer et al., 1997). With this in mind, a three-dimensional composite hydrogel, composed of chondroitin sulfate and poly(ethylene glycol) (PEG), has been engineered and was shown to closely mimic the native cartilage ECM (Hwang et al., 2008). These hydrogels provide an instructional microenvironment that enhances the clustering of mesenchymal cells, improves chondrogenic differentiation of MSCs, and increases cartilage extracellular matrix (ECM) deposition.

Collagen mimetic peptides (CMPs) are synthetic peptides that form triple helices that mimic the native protein structure of collagen and function by binding to natural ECM (Lee et al., 2006). CMPs cross-linked to PEG have been shown to provide a suitable microenvironment for sufficient chondrocyte maintenance (Lee et al., 2006), and enhanced chondrogenesis (Lee et al., 2008). Moreover, the CMP microenvironment inhibits hypertrophy, a phenotype that increases ossification and apoptosis of the tissue (Mueller & Tuan, 2008).

Biomaterials to interface with natural tissue

Improving the regenerative capabilities of injured/damaged tissue is an important

aspect of tissue engineering. In this regard, biomaterials are being developed to interface with the natural tissue, enhancing their capability of responding to diverse signals from cells in the vicinity of an implanted biomaterial scaffold (Lutolf & Hubbell, 2005). The ECM is a dynamic structure that is constantly receiving and sending signals to undergo remodeling, particularly during development, differentiation, and wound repair (Elisseeff, 2008). ECM degradation is controlled at multiple levels, and its dysregulation results in ECM damage that is common in many diseases. Matrix metalloproteinases (MMPs) are proteolytic enzymes that play a major role in the degradation and remodeling of the ECM. Specifically, MMP-13 is upregulated within 7–12 days of chondrogenesis (Sekiya et al., 2002), which corresponds to a decrease in fibronectin that includes the peptide RGD, the cell binding site. The presence of RGD plays an important role in initiating chondrogenic differentiation, as well as maintaining the overall fitness of cells encapsulated in hydrogels (Hwang et al., 2006). The perfectly orchestrated signaling for natural ECM remodeling is highly complex, adding to the difficulty of fully understanding the signals required for proper remodeling. Building materials that focus on mimicking individual components of EMC function will guide the field of tissue engineering to building more sophisticated materials that will improve their performance *in vivo*.

Heterogeneity in SC niche

When choosing the best cell type for regeneration purposes, it is also interesting to evaluate the presence of heterogeneity, and to eventually try the selection of a highly functional subpopulation. Emerging studies have suggested that significant heterogeneity exists within the satellite cell niche (Beauchamp et al., 2000; Collins et al., 2005; Kuang et al., 2007; Schultz, 1996; Sherwood et al., 2004). This is a fundamental question for their use in cell therapy and tissue engineering. A long-standing question has been whether such heterogeneity has any biological significance, for example hierarchical lineage relationships, or different developmental origins, of subpopulations of satellite cells. Furthermore, although satellite cells are known to be heterogeneous in their myogenic potential (Collins et al., 2005; Sherwood et al., 2004), it is unclear whether they are also heterogeneous in their intrinsic self-renewing capacity.

Most satellite cells are capable of self-renewal and the decision is likely to be

controlled by signals from the myofibre, from differentiating satellite-cell progeny or from the changing regenerating environment (Day et al., 2007; Zammit et al., 2004). Over time, however, the satellite cell population might evolve into a continuum of cells with more (or fewer) stem-cell characteristics, perhaps because some cells have been activated less frequently, or have undergone fewer divisions (as has recently been proposed for skin stem cells, see Clayton et al., 2007). Alternatively, the satellite-cell population might be composed of both lineage-based satellite 'stem' cells and myogenic precursors in the same anatomical location. However the satellite cell pool is organised, the expression of MyoD might remain a common step in the activation of all types of satellite cells. Not all satellite cells express markers such as Myf5-driven expression of β-galactosidase (Myf5nlacZ/+ mouse), and levels of Pax3-driven expression of eGFP (Pax3eGFP/+ mouse) vary between populations, although such phenotypic heterogeneity might simply reflect a dynamic state of protein expression (Beauchamp et al., 2000; Day et al., 2007; Kuang et al., 2007; Relaix et al., 2006). The constant emergence of new satellite-cell markers, such as lysenin (Nagata et al., 2006), caveolin 1 (Volonte et al., 2005) and the calcitonin receptor (Fukada et al., 2007), might help further to identify prospective sub-populations. On the functional level, a proportion of satellite-cell-derived myoblasts express myogenin within 8 hours of muscle injury, which shows that they commit to differentiation with little or no proliferation; by contrast, the remaining cells do not divide within the first 24 hours (Rantanen et al., 1995). *In vitro*, satellite cells exhibit heterogeneity in both their proliferation rate and their clonogenic capacity (Molnar et al., 1996; Schultz & Lipton, 1982).

A recent study by Rudnicki and colleagues has sought to address the question of satellite-cell heterogeneity directly (Kuang et al., 2007). The authors have shown that ~90% of satellite cells on myofibres of adult Myf5cre/+ mice had had a 'myogenic experience' and expressed Myf5 at some point (as shown by the presence of YFP from the recombined targeted *ROSA* locus). The remaining ~10% of satellite cells were YFP-negative, and were able to produce further YFP-negative and YFP-positive cells both *in vitro* and *in vivo*. When grafted into Pax7-null mice, these YFP cells gave rise to approximately three times more Pax7-positive satellite cells than the YFP-positive cells, and a quarter of these remained YFP-negative. It was proposed by the authors that these YFP-negative cells

correspond to a dedicated subset of satellite cells that have more stem-cell-like characteristics (satellite 'stem' cells), and that the YFP-positive cells are their transitamplifying progeny that can undergo limited symmetric proliferation to generate myonuclei (Kuang et al., 2007). Satellite 'stem' cells are defined by the absence of recombination at the ROSA-YFP locus, which is attributed to a lack of expression of Myf5-driven Cre; this phenotype could, however, result from too little (or too brief) an expression of Myf5-driven Cre for efficient recombination, or from an inability of the recombined ROSA locus to drive YFP expression in all quiescent satellite cells. Furthermore, the YFP-positive population might well contain – and, indeed, generate – cells in which Myf5 is no longer expressed (YFP-positive Myf5-Cre negative cells), which would have a phenotype that is equivalent to that of the YFP-negative population. Importantly, YFP-positive cells do give rise to satellite cells when grafted, albeit fewer than YFP-negative cells. A positive marker of YFP-negative cells (similar to one that has recently been described for crypt stem cells of the small intestine, see Barker et al., 2007) and the use of other targeted alleles (especially MyoD) to drive the expression of Cre would help to advance these important observations. The presence of satellite 'stem' cells has also been examined by pulsing regenerating muscle with halogenated thymidine analogues. A proportion of satellite-cell divisions *in vivo* and *in vitro* have been observed to be asymmetric, with the labelled DNA being transferred to the daughter cell that has the self-renewal phenotype (Conboy et al., 2007; Shinin et al., 2006). It has been proposed that this label retention identified satellite 'stem' cells, because the cells contained non-equivalent genomic DNA strands of which the older 'template' strand was protected from DNA replication errors according to Cairn's 'immortal DNA' hypothesis for stem cells (Cairns, 1975). However, label retention is not a universal characteristic of stem cells in all tissues (Waghmare et al., 2008), and it has recently been shown that even crypt stem cells of the small intestine may not retain label (Barker et al., 2007). It is crucial to determine how these label-retaining cells respond to further bouts of muscle injury: if they are satellite 'stem' cells, they should remain at a relatively constant level as they would retain the label by dividing asymmetrically to generate BrdU-negative myonuclei. A caveat is that BrdU is not simply a passive lineage marker, but can repress MyoD expression (Ogino et al., 2002) and inhibit myogenic differentiation (Bischoff and Holtzer, 1970). Rather than the prevention

of replication errors, the main purpose of non-random segregation of chromosomes might instead be to enable differential gene expression and, therefore, different cell fates of the two progenies – the ‘silent sister’ hypothesis (Lansdorp, 2007).

CHAPTER I

SKELETAL MUSCLE RECONSTRUCTION THROUGH *IN VIVO* TISSUE ENGINEERING

Background

Reconstruction of skeletal muscle after injury or in pathological conditions remains a complex and unsolved task, despite the present knowledge of the biological processes underlying muscle regeneration (Rosenblatt et al., 1995). *In vitro* approaches based on fabrication of functional muscle before *in vivo* transplantation showed several limitations (Yan et al., 2007), due to the intrinsic complexity of large organs reconstruction. Besides, it is well established that in mammals skeletal muscle can repair its damaged areas only in the presence of a supporting scaffold (Bach et al., 2004).

In this perspective, the aim of my work has been to combine myogenic cells and biocompatible scaffolds for developing an efficient *in vivo* strategy to restore mass loss in a model of partially ablated muscle in mouse. In particular my focus has been the setting up of a protocol that could be easily translated on bigger animal models and moreover be introduced as a clinical procedure for the reconstruction of muscle lost following injuries or for the substitution of muscle mass removed in surgical procedures.

The novelty of my work relies both in the way in which myogenic cells were derived and in the innovative biomaterial used. For the first time I used freshly isolated SCs and isolated single fibers in a tissue engineering protocol, at the light of some papers showing their huge regenerative potential when delivered into an injured or a dystrophic muscle through intramuscular injection. Moreover, the biomaterial used is innovative: it is an hydrogel, based on hyaluronic acid, one of the major components of the extracellular matrix, and it allows to resuspend cells in a solution, that is then photopolymerizable *in situ* in the place of injury (inside the muscle); in this way cells result embedded in the polymeric structure and can gradually begin to proliferate and migrate in the host muscle. Combining together these two component, my aim was to repair muscular tissue through an innovative approach, that has been defined "*in vivo* tissue engineering", in which the process of repair and reconstruction is performed totally inside the tissue, without any *in vitro* expansion and differentiation, or seeding on a biocompatible scaffold: this process minimizes the passages between cell isolation and cell implant. So this results to be the best way to mimic the canonical *in vivo* regenerative process.

Materials and Methods

Animals

Two and four-month old C57BL/6J wild-type mice and C57BL/6Tg (actin, beta–enhanced green fluorescent protein (EGFP)1Osb/J transgenic mice (Jackson Laboratories) were used. Animals were housed and operated onto at the Animal Colony of the ‘‘Centro Interdipartimentale Vallisneri,’’ University of Padova, under the conditions specified by the relevant Italian bylaws.

Hydrogel preparation and characterization

The hyaluronic acid–photoinitiator complex (HA-PI) is a hyaluronan ester obtained by chemical reaction between hyaluronic acid and 1-[4-(2-Hydroxyethoxy)-phenyl]-2-hydroxy-2-methyl-1-propane-1-one (HHMP, Irgacure 2959), which behaves as photoinitiator during the hydrogel cross-linking. HA-PI was synthesized by Fidia Advanced Biopolymers S.p.a (Abano Terme, Italy). Solution of HA-PI in physiological solution at the specified concentrations were prepared and sterilized in autoclave. A Bluewave50 lamp (Dymax) provided with a water-probe (0.5 cm diameter) emitting a 366 nm conical beam was used for hydrogel cross-linking.

Rheological analysis

A rheometer (Rheostress RS150 Haake) was used to evaluate viscoelastic and rheological properties. It was equipped with a temperature control (20.0±0.5° C) and a plate-cone sensor (1°) of 60 mm diameter. During measurements the distance between cone and plate was 0.051 mm. The solution rheological behaviour (before irradiation) was evaluated by analyzing the shear stress as function of rising deformation rates (0-5 s-1). From measurements on cross-linked hydrogels, elastic (G’) and viscous (G”) moduli were calculated as function of rising oscillation frequencies (0.1-10 Hz) at constant shear stress (τ = 1 Pa). Samples of different concentrations (10, 20 and 30 mg/ml) and exposition times (from 3 s up to 5 min) were analyzed.

Maximum flow rate

The data of viscosity (μ) of HA-PI solutions were used to evaluated the maximum injection flow rate (Q_{max}) as follow:

$$Q_{max} = \frac{\pi R^2 \tau_{max}}{2 \mu} \left(1 - \frac{2}{R}\right)^{-1}, \quad (1)$$

where R is the needle radius that is correlated with the needle gauge, τ_{max} is the higher shear stress allowed (1 Pa, see Hathcock et al., 2000).

Mesh size evaluation

Following the Flory-Rehner calculations, experimental data of hydrogel swelling can be used to calculate some important structural parameters of the hydrogel such as the mesh size, ξ (nm), defined as the length of the polymer chain between two following cross-links.

Swelling experimental data were obtained using disks of hydrogel of 22mm diameter that were gently dried at 37°C, weighed and than re-wetted with 10ml of physiological solution. The disks were weighed 3 days after dipping, when the equilibrium conditions were reached.

The hydrogel mesh size was calculated with the following equation (Cleland & Wang, 1970):

$$æ = Q_v^{1/3} \sqrt{r_0^2}, \quad (2)$$

where Q_V is the volumetric swelling ratio obtained from experimental data and $\sqrt{r_0^2}$ is the root-mean square distance between cross-links (nm). For HA, the following value was reported (Cleland & Wang, 1970):

$$æ = 0.1707 \sqrt{M_C} Q_v^{1/3}. \quad (3)$$

The average molecular weight M_C was calculated using a simplification of Flory-Rehner equation (Huang et al., 1997):

$$Q_v^{5/3} = \frac{õ M_c}{V_1} (0.5 - ÷), \quad (4)$$

where υ is the specific volume of dry polymer (0.893 cm^3/g), V_1 is the specific volume of solvent (1 cm^3/g) and χ is the Flory interaction parameter between polymer and solvent (0.473).

Hydrogel morphology

The morphology of cross-linked structure was analyzed by SEM (JSM-6490 Jeol). Two ml of solutions ranging from 10 up to 75 mg/ml were cross-linked in multi-well Iwaki of 22 mm diameter at 2 cm from the Triwood lamp for 5 min (4 mW/cm2). The samples were freeze-dried, gold sputtered and analyzed (Lyovac GT2 Leybold-Heraeus).

Single fiber isolation technique

Immediately after harvesting, muscles were digested for 1 hour at 37°C in 0,2% (w/v) type I-collagenase (Sigma-Aldrich), reconstituted in DMEM (high-glucose, with L-glutamine, supplemented with 1% penicillin-streptomycin, GIBCO-Invitrogen). Following digestion, muscles were transferred in DMEM medium (low-glucose, GIBCO-Invitrogen) on a horse serum (HS; GIBCO-Invitrogen) coated 10-cm dish (Falcon) and gently triturated with a wide-bore pipette in order to release single myofibers. These were then transferred one-by-one in another HS-coated 10-cm dish, under a phase-contrast inverted microscope. This passage was repeated three times, in order to avoid contamination of interstitial, endothelial and haematopoietic cells (Rosenblatt et al., 1995).

Myogenic precursor isolation

Single muscle fibers were isolated from *flexor digitorum brevis* (FDB), *extensor digitorum longus* (EDL) and *soleus* muscles from two-month old male C57BL/6J-GFP^{+} mice, as previously described (Rosenblatt et al., 1995). Groups of twenty myofibers were then placed in 2 ml Eppendorf tubes in 200 µl DMEM (low-glucose, GIBCO-Invitrogen). Isolated fibers were left to sediment on the bottom for 15 minutes, DMEM was then removed and replaced with 15 µl of HA-PI before injection. Freshly isolated SCs were stripped off the fibers by 20 passages through a 18G needle (Rossi et al., 2010). SCs were centrifuged at 300xg with a micro-centrifuge and resuspended in 15 µl of HA-PI. For myogenic precursors preparations, 20 single fibers were seeded onto a Matrigel®-coated 35 mm-dish according to single fiber culture technique (Boldrin et al., 2007). SCs left the parental fybers in around 36 hours and started to proliferate, and were then trypsinized before they got confluent, in order to expand them. At passage 1, 150000 cells were pelleted in 2 ml Eppendorf tubes and resuspended in 15 µl of

HA-PI. Separate preparations of fibers and cells were then mixed with liquid hydrogel and kept in ice until implant.

Surgical procedure

Four-month old male C57BL/6J mice were anesthetized using Forane® and ~4 mg wedge of tissue was removed by longitudinal cutting from the core of TA muscles. Removed tissue was weighed using a microbalance (Sartorius), in order to assess the repeatability of the ablation. Suspensions of cultured SCs, single fibers and freshly isolated SCs in HA-PI were placed in the created pocket with a micro pipette and then photo-polymerized for 55 seconds with the monochromator light. After polymerization, muscle was sutured with 7/0 Vycril, enclosing the hydrogel within its core; skin was then closed using 6/0 Prolene thread (Fig. 1).

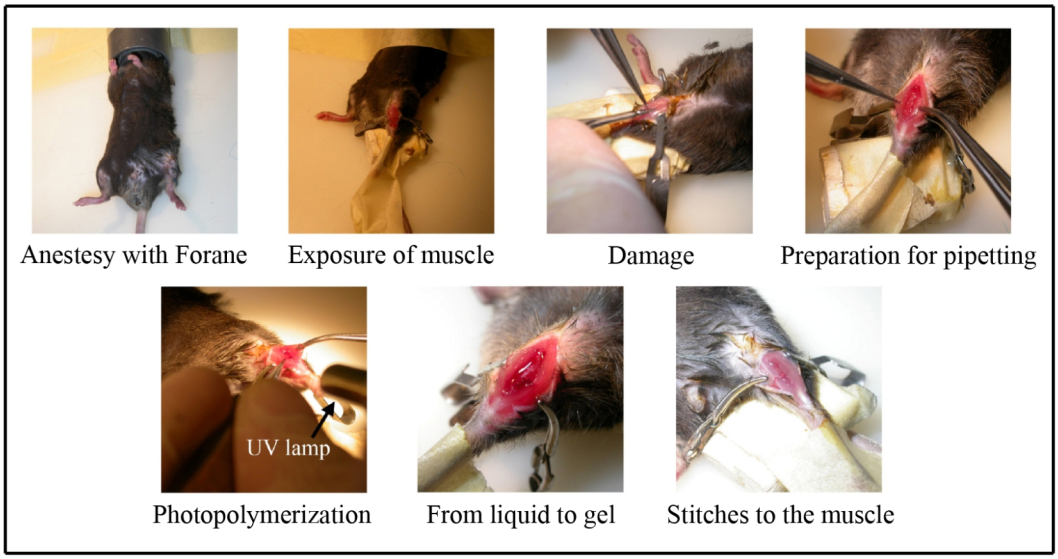

Figure 1. Procedure of surgical ablation and polymer implant.

Histological and immunofluorescence analyses

Treated muscles were frozen in 2-methyl-butane cooled in liquid nitrogen. 10 µm-thick sections were then prepared onto Superfrost slides (Thermo Scientific) for hematoxylin-eosin, Masson's trichrome (Biooptika) and immunofluorescence analyses. Slides were fixed with 4% paraformaldehyde in phosphate buffered saline (PBS) and permeabilized with 0.5% Triton X-100 in PBS. For GFP detection they were directly mounted with fluorescent mounting medium (DAKO) containing DAPI as nuclear counter stain. For immunological analyses we used mouse anti-Pax7 antibody (DSHB; dilution 1:50), rabbit anti-laminin (Sigma;

1:150), mouse anti-fetal myosin BF-G6 (a kind gift from Prof. S. Schiaffino; dilution 1:100), rabbit anti-GFP 594 (Invitrogen; 1:150), rabbit anti-von Willebrand factor (Dako cytomation; 1:100). Where indicated, slides were also incubated with Alexa anti-α-bungarotoxin 488 (Invitrogen), in order to mark the neuromuscular junctions.

Morphometric analyses

Average cross-sectional area of muscle sections were measured using Scion image software (http://www.scioncorp.com). Centrally nucleated myofibers, GFP^+ myofibers and vessels (stained positively for von Willebrand factor) were counted in muscle sections with Adobe Photoshop.

Weight recovery assessment

In order to assess weight recovery, removed muscle tissue was weighed at the time of operation and total muscle weight was inferred through a regression curve (see Fig. 9). After 6 weeks from the operation, muscles were harvested and weighed. % of muscle recovery was calculated using the following formula: (weight of muscle after 6 weeks) / ((inferred weight at operation) – (removed muscle tissue weight)).

Cell proliferation assay

Six–week operated TA muscles were further damaged by injecting 50 μl of bupivacain 0.5%. Three days later EdU (5-ethynyl-2'-deoxyuridine), resuspended in PBS was injected intraperitoneally (150 μl, at the concentration of 1 μg/μl), according to Salic & Mitchison, 2008. After 48 more hours mice were sacrificed and TA muscles harvested, frozen and sectioned at 10 μm. Click-iT staining for EdU labeled cells was then carried out according to manufacture's instructions (Invitrogen).

Force measurement

Contractile performance of treated and control muscles was measured *in vivo* using a 305B muscle lever system (Aurora Scientific Inc.) in animals anesthetized with a mixture of Tiletamine, Zolazepam and Xilazine (Blaauw et al., 2008). Mice were placed on a thermostatically controlled table, with the knee kept stationary

and the foot firmly fixed to a footplate, which was in turn connected to the shaft of the motor. Contraction was elicited by electrical stimulation of the peroneal nerve. Teflon-covered stainless steel electrodes were implanted near to the branch of the peroneal nerve as it emerges distally from the popliteal fossa. The two thin electrodes were sewed on both side of the nerve and the skin above was sutured. The electrodes were connected to an AMP Master-8 stimulator (AMP Instruments). Isometric contractions induced by single stimuli (twitches) and by trains of stimuli (frequency 150 Hz, duration 0.5 s) were recorded.

Microscope and imaging system

Phase-contrast and histological analyses were carried out using an inverted microscope (Olympus IX71). Immunofluorescence analyses were performed using a direct microscope (Leica B5000).

Statistical analysis

Values are reported as means ± SEM. Coupled data sets were compared by Student's t-test. Statistical significance was accepted when $p<0.05$.

Results

In this work I developed, in collaboration with the Department of Chemical Engineering, a biodegradable, injectable and photo-crosslinkable hydrogel (HA-PI), based on ester of hyaluronic acid, one of the main components of the extracellular matrix, ligand of protein CD44, expressed by SCs; see Boldrin et al., 2007) linked to a synthetic photoinitiator (Revell et al., 2005); this latter allows the transition from liquid to gel when the compund is exposed to monochromatic UVA light at 366 nm (Fig. 2).

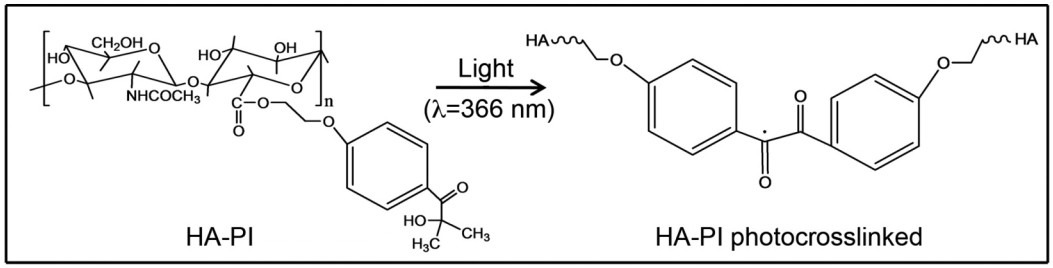

Figure 2. Chemical structure of the hyaluronic acid-photoinitiator complex (HA-PI, left). This molecule reacts after UVA light exposure, producing cross-linkings and giving the final structure of the hydrogel (right).

The first part of the study has been the characterization of the biomaterial, in order to maximize cell survival and myogenic potential; in this context various parameters of the biomaterial needed to be considered. First of all, the shear stress acting on cells during injection depends on the variables: viscosity of the solution, needle gauge and flow rate. Apparent viscosity of HA-PI solution at different concentrations was hence measured (Fig. 3a). The maximum injection flow rate was then evaluated (see Materials and Methods) as function of the needle gauge in order to maintain the shear stress below 1Pa: this is important in order to avoid cell membrane damages (Fig. 3b, see Hathcock et al., 2000). After light exposure, the reaction of photopolymerization takes place and HA-PI constitutes a semisolid hydrogel (Fig. 3c, left), whose microstructure, at different concentrations, was characterized through SEM microscopy (Fig. 3c). HA-PI has the advantage of not requiring mixing between two separate solutions, as the photoinitiator and the hyaluronic acid chain are linked in one molecule. This property ensures structural uniformity at every concentration, as shown in Fig. 3c, and ensures the reduction

of toxicity of the photoinitiator of polymerization, that is usually used at higher concentrations than required. Other parameters evaluated were the elastic modulus and the dimension of the cross-linking reticulum of polymerized HA-PI (see Materials and Methods), that were both dependent on the irradiated light energy up to 20 J/cm^2, whereas higher energy did not affect hydrogel properties. This finding ensured repeatability of results and defined the "safe" operative zone (Fig. 3d). It is important to note that the dimension of cross-linking reticulum (Fig. 3e) ensures free diffusion of biomolecules, thereby allowing cell-tissue cross talking, while preventing the host's inflammatory cells from reaching the implanted cells. On the basis of *in vitro* results, we used a HA-PI concentration of 50 mg/ml and an exposure time of 55 sec, the light source being placed at a distance of 3 cm.

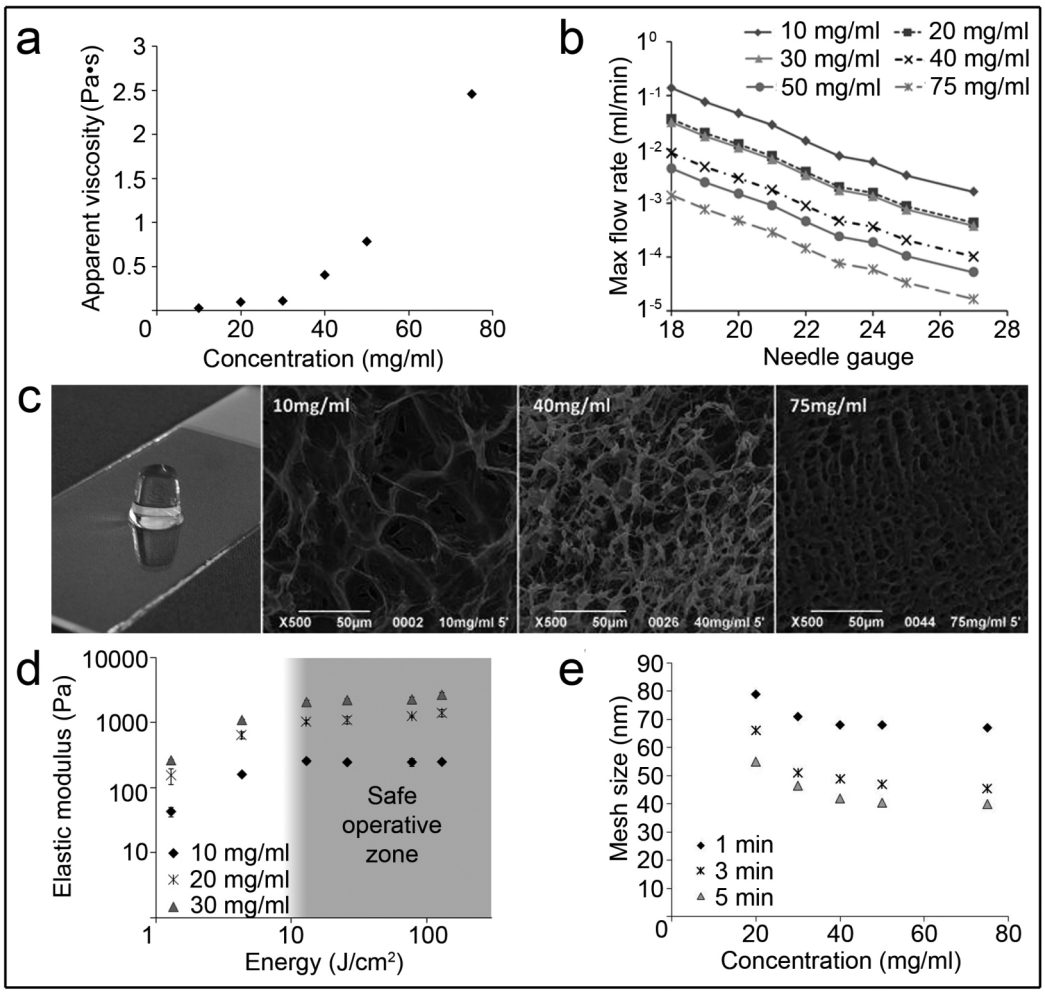

Figure 3. (a) Apparent viscosity of HA-PI calculated as function of the concentration in physiological solution. **(b)** Maximum flow rate that can be used during the injection of cells suspended into HA-PI solution, in order to ensure no cell membrane damages (shear stress ≤ 1Pa). The maximum flow rate as function of the needle Gauge is reported for different HA-PI concentrations in solution. **(c)** from left to right: image of a cylinder of

photo-crosslinked Hydrogel, SEM images of dehydrated hydrogel obtained from HA-PI solutions at the concentration of 10mg/ml, 40mg/ml and 75mg/ml respectively (bar=50 µm). **(d)** Elastic modulus of photo-crosslinked hydrogel as function of the light energy used for the photo-crosslinking. Values for three compositions of the initial solution are reported. The grey area indicates the region where the elastic modulus does not depends on exposure time and thus where is "safe" to operate. **(e)** Average dimensions of the crosslinking reticulum of the hydrogel as function of the HA-PI concentration. Values for three exposure times are reported.

Another parameter that we needed to characterize was the *in vivo* degradation rate of HA-PI, a crucial parameter for cell homing after delivery (Freed et al., 1994). Upon surgical ablation of about 15% w/w of *tibialis anterior* muscle and polymer implantation, animals were sacrificed at short time points of 48 hours in the first 8 days. Then a morphometric software (see Materials and Methods) has been used, in order to measure the area of polymer present in H&E stained muscle sections (Fig. 4). After the first 48 hours, 70±14% of muscle sections were filled by HA-PI, while after 8 days hydrogel (14±9%) was mostly replaced by regenerating muscle formed by resident SCs and/or by connective tissue. These findings confirmed that, as desired, hydrogel was present in the muscle only during the massive first wave of inflammation after damage (from 2 to 4 days, see Malm, 2001), and was therefore suitable for protecting delivered myogenic cells before fiber formation.

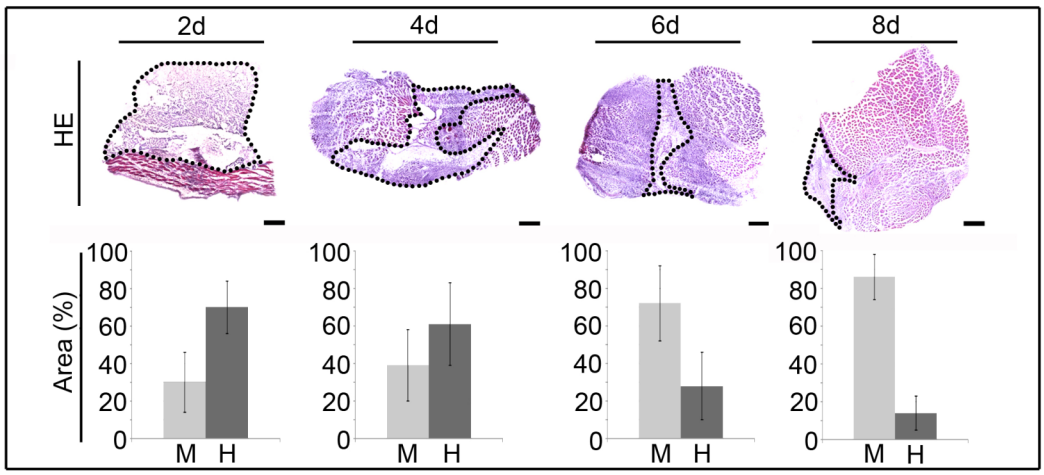

Figure 4. *In vivo* degradation study of HA-PI implanted in mouse TA muscle. Haematoxylin/eosin (HE) staining on muscle sections 2, 4, 6 and 8 days after transplant (n=4, bar=100 µm, upper panel). Proportion of total cross-sectional muscle area (%) occupied by HA-PI (H) or muscle (M) at the same time points (lower panel).

In the second set of experiments, the regenerative process associated to the mode of isolation of SCs has been analysed. Three different protocols have been used for SC isolation, that subsequently have been delivered *via* HA-PI in partially ablated muscles. 150.000 cultured MPCs (passage 1 from a culture of 20 single fibers, see Materials and Methods and Rosenblatt et al, 1995) were produced, then 20 isolated single fibers (Collins et al., 2005) or 250 freshly isolated SCs (mechanically dissociated from 20 single fibers, see Rossi et al., 2010), all derived from syngeneic C57BL/6J-GFP^{+} mice muscles (*flexor digitorum brevis*, *extensor digitorum longus* and *soleus*). Fifteen days after surgery, implanted muscles were analyzed to assess muscle regeneration vs. infiltration (the respective areas were measured by morphometry, see Materials and Methods). The results show that in average the presence of cells within the polymer reduces the infiltration in treated muscles. In muscles treated with only HA-PI, cell infiltrate constituted the 66±8% of the whole muscle section, compared to 34±6% of muscle tissue. In muscles treated with MPCs embedded in HA-PI, infiltration was 44±6% compared to the 56±7% of muscle (*p<0.05). In muscle treated with fibers and SCs, both embedded in HA-PI, the area of cell infiltrate was reduced to the 32±6% and 25±6% respectively, compared to an increase in muscle mass, with a proportion of 68±9% and 75±5% respectively (Fig. 5). Notably the central part of muscles, where mass was ablated and polymer with cells were implanted, showed the presence of newly generated myofibers, that constituted the first evidence of the efficiency of the system HA-PI ± fibers or SCs in reconstructing muscle tissue after severe ablation.

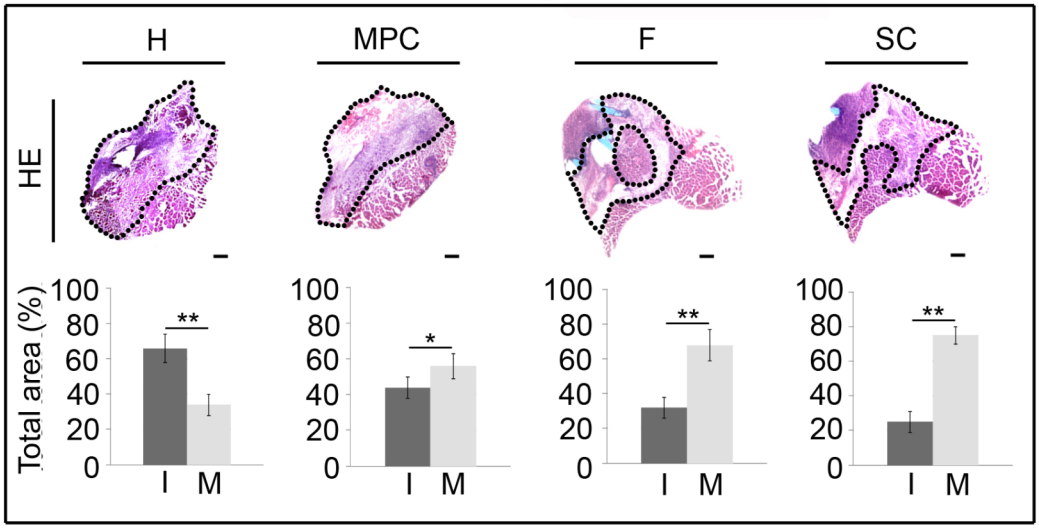

Figure 5. Histological and morphometric analysis of muscles 15 days post-treatment with HA-PI alone (H), or HA-PI with cultured MPCs (MPC), single fibers (F) or freshly isolated SCs (SC); n=8 in all cases. H&E staining on muscle sections (bar=100 µm, upper panel). Proportion of total cross-sectional muscle area (%) occupied by infiltrate (I) or muscle (M) (*p<0.05, **p<0.01; lower panel).

In order to quantify the regenerative process in treated muscles, the number of centrally nucleated fibers per section were counted (see Materials and Methods). The result confirmed what was already evident from H&E staining: the number of centrally nucleated myofibers was higher when fibers (97±6) or SCs (84±8) were used (***p<0.001). MPCs (48±7) also yielded more regenerating fibers than HA-PI alone (18±6, ***p<0.001) (Fig. 6).

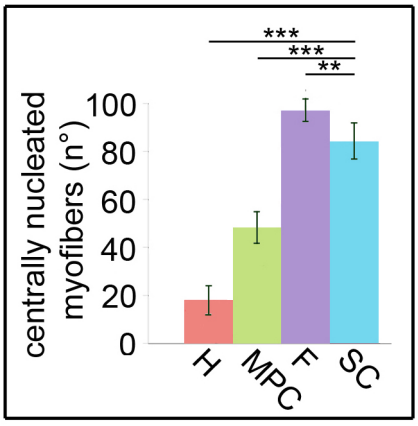

Figure 6. Quantification of new myofibers in the engineered muscle (**p<0.01, ***p<0.001) showed that a higher number of centrally nucleated fibers was present when fibers (F) and SCs (SC) were used. Significativity is shown only for SC in order to avoid confusion.

Reconstruction of the engineered muscle was evaluated after 6 weeks from surgery. Muscles were harvested and analysed through hystology (H&E and Masson's trichrome stainings) and morphometry, the latter in order to evaluate of the total area of muscles sections. Two controls have been used: the first were the "sham-operated" muscles, in which the central part of the tissue was removed (according to Materials and Methods) and then the muscle was closed with stitches, and the second were the muscles ablated and filled with HA-PI without cells. Histological and morphometric analyses of muscles treated with 20 single fibers or 250 freshly isolated SCs showed extensive and consistent regeneration of

the ablated region in TA muscles with little scar tissue formation after 6 weeks, as evidenced by Masson's trichrome staining. On the contrary, "sham-operated" (i.e. muscle ablation alone) and hydrogel-only implanted muscles showed a dramatically altered morphology, with large infiltrations of connective tissue. Muscles that received MPCs showed limited regeneration, with presence of connective tissue in the central part of the sections (Fig. 7).

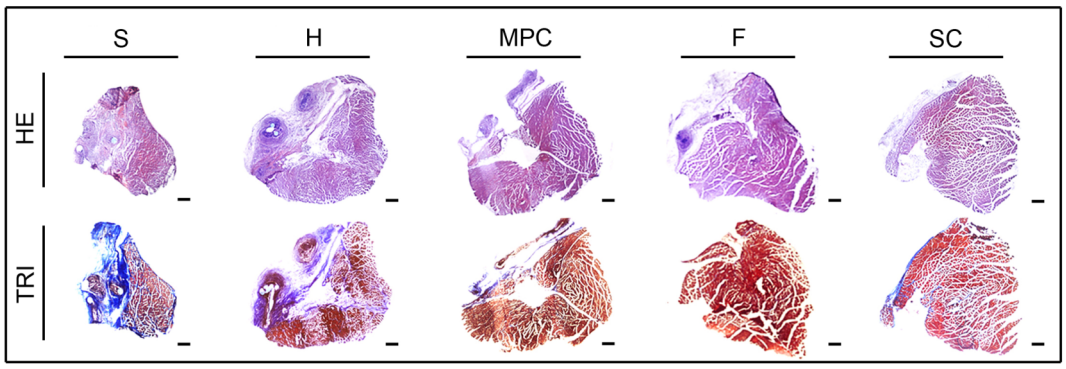

Figure 7. Histological analysis of operated muscles 6 weeks post-treatment. Haematoxylin/eosin (HE) and Masson's trichrome (TRI) staining on muscle sections (bar=100 μm) confirmed extensive regeneration and few scar tissue when fibers (F) and SCs (SC) were delivered with HA-PI; n=10 for F and SC; n=19 for HA-PI alone, H; n=12 for sham operated controls, S.

To better quantify muscle mass reconstruction, the ratio between the post-operatory and the pre-operatory weight was also calculated (Fig. 8). Muscles treated with MPCs or SCs were heavier than sham-operated (120±22% and 112±23% of recovery vs. 82±32%; $^{**}p<0.01$ and $^{*}p<0.05$) whereas HA-PI implanted (99±27%) and fibers-treated (100±35%) muscles did not show any significant difference with controls.

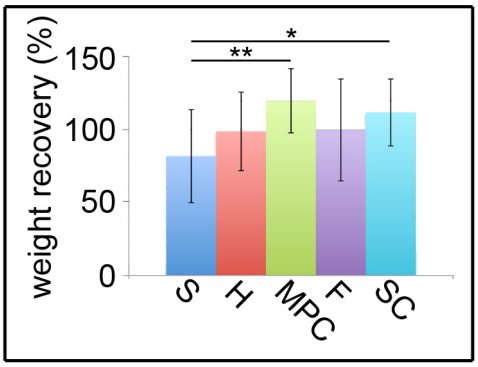

Figure 8. Weight recovery analysis (%) on treated muscles demonstrated that MPC- and SC-treated muscles were heavier than sham-operated.

Muscle weight at time of surgery was inferred from a regression curve plotting the correlation between tibialis anterior and total body weight (n=15, Fig. 9).

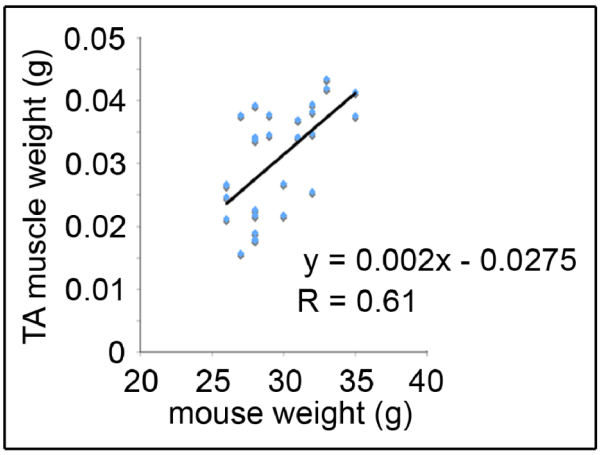

Figure 9. Correlation between weight of TA muscle and total weight of C57BL/6J mouse. Regression curve was derived using fifteen C57BL/6J mice. After being weighed the mice were sacrificed and their TA muscles were harvested and weighed.

The average cross-sectional area of the treated muscles was also examined: this is an important parameter to evaluate the quality of the reconstruction of muscles. It has been measured on transversal sections taken from the part of the muscle in which ablation was performed and HA-PI was implanted (this means from the center of the muscle until ~3 mm from tendons, in both sides). Muscles treated with freshly isolated SCs presented a cross-sectional area of 8.2±0.8 mm^2, which was bigger (***$p<0.01$) than all the other treatments and was not significantly different from that of age-matched wild-type. This highlights the regenerative properties of freshly isolated SCs, able to give rise to a process of reconstruction that after only 6 weeks restored the structure of muscles making it comparable to

that of an untreated animal. The area of sections from "sham-operated" was 3±1.6 mm^2, from hydrogel-implanted 3.2±1.2 mm^2, and from MPCs treated muscles 4.6±1 mm^2: all these values were statistically different from SCs (***p<0.001); this means that muscle that undergo severe ablation is not able to recover its structure, even if there is a supply with HA-PI, and there is another confirmation that MPCs are not able tu sustain a process of regeneration, even if delivered through a biopolymer, because they display reduced proliferation and migration. Fibers-implanted muscles had an average area of 6.1±1.5 mm^2, that was not significantly different from other conditions, but was significantly inferior if compared to wild-type untreated muscles (*p<0.05, see Fig. 10).

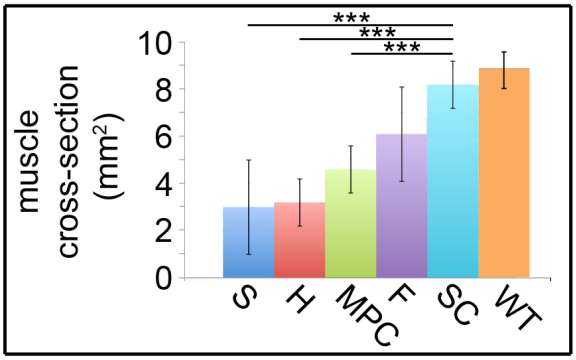

Figure 10. Average cross-sectional muscle area (mm^2) of treated and untreated (WT) muscles. Statistical significance is reported only for SCs, in order to avoid confusion in the diagram (***p<0.001).

In order to quantify the contribution to muscle reconstruction, green fluorescent protein (GFP) epifluorescence was examined at 7 and 15 days and at 6 weeks (Fig. 11). The tracking of implanted cells through the GFP is useful in order to evaluate the contribution to muscle regeneration and reconstruction, in part given also by the host resident cells, that were not inactivated.

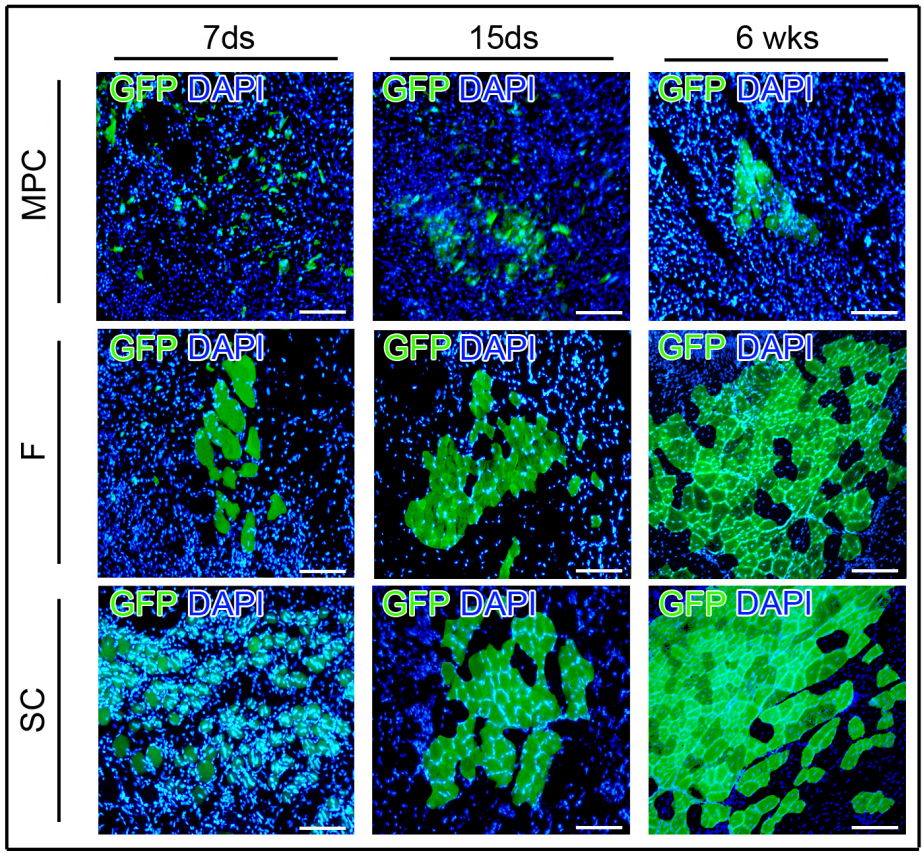

Figure 11. Contribution to regeneration of donor myogenic precursors, evaluated through epifluorescence for GFP (counter stained with DAPI) on muscles treated with cultured MPCs (MPC), single fibers (F) or freshly isolated SCs (SC) 7, 15 days and 6 weeks post-operation (bar=100 μm).

Positive fibers were blind-counted by 2 investigators. Both fibers and SCs were much more effective than MPCs in contributing to neo-fibers formation at each time point (***$p<0.001$). After 7 days no GFP^+ myofibers were present in muscles treated with HA-PI and MPCs, but only cells and small myotubes were detected; the situation was extremely different in the muscles implanted with HA-PI and fibers, with 21±8 fibers per section, and HA-PI plus SCs, with 32±12 neofibers. After 7 days there was no significant difference in contribution of newly generated fibers between hydrogel with fibers and hydrogel with SCs; the only difference between these two treatments was a trend in GFP^+ fiber area, that seemed to indicate a slight hypertrophy of fibers in muscles treated with hydrogel and fibers. This can be an indication of a faster maturation of neofibers, that probably depends on a faster engraftment and activation of SCs in the host muscle, due to the fact that they are implanted in their niche inside parental parental myofiber. After 15 days, some GFP^+ fibers were detectable in muscles

operated with hydrogel and MPCs (9±4), but only few; hydrogel and fibers contributed with 48±21 neofibers and hydrogel and SCs with 76±23, with SCs being the most efficient (*p<0.05). 6 weeks post treatment hydrogel plus MPCs produced 35±12, and definitively more inefficient if compared to hydrogel with fibers (137±15) and with SCs (198±24), that resulted to be the most effective (***p<0.001 Fig.12). These data confirmed the histologies showing a great potential of SCs in reconstructing ablated muscles, when delivered in combination with HA-PI.

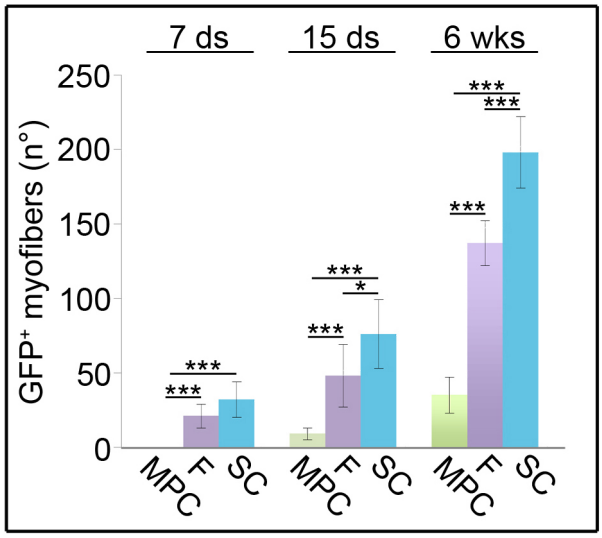

Figure 12. Quantification of GFP^+ myofibers in muscles treated with hydrogel plus MPCs, or fibers (F) or freshly isolated SCs (SC) after 7 or 15 days and 6 weeks from treatment (*p<0.05, ***p<0.001).

Another important parameter in muscle regeneration studies is the contribution of the implanted myogenic cells to the reconstitution of the niche of SCs (Collins et al., 2005). This is crucial, expecially in case of pathologies disrupting SC niche for excessive SC activation and cycle, like Duchenne Muscular Dystrophy, and even more important in case of muscle reconstruction, to assess the functionality of newly formed muscle tissue. Paired-box 7 (Pax7) transcription factor, known as universal marker of quiescent SCs (Seale et al., 2001), was used to identify SCs (Fig. 13, upper panel). Another way to assess the integration of the delivered SCs in host muscle is to verify the position of GFP^+ cells in the canonical SC position, i.e. under the basal lamina (Mauro, 1961). So I performed a staining with anti-laminin antibody and verified the presence of GFP^+ cells under the basal lamina, inside muscle fibers (Fig. 13, middle panel). In order to assess if SCs engrafted in

the niche were functional, two different experiments were performed. In the first treated muscles were harvested 6 weeks post treatment, and single fibers were isolated *via* collagenase digestion and cultured, in order to release SCs (Rosenblatt et al., 1995). In culture many GFP^+ fibers were present, with GFP^+ SCs associated with both GFP^+ and GFP^- fibers, confirming the data shown before. More interestingly, GFP^+ SCs proliferated from fibers and were able to align and fuse to form myotubes, also with host SCs (Fig. 13, lower panel).

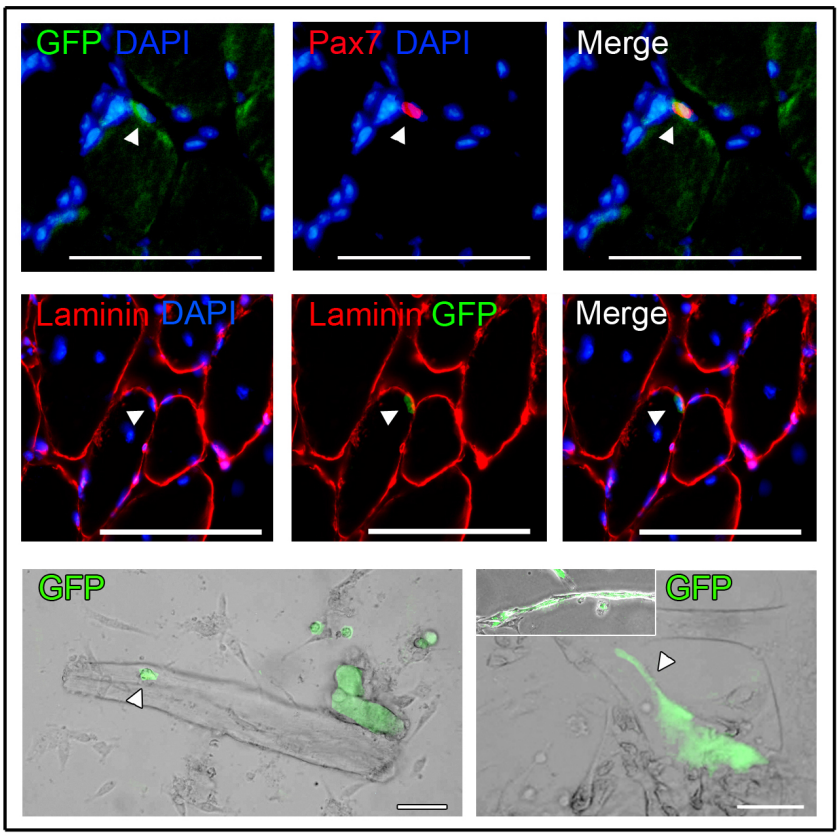

Figure 13. Generation of a SC niche within engineered muscle. Immunostaining for Pax7 and epifluorescence for GFP (counter stained with DAPI) on treated muscles (bar=100 µm, upper panel). Immunostaining for laminin and epifluorescence for GFP (counter stained with DAPI) on treated muscles (bar=100 µm, middle panel). Phase contrast microscopy and epifluorescence for GFP on fibers derived from treated muscles. GFP^+ SCs were able to align and fuse to form myotubes (bar=100 µm, lower panel).

In the second, 6-weeks treated muscles in different conditions were reinjured *in vivo* with bupivacaine in order to activate SCs, and after 3 days EdU was injected intra *peritoneus,* in order to mark proliferating cells (see Materials and Methods). 48 hours later animals were sacrificed and TA muscles harvested and processed.

In the sections EdU^+-GFP^+ cells were detected, showing that they were functionally activated after damage (Fig. 14).

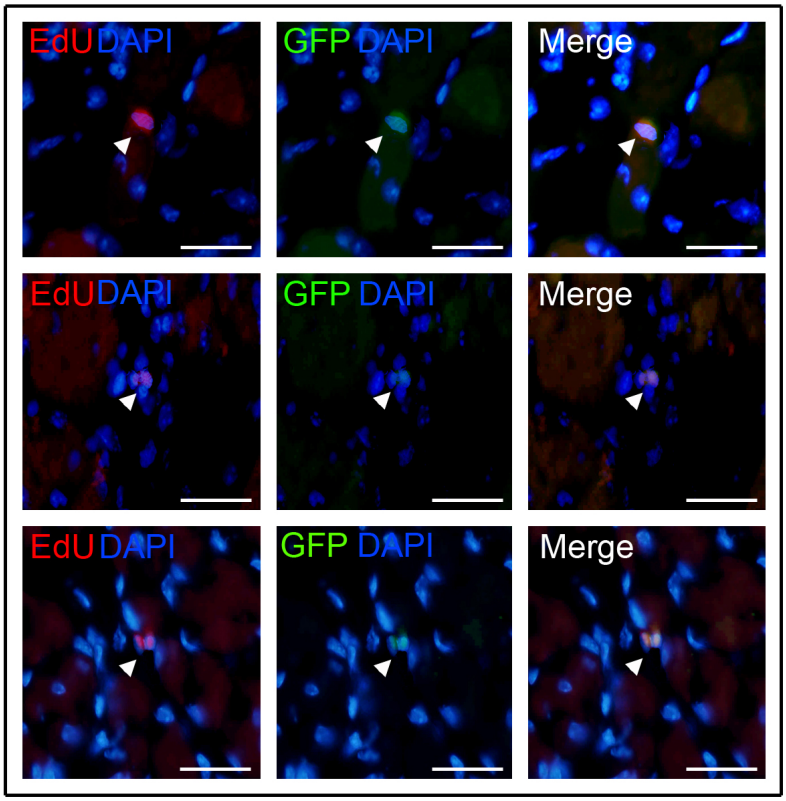

Figure 14. Cell proliferation assay on treated muscles. Six C57BL/6J mice (2 implanted with hydrogel and MPCs, 2 with hydrogel and fibers and 2 with hydrogel and SCs) were reinjured with bupivacain and injected with EdU, after 6 weeks from transplantation. Muscle slides were EdU-labeled and GFP was detected through epifluorescence (bar=100 µm).

In order to quantify the repopulation of SCs in treated muscles, the amount of cells that were derived from the GFP^+ implanted precursors, and were positive for the canonical SC marker Pax7, was counted. The percentage of $Pax7^+GFP^+$/total $Pax7^+$ cells per section was 38.7±4.8% in muscles reconstructed with SCs, while only the 19.3±3.8% in those receiving single fibers and just 12.6±5% in those with MPCs (Fig. 15).

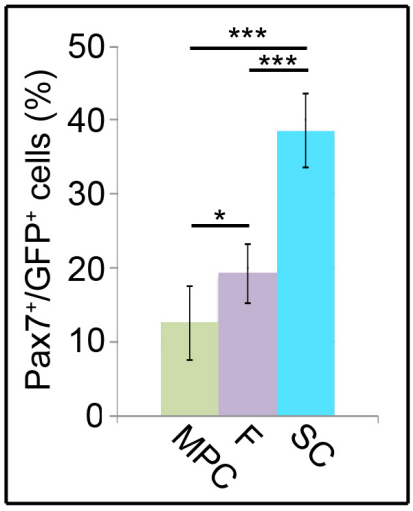

Figure 15. Pax7^{+}/GFP^{+} cells in muscles treated with cultured MPCs (MPC), single fibers (F) and freshly isolated SCs (SC) (*p<0.05, ***p<0.001; right).

Freshly isolated SCs were hence the most efficient in repopulating the satellite niche (***p<0.001). This constitutes the first demonstration of complete functional integration in a tissue-engineered muscle, similar to what has been shown previously after cell tranplantation without tissue ablation (Collins et al., 2005).

At this point of my work I was able to obtain an almost complete reconstruction of muscles after severe ablation, both in architecture and in SC niche, documented through histological and immunofluorescence analyses. Nevertheless, it is fundamental to prove that the regenerative processes led to the formation of functional muscle. There are many components connected with a correct physiology: first of all the muscle structure itself, e. g. fiber orientation, but also innervation and vascularization. Then it is important to assess if the regeneration led also to recovery of muscle force. The first experiment performed has been the force measurement with an innovative technique. We used a set up, that is different from the commonly used assays, that require muscle isolation after the sacrifice of the animal, with the whole analysis performed *ex vivo* and *ex situ*. In my setting, I was able to measure the response of the operated muscles, 6 weeks after treatment, through the electrical stimulation of the peroneal nerve *in vivo*, i. e. on the anesthetized animal, and *in situ*, i. e. on the system of the hindlimb (see Material and Methods). The analyses were performed in animals with or without transplantation, and in age- and weight-matched control mice. The absolute force

was calculated in the different samples giving a stimulus of 150 Hz, in order to reach muscle tetanus. The results were very interesting and confirmed what was clear from histologies and immunofluorescences. Freshly isolated SCs yielded the best functional recovery (Fig. 16, left). They showed significative improve in force, when combined with the polymer, in comparison with the "sham control" and the hydrogel-only muscles (***$p<0.001$), and even more interestingly with MPCs (**$p<0.01$). This is the first demonstration that freshly isolated SCs allow a better force recovery than MPCs, when combined with a biopolymer, in presence of muscle ablation. Nevertheless, the absolute force on SC treated muscles was inferior when compared with age-matched untreated animals, meaning that the reconstruction after 6 weeks from surgery was not sufficient to reconstitute the normal force of the muscle. In this concern, it is possible that a longer time is required to completely restore muscle force. Normalization of the absolute force values against the weight of muscle provides information about the quality of muscle reconstruction, i. e. the force produced by each unit of weight. SCs treated muscles resulted to be the most efficiently reconstructed, displaying a normalized force value that was significantly higher than "sham-operated" (**$p<0.01$), hydrogel-only (***$p<0.001$) and MPC treated muscles (**$p<0.01$). Interestingly SC treated muscles did not display any significantly difference with normalized force of age-matched untreated mice muscles, underlining how the quality of the reconstructed muscle was not different from that of a normal not-ablated muscle. This is a very important parameter, because the quality of muscle force depends on its structure, i. e. the correct alignment of fibers; as it results evident from Fig. 16, right, treated muscles that presented consistent infiltration of connective tissue had minor force, due to uncorrect alignment of fibers from tendon to tendon, and sometimes to the presence of bifurcated myofibers.

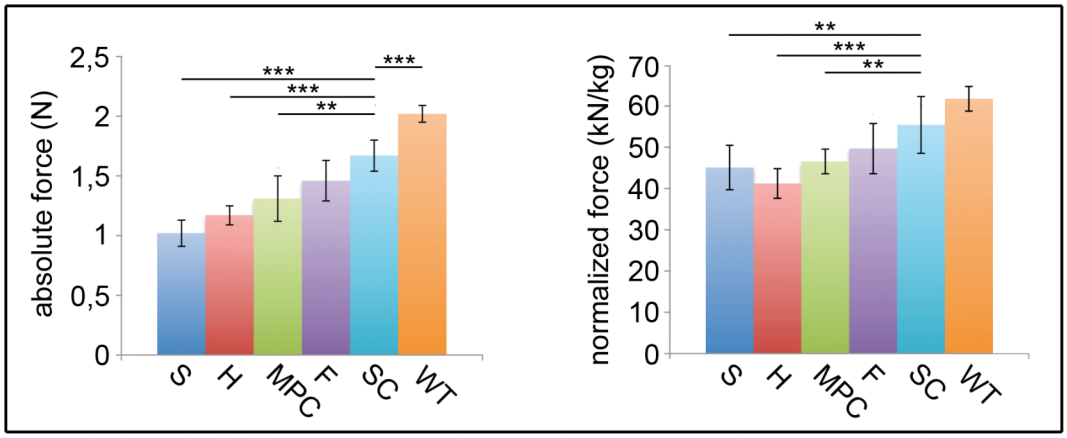

Figure 16. Force measurement on treated muscles compared to untreated controls. Measurements were carried out 6 weeks after treatment. Significance is reported only against SCs, in order to avoid confusion in the diagram. Left panel: absolute force values (N) in the different conditions (sham (S), HA-PI alone (H), HA-PI with cultured MPCs (MPC), HA-PI with single fibers (F), HA-PI with freshly isolated SCs (SC) and wild-type untreated animals (WT), **p<0.01, ***p<0.001; left). Right panel: normalized force-weight values (kN/kg) in the different conditions (**p<0.01, ***p<0.001; right).

An immunofluorescence staining for myosin BF-G6, an isoform of embryonic myosin used as a marker of regenerative processes (Schiaffino et al., 1986), has been performed, in order to assess if the regenerative process in treated muscles was still ongoing after 6 weeks from treatment. I found the presence of various clusters of GFP^+ myofibers in muscles delivered with fibers or SCs embedded in HA-PI, that stained positively also for BF-G6 (Fig. 17). This might also correlate with the lack of a complete recovery in force of SC treated muscle, that probably could be achieved in a time longer than the 6 weeks.

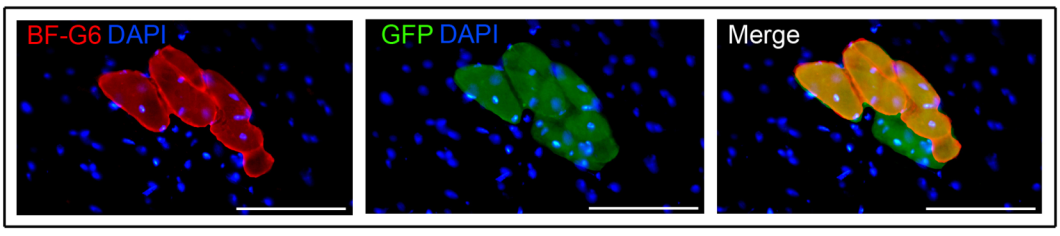

Figure 17. Immunostaining for embryonic myosin isoform BF-G6 (left), epifluorescence for GFP (center) and merge (right, bar=100 µm).

This is the first demonstration that freshly isolated SCs have the best potential for functional muscle reconstruction, both for SC niche repopulation and force

recovery. Nevertheless, the reconstruction of muscle is strictly dependent on the formation of a functional network of nerves and of vessels. This has represented a major limitation in previous studies (De Coppi et al., 2006a; Yan et al., 2007), and growth factors have been suggested to implement nerve regeneration (Rumsey et al., 2008) and new capillary formation (De Coppi et al., 2005; Borselli et al., in press). The force measurement assay provides an indirect indication of the reinnervation of ablated muscle, because the stimulation that produces muscle tetanus derives from electrical impulses of the peroneal nerve. The innervation at the level of regenerated fibers was evaluated through a common immunofluorescence assay, in which bungarotoxin, a toxin derives from venomous snakes and with the capacity to bind cholinergic receptors, is linked to a fluorophore, that allows the localization of neuromuscular junctions. In this way it was possible to observe how regenerated fibers (GFP^+) were regularly innervated, in comparison with GFP^- host fibers (Fig. 18). It is not easy to quantify the incidence of neuromuscular junctions in muscle sections, because every single fiber presents only one point of innervation, that is randomly distributed in its total lenght. This gives another important information about the quality of the reconstructed muscle.

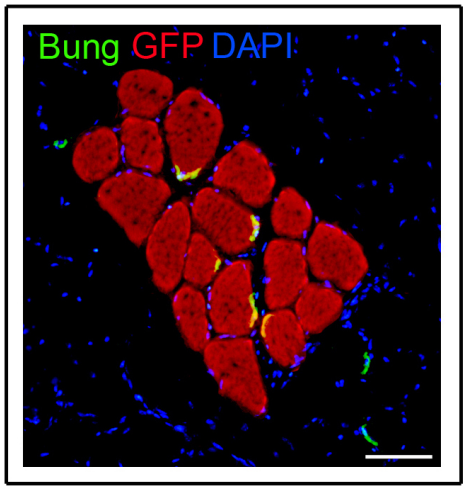

Figure 18. Immunostaining for 488-bungarotoxin identifies neuromuscular junctions, and anti-GFP the regenerated fibers (counter stained with DAPI) (bar=100 µm).

Another pivotal issue is the vascularization of the reconstructed muscle, fundamental for the support of oxygen and nutrients. In the ablated part of the muscle all the tissue was removed, even the vascular components, that needed to be recreated *in toto*. In order to verify the status of vascularization in treated

muscles 6 weeks post treatment, an immunofluorescence staining for von Willebrand factor (a specific marker of vessels) has been performed (Fig. 19, left). Some results have been unexpected: muscles reconstructed with SCs or fibers, together with HA-PI, presented an amount of vessels that was not significantly different from "sham-operated" and hydrogel-only muscles. This means that freshly isolated SCs and fibers were not actively contributing to a regeneration of the vascular network, because there was no difference between the presence or the absence of cells. Hydrogel-only treated muscles showed a better contribution to vascularization, when compared with "sham-operated" (*$p<0.05$). MPCs, combined with HA-PI, were the most effective delivered cells able to promote vascular network formation, showing significative difference when compared with fibers and SCs. It is very interesting to notice how hydrogel-only and MPC treated muscles did not differ from untreated, age-matched controls (Fig. 19, right). I hypothesised that MPCs, delivered in the amount of 150000 cells, were most effective in promoting vascular network formation due to the major amount of released factors; it is well known that stem cells in general, embryonic or adult, retain a huge paracrine potential on sorrounding cells and tissues. Nevertheless, they were not actively involved in transdifferentiation towards the endothelial lineage, because no co-staining between GFP^+ and von Willebrand factor was found. A contrasting point is that also hydrogel only treated muscles presented no significative differences with untreated controls: the initial scaffolding guarantees a major area of muscles, and this explains the significative difference in comparison with "sham-operated". On the other hand, it seems that hydrogel itself is self sufficient in promoting vessel formation and reconstitution, probably because it is made of hyaluronic acid and it produces the ideal environment for the colonization from endothelial precursors.

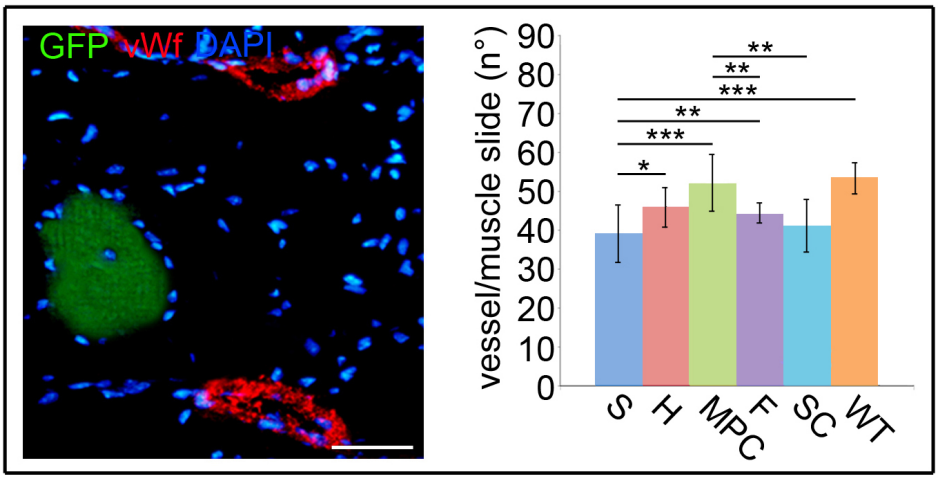

Figure 19. Immunostaining for von Willebrand factor and epifluorescence for GFP (counter stained with DAPI) to mark blood vessels (bar=100 µm, left). Quantification of the number of vessels per muscle slide in the different treatment conditions (right).

These results were encouraging, especially when considering that regeneration was not complete in muscles treated with fibers and SCs, but I believe that vascularization and innervation in the engineered muscle will likely need to be improved when considering translation to human. This could be achieved in our system by spiking the HA-PI with microspheres containing growth factors (Borselli et al., in press) or by genetically engineering implanted cells (De Coppi et al., 2005).

Discussion

In this study I demonstrated for the first time that cell transplantation *via* an injectable and photo-crosslinkable hyaluronan-based hydrogel promote *in vivo* functional skeletal muscle reconstruction. Moreover, I demonstrated that muscle reconstruction after ablation (about 15% w/w) could be achieved much more efficiently by using freshly isolated SCs than MPCs, that have been the preferred source of myogenic precursors used for cell transplantation. The interesting point is that with just 250 SCs it has been possible to achieve a normal muscle architecture, that is 1:20000 of the minimum amount of MPCs that can be used in order to obtain a mild regenerative effect in damaged mice muscle (Boldrin et al., 2007). This is encouraging for cell therapy in human, that requires a huge number of myogenic precursors, due to the dimension of muscles. The reconstruction obtained comprises neofiber formation and the construction of a muscle stem cell niche throughout the whole muscle volume: this means that other than forming new myofibers, there is also a high engraftment of SCs in the brand new niche, due to self-renewal (Collins et al., 2005). Obtaining the reconstitution of SC niche is fundamental, because it guarantees muscle regeneration in case of injuries, and it is particularly important in the treatment of diseases, as Duchenne Muscular Dystrophy (DMD), in which SCs are exhausted because of high turnover (Webster & Blau, 1990). For the first time the force exerted by the engineered muscle was evaluated. It was clearly demonstrated that the quantitative histological reconstruction was proportional to a qualitative force recovery. The reconstructive processes were also associated to reinnervation of the newly formed fibers and revascularization. I strongly believe that this approach to skeletal muscle tissue engineering could be advantageous for the reconstruction of diseased or damaged muscles and could improve the functional recovery that has been associated with previous strategies of muscle replacement.

CHAPTER II

CHARACTERIZATION OF SATELLITE CELL HETEROGENEITY

Background

Initially, SCs were considered unipotent stem cells with the ability of generating a unique specialized phenotype (Bischoff & Heintz, 1994), whilst subsequently, it was demonstrated in mice that opposite differentiation towards osteogenic and adipogenic pathways was also possible (Asakura et al., 2001). Recently, it was also shown that both human and porcine SCs can differentiate under appropriate stimuli into mature adipocytes (De Coppi et al., 2006b; Singh et al., 2007). However, even though the pool of SCs is accepted as the major, and possibly the only, source of myonuclei in postnatal muscle, it is most likely that SCs are not all multipotent stem cells (Kuang et al., 2007). Thus, evidences for diversities within the myogenic compartment have been described both *in vitro* and *in vivo* (Beauchamp et al., 2000; Rouger et al., 2004). Alternative sensitivity to high-dose irradiation revealed that at least two populations of SCs are present (Heslop et al., 2000): they are distinguishable by proliferative and myogenic capacities (Molnar et al., 1996) with a proportion that varies according to the age (Grounds, 1998). Similarly, after bupivacain injection, two SCs subpopulations get activated: committed myogenic precursors and "stem" satellite cells (Rantanen et al., 1995; Schultz, 1996; Cornelison & Wold, 1997). Intrinsic heterogeneity was indeed evident when the activating sequence of myogenic regulatory factors (MRFs) was exploited (Cornelison & Wold, 1997). Among others, Myf5 expression has led to the existence of hierarchical subpopulations of SCs (Beauchamp et al., 2000; Kuang et al., 2007). In particular, SCs have been shown to be composed of about 10% stem cells ($Pax7^+/Myf5^-$) and 90% committed myogenic progenitors ($Pax7^+/Myf5^+$) (Kuang et al., 2007). More recently, variation in the expression of various non-specific myogenic markers such as nestin (Day et al., 2007), CXCR-4 and b1-integrin (Cerletti et al., 2008), and ABCG2 and Syndecan-4 (Tanaka et al., 2009) have also been described. Despite the evident heterogeneity, the phenotypical characteristics of these subpopulations were hard to elucidate because their behavior *in vitro* has been difficult to investigate. Using a new experimental maneuver that permits clear and correct isolation of SCs from the fiber of origin, I report, for the first time, that two subpopulations of SCs coexist in fixed proportions on the single fiber: the low proliferative (LPC) and the high proliferative clones (HPC) which show alternative myogenic potential *in vitro*

retained also *in vivo*. Intriguingly, although the HPC give spontaneously rise to adipocytes their myogenic potential can be boosted if co-cultured with LPC. Besides assessing the regenerative and proliferative potentials of SCs, I also investigated functional cellular markers attributable to mitochondrial function. Thus, I exploited the mitochondrial membrane potential ($\Delta\Psi_m$) (Duchen et al., 2003), the pathways of ATP production and the rate of Reactive Oxygen Species (ROS) generation discovering that LPC and HPC remarkably differ in every of these parameters accounting for differences in basal cell signaling and metabolism. In this way, we do not just provide experimental evidences for different populations of SCs but also indications for readouts that may lead to applied studies of regenerative medicine.

Materials and Methods

Animals

Three to four month-old Sprague-Dawley wild type rats (Harlan, Indianapolis, USA) and transgenic rats, with expression of the enhanced GFP, under the control of the cytomegalovirus (CMV) enhancer and the chicken beta-actin promoter (Mothe et al., 2005), were used in this study. Animal care and experimental procedures were performed in accordance with "D.L. 27-1-1992, number 116, applicative declaration of Healthy Minister number 8 22-4-1994".

Isolation of single fibers from flexor digitorum brevis (FDB) muscle

Single muscle fibers with associated SCs were isolated from FDB muscles as previously described (Fig. 1, see Rosenblatt et al., 1994). In brief the hind limb FDB was digested for 3 hours at 37°C in 0.2% (w/v) type I-collagenase (Sigma-Aldrich), reconstituted in DMEM (high-glucose, with L-glutamine, supplemented with 1% penicillin-streptomycin, GIBCO-Invitrogen). Following digestion, the muscle was transferred in plating medium (DMEM low-glucose, 10% HS, 1% penicillin-streptomycin, 0.5% chicken embryo extract, GIBCO-Invitrogen) and gently triturated with a wide-bore pipette to release single myofibers. In each preparation, under phase contrast microscope, 50 single fibers were carefully sucked up through a 100 μl pipette and transferred in a 10 cm-plate containing 10 ml of muscle plating medium (1° dilution). Each single fiber was subsequently transferred in another 10 cm plate containing 10 ml of muscle plating medium (2° dilution). Finally, each fiber was collected into one 50 ml Falcon tube with 1 ml of muscle proliferating medium (3° dilution in DMEM low-glucose, 20% FBS, 10% HS, 1% penicillin-streptomycin, GIBCO-Invitrogen, 0.5% chicken embryo extract, MP Biomedicals). Serial dilution was performed in order to avoid the presence of contaminant cells. An aliquot of each preparation was used to perform immunofluorescence staining for CD45, CD163 and CD31 to further exclude respectively macrophages, haematopoietic and endothelial cells contamination after muscle dissociation (1° dilution), first (2° dilution) and second passage (3° dilution).

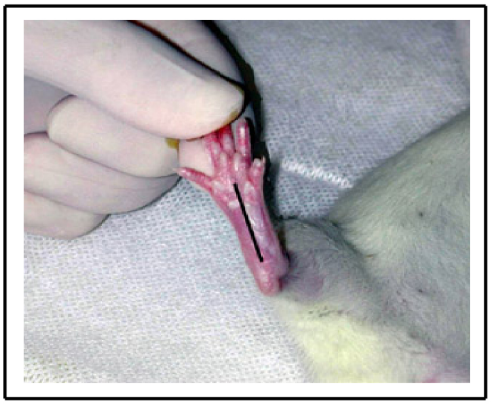

Figure 1. Isolation of *flexor digitorum brevis* (FDB) muscle from rat.

Single fibers culture in suspension in hanging drops

Freshly isolated single fibers were transferred with Pasteur pipette to drops of proliferating medium. Each 30 µl drop contained only one single fiber devoid of contaminating cells. Twenty drops were made on the upper part of 10 cm Petri dish (Falcon) which was then turned while the lower part of dish was filled with PBS to prevent evaporation, similarly to what is commonly done for embryoid bodies' cultures (Keller, 1995). Fibers were cultured for 5 days at 37.5°C, 5% CO_2 in a humidified tissue culture incubator (Heraeus BDD 6220) and then fixed and immunostained.

Cloning satellite cells from single myofibers

Clones of SCs were derived from FDB myofibers of Sprague-Dawley rats (both wild type and GFP-transgenic). For each experiment, 10 myofibers were transferred, after dilution, into a separate tube containing 1 ml DMEM. They were then triturated 20 times using a 18G needle mounted onto a 1 ml syringe, to disengage SCs (Shefer et al., 2004). The resulting cell suspension was filtered through a 40 µm cell strainer (Falcon) and diluted with 18.2 ml of muscle proliferating medium, and then dispensed into five 96-well petri dishes in 0.2 ml of growth medium (DMEM low-glucose, 20% FBS, 10% HS, 1% penicillin-streptomycin, GIBCO-Invitrogen, 0.5% chicken embryo extract, MP Biomedicals) with limiting dilution (0.5 cell/well). Dishes were incubated at 37.5°C, 5% CO_2 in a humidified tissue culture incubator. Clones were then followed counting the amount of cells at 5, 10 and 20 days with inverted-microscope analysis and Bürker counting chamber. Duplication time was assessed

through the formula: duplication time (hours) = Δt / $\log_2$ (number of cells at second count / number of cells at first count), with Δt = interval (in hours) between the first and the second count.

Immunofluorescence analyses

Immunofluorescence analysis was conducted on freshly isolated single myofibers, myofibers cultured in suspension in hanging drops, SCs disengaged from fibers but not cloned and SCs cloned with limiting dilutions. Freshly isolated single myofibers were collected in 0.5 ml DMEM, 5% HS in an Eppendorf tube. Fibers and SCs were fixed with 4% paraformaldehyde (PFA; Sigma-Aldrich) in phosphate buffered saline (PBS, GIBCO-Invitrogen), rinsed in PBS and permeabilized with Triton X-100 (Fluka) 0.5% in PBS. After washing, fibers and/or cells were incubated with primary antibodies overnight at 4°C or 1 hour at 37°C. Non specific interactions were blocked with 20% goat serum (Vector). They were then washed and incubated with labeled secondary antibodies for one hour at room temperature. SCs were then mounted with fluorescent mounting medium (DAKO) plus DAPI 100 ng/ml (Sigma-Aldrich). Fibers were collected and moved onto a polilysine microscope slide, and then mounted. Immunofluorescence for Pax7 on isolated single fibers was conducted in order to determine the average number of SCs per fiber. The following primary antibodies were used: mouse anti-rat Pax7 (DSHB, Iowa, dilution 1:50), rabbit anti-rat Myf5 (Santa Cruz, dilution 1:50), rabbit anti-rat MyoD (Santa Cruz, dilution 1:50), rabbit anti-rat desmin (Abcam, dilution 1:50), mouse anti-rat CD45 (Chemicon, dilution 1:50), mouse anti-rat macrophages CD163 (Serotec, dilution 1:50), mouse anti-rat CD31 (Chemicon, dilution 1:50), rabbit anti-rat leptin (Santa Cruz, dilution 1:10), rabbit anti-rat perilipin A (Abcam, dilution 1:500), rabbit anti-rat laminin (Sigma, dilution 1:100). Secondary antibodies used were Alexa Fluor goat anti-mouse 488, Alexa Fluor donkey anti-mouse 594 and Alexa Fluor chicken anti-rabbit 594 (Molecular Probes).

Cell proliferation assay

For the quantification of cell proliferation we used the Click-iT Edu Breakthrough cell proliferation assay (Invitrogen) based on an analogous of bromodeoxiuridine: EdU (5-ethynil-2'-deoxyuridine), according to manufacturer's protocol.

Standard PCR analysis

PCR analysis has been conducted on pools of LPC and HPC, in order to get enough material for the assay. Total ribonucleic acid (RNA) was extracted using a kit (Rneasy Micro, Qiagen), following the supplier's instructions from SCs of both LPC and HPC. All material collected (due to the little number of total cells obtained from a single cloning) was firstly treated with Dnase and removal reagents (Ambion, USA) before being reverse-transcribed using Superscript II reverse transcriptase (Invitrogen).

Real-time PCR

PCR was carried out using a DNA Engine (Opticon 2 Continuous Fluorescence Detection System; MJ Research). Reactions were performed two times with SYBR Green PCR Master Mix (Applied Biosystems) and 5 to 10 ng of cDNA as previously described (Milan et al., 2004). Standard curve was obtained using cDNA derived from LPC and HPC for the MRF MyoD, myogenin and UCP-1. Results were normalized by beta-2-microglobulin mRNA content and reported as arbitrary units ratio.

Imaging mitochondrial membrane potential

For the majority of experiments, we used tetramethyl rhodamine methyl ester (TMRM, 50 nM, Invitrogen) in "redistribution mode" (Duchen et al., 2003): the dye was allowed to equilibrate and was present continuously. TMRM distributes between cellular compartments in response to different potentials and, at concentrations ≤50nM, the fluorescent signal shows a simple relationship with the dye concentration, so that signal intensity maps to mitochondrial potential. TMRM fluorescence intensity was quantified by removing all background signal by "thresholding" and measuring the mean TMRM fluorescence intensity in the pixels containing mitochondria. Thus the signal is independent of mitochondrial mass and only reflects the dye concentration within individual mitochondrial structures. Mitochondrial depolarization is seen as the movement of dye from mitochondria into the cytosol. Experiments were the normalized in response to mitochondrial depolarization by 1μM carbonyl cyanide 4-(trifluoromethoxy)phenylhydrazone (FCCP), which was done at the end of every experiment.

$[Mg^{2+}]_c$ measurement

For measurements of the free cytosolic Mg^{2+} concentration $[Mg^{2+}]_c$ as an index of ATP hydrolysis (since ATP has a higher affinity than ADP for Mg^{2+}), the Mg^{2+} sensitive dye Magnesium Green (5 μg/ml; Molecular Probes) (K_d = 1 mM) was used (Leyssens et al., 1996). Fluorescent images were captured on Zeiss 510 LSM confocal microscope equipped with a 40X oil-immersion lens.

ROS production measurements

Coverslips were transferred to small chambers for microscopy. Cells were imaged while bathing in a modified HBSS solution containing (in mM) 156 NaCl, 3 KCl, 2 MgSO4, 1.25 KH2PO4, 2 CaCl2, 10 glucose, and 10 HEPES, pH adjusted to 7.35 with NaOH. Dihydroethidium (DHE; 10 μM) was added immediately before the start of an experiment and remained in the solution for the duration. Images were obtained using a Zeiss 510 LSM confocal microscope equipped with a 40X oil-immersion lens. Excitation was provided by the 543 line of the helium-neon laser line and emitted fluorescence collected >560 nm. In all experiments using DHE, data were collected every 10 s. The rate of DHE oxidation was compared between LPC and HPC cells. The rate was calculated in every cell in a field of view was analyzed and included in the final measurements.

Oil-red-O staining for lipid droplets

Presence of adipose elements in cell culture was determined by Oil-Red-O staining (Sigma-Aldrich) (Ramirez-Zacarias et al., 1992). The slides were fixed in 10% formalin for 1 hour, washed in deionized water, and air-dried. The cells were incubated with Oil-Red-O staining solution for 15 min, counterstained with Mayer's hematoxylin (pH 4), and rinsed in deionized water.

In vivo experiments

In order to test SCs muscle regeneration potential, a model of muscle damage was tested similarly to what previously described (Hall-Craggs, 1994). Six Sprague-Dawley female rats were injected with 150 μl of bupivacain 0.5% (w/v, with adrenalin 5 g/ml) in both tibialis anterioris (TA) muscles. After 3 days a pool of HPC GFP+ SC clones (20000 cells) and a pool of LPC GFP+ SC clones (20000

cells), counted after trypsinization, were resuspended in 50 μl of DMEM, and injected separately in left and right TA muscles respectively. Animals were left for 3 weeks, then they were sacrificed and TA muscles were collected, fixed in PFA 2% for 1 hour and left in sucrose 30% overnight. The following day muscles were frozen in isopentane cooled in liquid nitrogen, and subsequently processed using a criostate (Leica) to produce 10 μm sections for staining. GFP-positive fibers have been counted for each muscle section, and average number of positive fibers for each of the six animals has been evaluated.

HPC-LPC co-cultures and HPC in LPC conditioned medium

Twenty single HPC were co-cultured with 20 single LPC. Each HPC has been detached with trypsin and seeded on a single LPC. Every experiment has been performed in a single well of 96-well plate (Falcon). Culture of 20 HPC in LPC-conditioned medium has also been performed. LPC-conditioned medium was prepared filtering the supernatant of culture of LPC with 0.22 μm syringe filters (Nalgene) mounted on 2 ml-syringes (Falcon), in order to avoid any LPC-cell contamination in HPC. LPC-conditioned medium was added to HPC very 2 days for all the period of culture (20 days).

Microscope and imaging system

Phase-contrast and hystological analyses were conducted using an inverted microscope (Olympus IX71); immunofluorescence analyses were performed using a direct microscope (Leica B5000). GFP-positive fibers were counted through analysis for GFP epifluorescence.

Statistical analysis

Data are presented as mean ± s.d. Comparison between groups used the t-test assuming two-tailed distribution, with an alpha level of 0.05.

Results

Single fibers isolated by enzymatic digestion and mechanical dissociation from rat FDB muscles were cultured in hanging drops, a technique that has been commonly used for embryonic stem cells culture in order to avoid cell adhesion and promote cell differentiation (Fig 2; see Keller et al., 1995).

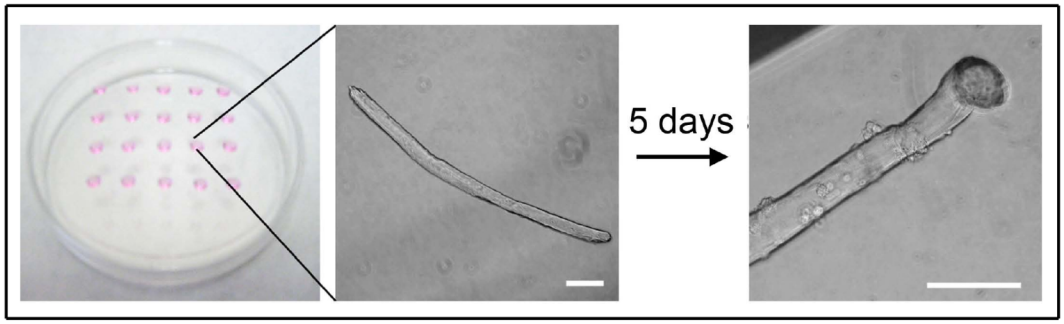

Figure 2. Culture of single fibers in suspension in hanging drops: 20 drops containing a single myofiber each were posed on the lid of a petri dish. It was then turned, in order to perform a suspension culture in hanging drops. On the right, after 5 days SCs emanate from the fiber and clones were easily distinguishable between LPC and HPC.

In order to quantify SCs present in average in FDB single fibers, immunofluorescence for the canonical marker Pax7 was performed in suspension. About 5 SCs were associated to each single FDB muscle fiber (5.0±0.6, n=200 fibers) (Fig. 3 and 4) and underwent rapid activation, revealed by MyoD expression and proliferation in culture.

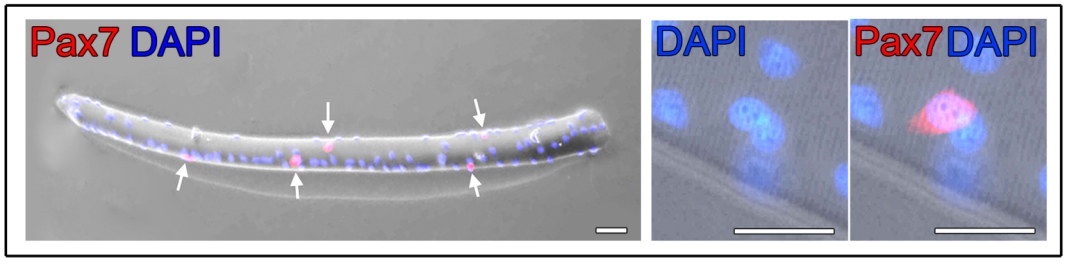

Figure 3. Evaluation of the average number of SCs per single fiber. Isolated FDB single fibers were immunostained with anti-Pax7 antibody and merged with DAPI immediately after isolation, in order to count the SCs (white arrows) per fiber (left; high magnification on the right).

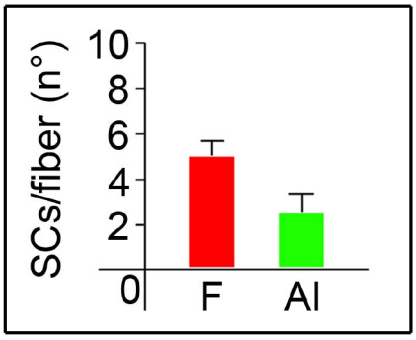

Figure 4. Evaluation of SCs number per isolated single fiber before and after fiber disaggregation: isolated FDB fibers were immunostained for Pax7 and DAPI. SCs were counted in order to evaluate the average amount present per single, isolated fiber (as in Fig. 2). Diagram shows the average amount of SCs on fiber (F column) and after fiber disaggregation and isolation (AI column, mean ± s.d.).

This system of culture is useful, because proliferating SCs do not leave the native fiber, as normally happens when plated onto a rigid substrate, as in normal single fiber cultures (Rosenblatt et al., 1995). SCs remain in their niche under the basal lamina, thus allowing the comparison of different clones arising from each SC. When fibers were maintained in suspension for 5 days, two types of clones were observed on the myofiber surface: low proliferation clones (LPC), containing equal or less than 4 cells, and high proliferation clones (HPC), containing more than 4 cells (Fig. 5). Interestingly, analysis of 70 fibers from 3 different animals revealed that SC clones, identified for the expression of Pax7 and MyoD (Fig. 6), were present in fixed proportion in each fiber: 3.7±0.9 (about 76%) gave rise to LPC, whilst 1.2±0.6 (about 24%) SCs gave rise to HPC (Fig. 1a, bottom right).

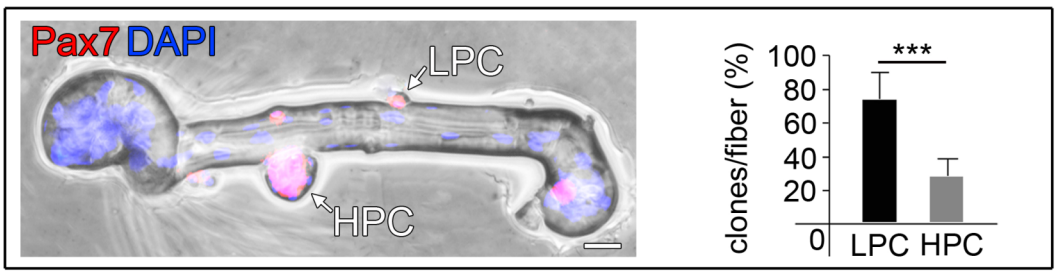

Figure 5. Single fibers were also cultured in suspension for 5 days and SCs were evaluated. LPC and HPC are distinguishable on the fiber (indicated with LPC and HPC). SCs were immunostained with anti-Pax7 antibody and merged with DAPI (bottom left, bar=100 µm). In the diagram percentage of LPC and HPC per single fiber (n=50) is reported (bottom right, mean ± s.d., ***p<0.001).

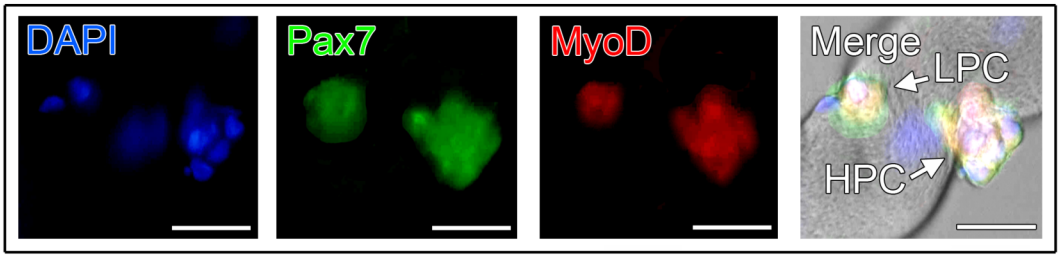

Figure 6. Immunostaining for Pax7 and MyoD, merged with DAPI, was performed on both LPC and HPC on fiber, showing that SCs in both clones are positive for such markers after 5 days in suspension culture (bar=100 µm).

In order to verify that LPC and HPC derived from distinct SC sub-populations, clonal cultures of freshly isolated SCs, mechanically disaggregated from their parental myofibers immediately after isolation, were established. In order to be statistically consistent, more than 500 fibers out of 10 different animals were analyzed. Purity of stripped cells was confirmed performing an immunofluorescence for the canonical markers of quiescent and activated SCs. The results was that 97±1% of stripped cells resulted positive for Pax7, 92±8% for Myf5 and 95±3% for MyoD, immediately after adhesion (4 hours from seeding, 500 cells examined for each marker, 10 random fields evaluated at 10X magnification, 5 different experiments; Fig. 7).

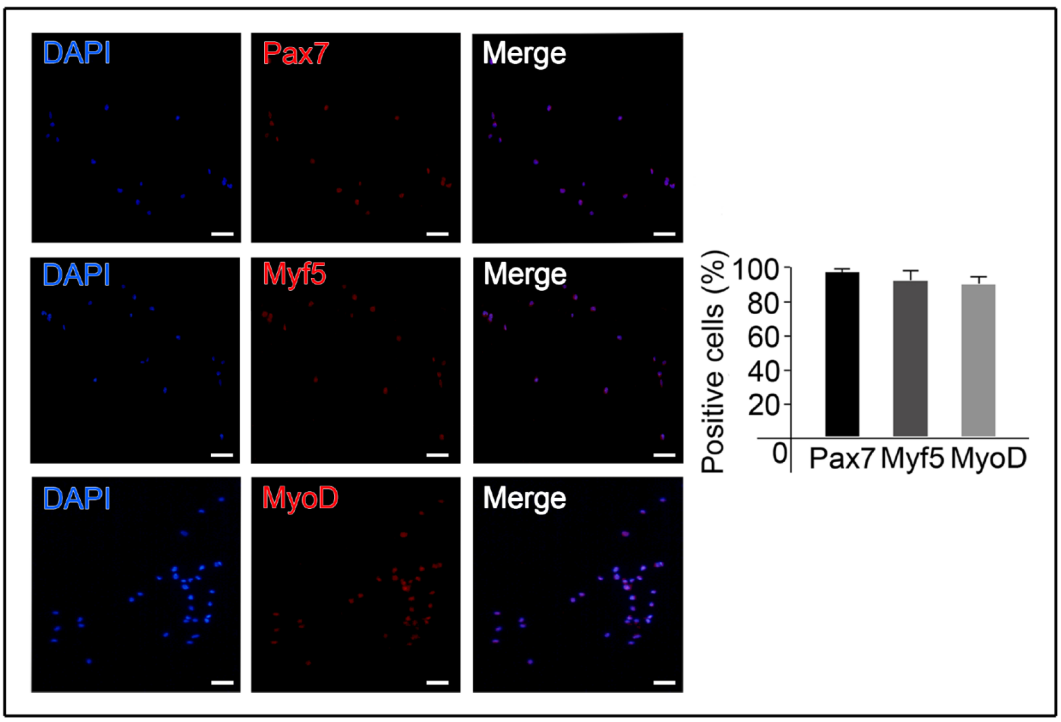

Figure 7. Characterization of freshly isolated SCs. SCs were mechanically dissociated from isolated myofibers and were then seeded on gelatin-coated slides (in order to improve the adhesion). Immunofluorescence for the canonical marker Pax7 and the myogenic markers Myf5 and MyoD were performed. Diagram indicates percentage of positive cells (mean ± s.d.).

In this study of characterization of heterogeneity in a cell population, it was fundamental to exclude from the analyses other contaminant cell types, present in muscle, in order to avoid experimental mistakes. To confirm this, immunofluorescence for the common markers of the non-muscle cells was performed: the absence of CD45 excluded the presence of haematopoietic cells, while no CD163 staining confirmed the absence of macrophages, and CD31 the absence of contaminant endothelial cells (Fig. 8). It was important in particular to exclude the latter, because it has been widely demonstrated in literature that some endothelial cells are endowed of myogenic potential, and are recruited in processes of muscle regeneration.

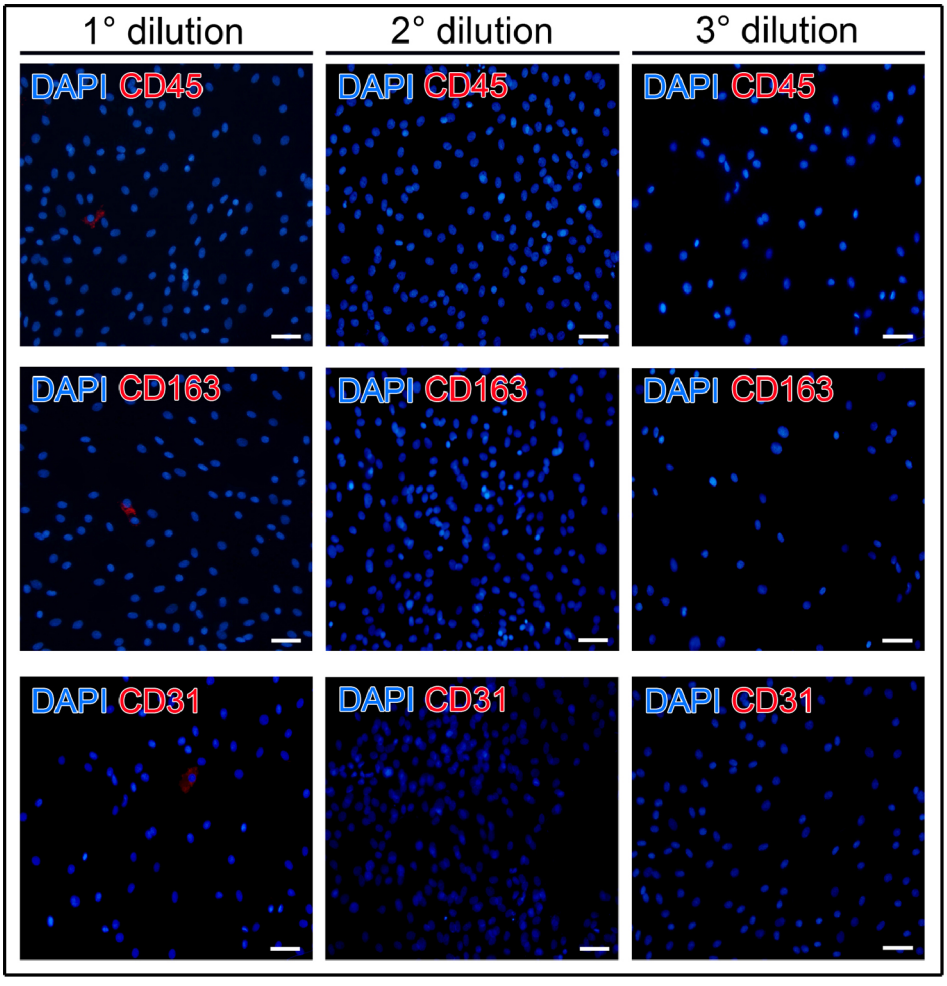

Figure 8. Immunostaining for CD45, CD163 and CD31 on preparations of SCs: freshly isolated SCs were immunostained for haematopoietic cell marker CD45, macrophage marker CD163 and endothelial marker CD31, at each of the 3 passages of dilution (see Materials and Methods). They resulted negative for all contaminant cell markers immediately after the second passage of dilution.

Similarly to what previously reported for other stem cell sources (De Coppi et al., 2007), limiting dilutions in 96-well dishes technique was used to determine SC phenotype at single cell level. Single cell were seeded and left to divide in proliferating medium (Rosenblatt et al., 1995) for 10 days, and examined daily at phase contrast microscope, in order to follow the grow kinetics. After the limiting dilutions, the number of clones obtained from a single fiber was 2.4±0.7: considering that this number is inferior to that of the SCs carried by each single fiber, this further confirms the absence of contaminant cells in the preparation (Fig. 4). By phase-contrast microscopy, SC clones were easily distinguished on the basis of their proliferation rate into LPC (Fig. 9, left) and HPC (Fig. 9, middle), similarly to what observed in single fiber cultures (cells were counted after being stained with haematoxylin, in order to mark nuclei, very useful in particular for HPC). Pax7 and MyoD immunostainings were performed in order to further verify the purity of preparation and to quantify the levels of expression of such markers, that provides information about the balance quiescence/differentiation. These assays were performed after 5 and 10 days of culture (Fig. 9, right).

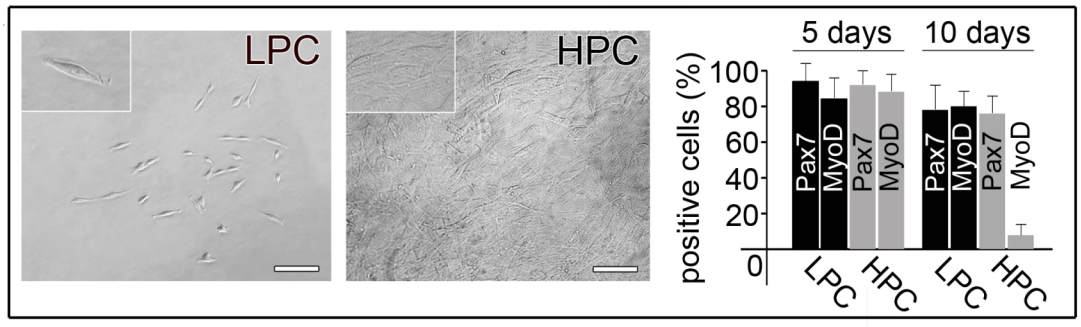

Figure 9. Cloning of freshly isolated SCs through limiting dilutions in 96-well dishes. LPC and HPC are distinguishable after phase-contrast microscope analyses (left, bar=100 μm, insets with higher magnification). In the diagram on the right the % of cells staining positive for Pax7 and MyoD, both in LPC and in HPC, after 5 and 10 days of culture respectively, is reported.

Moreover, the relative proportion of LPC (1.8±0.4; 75%) and HPC (0.6±0.3; 25%) (Fig. 10, left) resemble what we have observed in the cultures of single fibers (compare with Fig. 5). This constitutes the first demonstration that differences between the 2 subpopulations of SCs are not dependent from the niche. After 10 days in culture, 50 to 400 cells (323±201) in LPC and 800 to 3.700 (1.432±903) cells in HPC were present (Fig. 10, center). This was related to a marked difference in the duplication time of LPC and HPC that was 50.4±8 and 18.5±7 hours, respectively. Differences in proliferation were further confirmed by evaluating the amount of EdU (5-ethynyl-2'-deoxyuridine) incorporated by duplicating SCs in an interval of 48 hours. 3±2% of cells in LPC and 29±11% of cells in HPC ($p<0.001$) were in active DNA synthesis (Fig. 10, right).

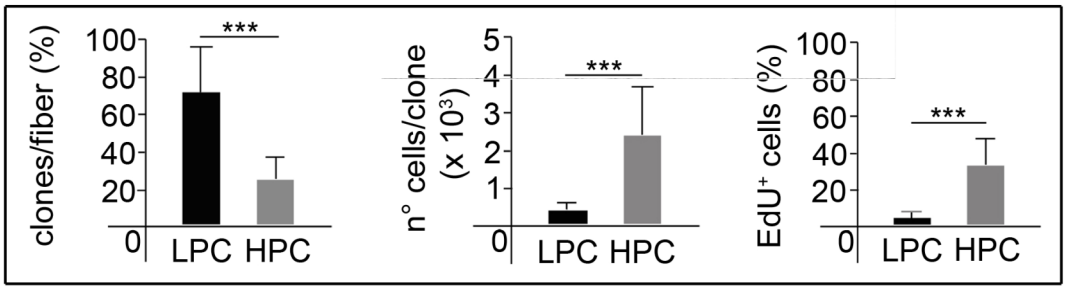

Figure 10. In the diagram on the left, percentage of LPC and HPC derived from cloning of freshly isolated SCs per single fiber, then diagrams showing that average number of cells (center) and percentage of EdU-positive cells in LPC and HPC (mean ± s.d., ***$p<0.001$) (right).

For PCR analyses, various LPC and HPC were pooled, in order to collect enough material compatible to the sensibility of the technique. Standard PCR on LPC and HPC showed that both clones expressed Pax7 and Myf5, while the expression of MyoD was not detectable in HPC at day 10 (Fig. 11, left). At the same time point, quantitative real time PCR analysis showed that expression of MyoD was present, but it was a significantly reduced in HPC (Fig. 11, center), and consequently also myogenin expression was very low (Fig. 11, right).

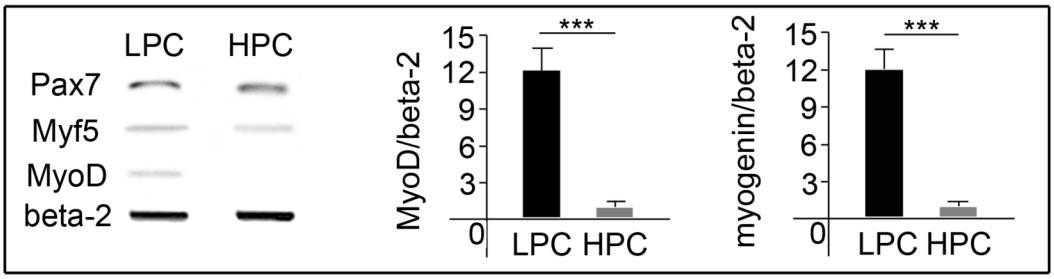

Figure 11. Semiquantitative PCR analysis for myogenic markers Pax7, Myf5 and MyoD (house-keeping gene: beta-2-microglobulin) (left), and real-time PCR analysis for MyoD (center) and myogenin (right) (mean ± s.d., ***p<0.001, normalized against housekeeping gene beta-2-microglobulin) on pools of LPC and HPC.

Finally, HPC were successfully subcloned using serial dilution technique and they were able to generate LPC and HPC, in a proportion comparable to the one obtained in the first clonal generation (82±16% LPC and 18±10% HPC, see Fig. 12).

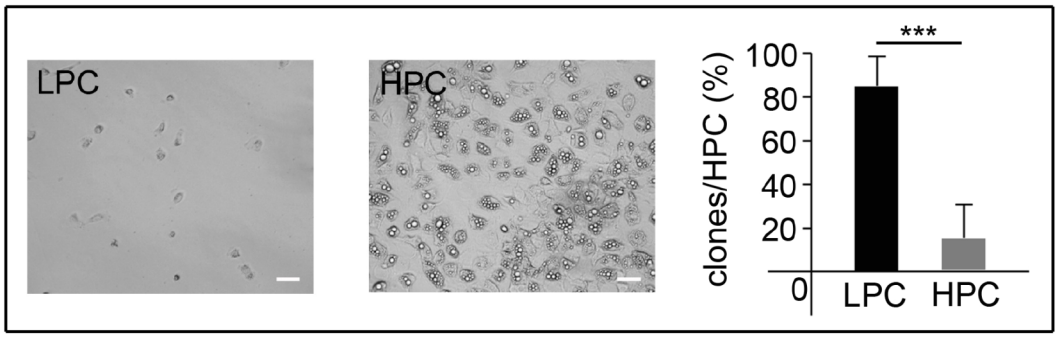

Figure 12. Sub-cloning of HPC: HPC clones (n=10) were sub-cloned in 96-well dishes with limiting dilutions. After 10 days of culture it was possible to distinguish LPC (left) and HPC (center), the latter with adipogenic potential. Their relative proportion was evaluated and reported in diagram (right, mean ± s.d., ***p<0.001). In the table below the developmental potential of each single sub-cloning is reported.

HPC clone (n°)	LPC clones	HPC clones
1	115	0
2	107	0
3	118	7
4	109	11
5	105	13
6	92	23
7	91	25
8	97	28
9	84	36
10	85	39

Heterogeneity of SCs has been extensively described in the last few years. It is believed that SCs, 24h after activation, express Pax7 and MyoD, but then a proportion of them (around 20%) withdraw from cell cycle to return in a quiescent state ($Pax7^+$ $MyoD^-$) that is linked to the maintenance of the SCs pool (Zammit et al., 2002). This SCs proportion is considered to retain a multipotent differentiation potential (Shefer et al., 2004) but it has remained unclear for many years if they represented a distinct population or a dynamic state during SC activation (Cornelison & Wold, 1997). We found that the proportion of SCs able to proliferate at high rate at clonal level (HPC) was around 25% of the total. Noteworthy, this could plausibly be the subset with stem cell characteristics. Similarly to adult stem cells in fact, they rapidly grow in culture when exposed to proper stimuli, as partly showed before (Zammit et al., 2004), and could be clonally expanded in culture (De Coppi et al., 2007) containing high serum.

Intrigued by the differences in proliferation we then investigated whether these two populations of cells might differ also for metabolic markers. Therefore, parameters attributable to the efficiency of mitochondrial function were readily investigated. Assessment of the mitochondrial membrane potential ($\Delta\Psi_m$) with the potentiometric dye tetramethyl rhodamine methyl ester (TMRM) showed that

LPC have reduced $\Delta\Psi_m$ than HPC cells (Fig. 13), suggesting that differences in the coupling of the mitochondrial F_1Fo-ATPsynthase are likely to occur. Thus, resting $\Delta\Psi_m$ may be a short-hand for protons motive force throughout the Electron Respiratory Chain (ERC) hence a direct function of the F_1Fo-ATPsynthase in intact cells (Campanella et al., 2008; Campanella et al., 2009) whereas an increased H^+ flux through the F_1Fo-ATP synthase reduces the $\Delta\Psi_m$ and conversely a reduced H^+ flux increases it.

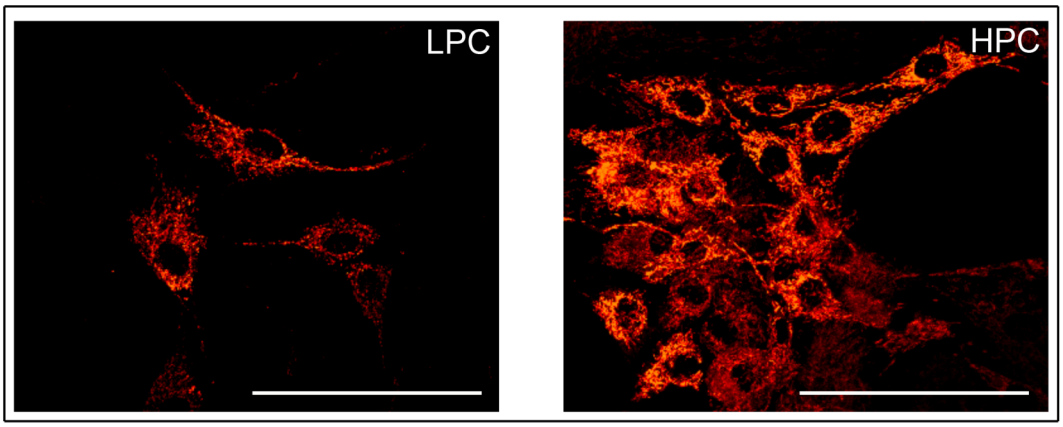

Figure 13. Confocal images showing TMRM fluorescence as measurement of mitochondrial potential ($\Delta\psi_m$). LPC (left) shows, in this culture condition, a lower $\Delta\psi_m$ compared to HPC (right).

To confirm that, clones were subsequently exposed to 2.5 µg/µl oligomycin, a selective inhibitor of the F_1Fo-ATP synthase activity and the $\Delta\Psi_m$ monitored over time. As a result of an active respiration, the continued efflux of protons increased $\Delta\Psi_m$ (Fig. 14, left) and this increase was more sustained in LPC than in HPC although both clones eventually reach a final state that normalizes the initial differences (control conditions, LPC: 1121.68±118.95 and HPC: 1595.52±184.18 arbitrary units; after Oligomycin, LPC: 2735.95±499.28 and HPC: 2349.95±224.53 arbitrary units; ***$p<0.001$, n=7 distinct cultures) (Fig. 14, right).

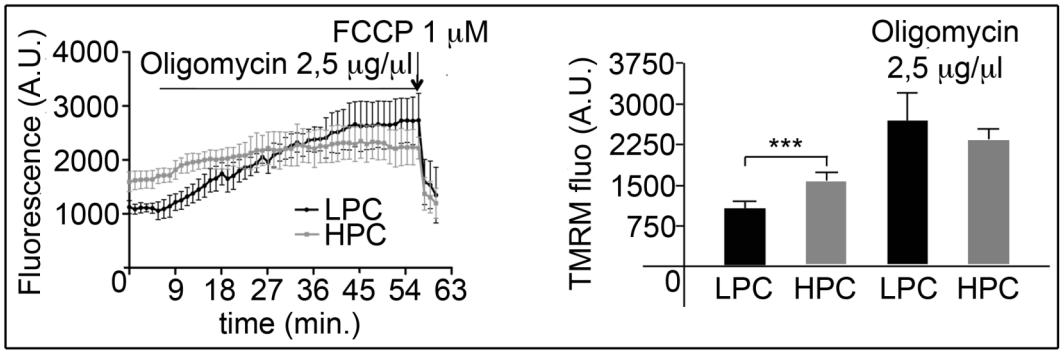

Figure 14. $\Delta\psi_m$ was measured in real time in LPC and HPC using TMRM fluorescence and confocal imaging. Cells were treated with oligomycin (2.5 μg/μl) to block the F_O component of the F_1F_O-ATPasynthase. 1 μM FCCP was added at the end of each experiment to completely depolarize the mitochondria. Diagram on the left shows the trend over time. Values derived from 21 individual cells before and after oligomycin addition for LPC and HPC are summarized in diagram on the right (***p<0.001).

If this interpretation is correct, the ATP generated from mitochondrial oxidative phosphorylation (OXPHOS) should be the main source of energy in LPC and since these cells could not be transfected with intracellular targeted luciferase (Jouaville et al., 1999) (data not shown) to gain a discrete measurement of ATP dynamics, we quantified the concentration of free magnesium $[Mg^{2+}]_c$ as alternative read-out of ATP fluxes (see Materials and Methods; Leyssens et al., 1996). Oligomycin was also employed in this experiment to block the F_1Fo-ATPsynthase and monitoring the decay of ATP (corresponding to a rise in $[Mg^{2+}]_c$) in both LPC and HPC. Consistently, the ATP level dropped quite instantly in LPC whilst in HPC a visible effect took over ~60 minutes to occur (Fig. 15, left). The kinetic of $[Mg^{2+}]_c$ was then calculated and plotted as histogram (Fig. 15, right) (LPC: 1.42±0.49 and HPC: 0.42 ±0.07 arbitrary units, ***p<0.001, n=3 different cultures).

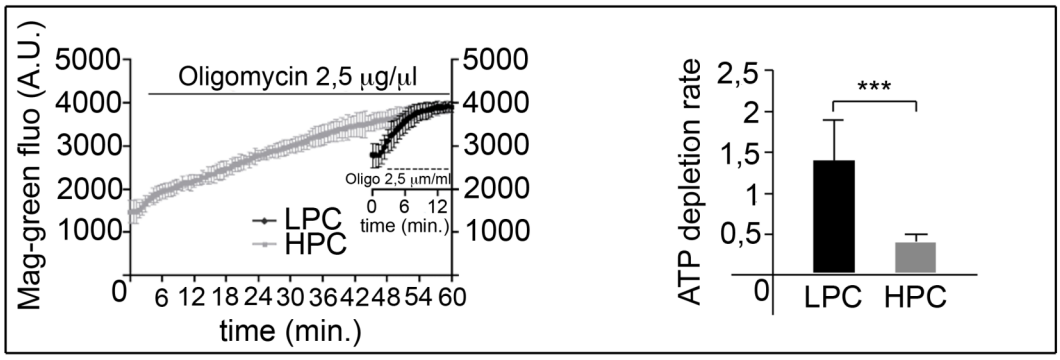

Figure 15. Cellular ATP was followed in real time by measuring intracellular $[Mg^{2+}]_c$ using the fluorescent dye Magnesium Green (Mag-green). LPC and HPC were treated with oligomycin (2.5 μg/μl) and (left) traces trend monitored over time (traces are mean ± s.d. of 10 individual experiments for cell type); plotted values of $[Mg^{2+}]_c$ rate (mean ± s.d.) is presented in diagram on the right (***$p<0.001$).

These data suggest that HPC metabolism seems to be more glycolytic than that of the LPC in which mitochondria appear more coupled and act as the principal source of intracellular energy. Glycolysis is a feature of every highly proliferative cell (e.g. cancer cells) (Zhivotovski & Orrenius, 2009) and also contributed by alterations in fundamental signalling mechanisms the most representative of which is Reactive Oxygen Species (ROS) generation (Pelicano et al., 2008), which we have therefore evaluated (Aguiari et al., 2008). This was done using the fluorescent probe dihydroethidium (DHE) which forms a fluorescent product (ethidium) when oxidised allowing a real time detection of basal generation of ROS (Bindokas et al., 1996). The traces reported in Fig. 16 show that in HPC the DHE oxidation is significantly faster than in LPC indicating that the HPC have an increased rate of ROS generation at resting conditions. Values summarized in panel d right (LPC: 1.13±0.41 and HPC: 2.92±0.87; rates from normalized arbitrary units, **$p<0.01$, n=2 different cultures) confirm that cellular ROS are more prominent in HPC than LPC, consistent data with the findings on $\Delta\Psi_m$ and ATP.

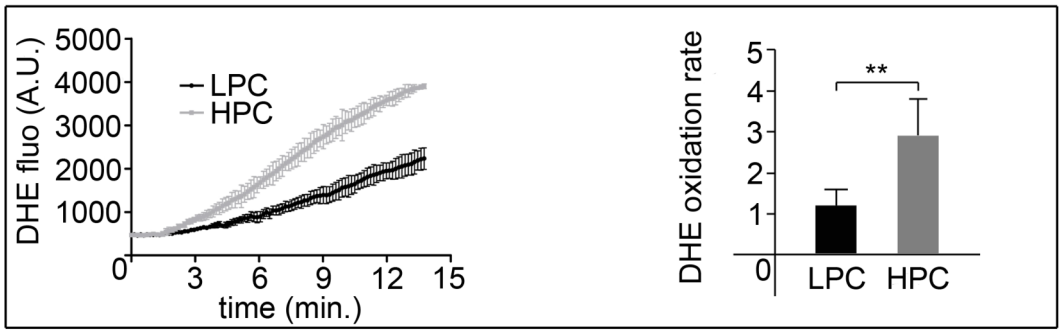

Figure 16. ROS production was measured using 5 μg/ml dihydroethidium (DHE). Diagram on the left shows an increase in DHE fluorescence in LPC and HPC recorded in real time and diagram on the right the rate values (mean ± SD) of three different experiments are summarized (**p<0.01).

In order to reproduce what was performed on single fibers in hanging drops, I tried to evaluate if there were some characteristic metabolic patterns that could reveal differences in the whole popolation of freshly isolated SCs, immediately after seeding. I found that after loading of cells with the potentiometric dye tetramethyl rhodamine methyl ester (TMRM), heterogeneity concerning mitochondrial membrane potential ($\Delta\Psi_m$) was present, and, more interestingly, it allowed to distinguish 2 different subpopulations. First of all, a threshold was evident in the values of TMRM fluorescence intensity, that allowed to distinguish low TMRM uptake cells (812±398 a. u.) and high TMRM uptake cells (2043±362 a.u.). On this basis the proportion of low TMRM uptake cells has been calculated in 78.2±9.8% and that of high TMRM uptake cells in 21.8±9.6%: this resembles the relative quantities calculated in the other experiments, and seems to indicate that SCs are distinguishable from the beginning for bioenergetic patterns (Fig. 17).

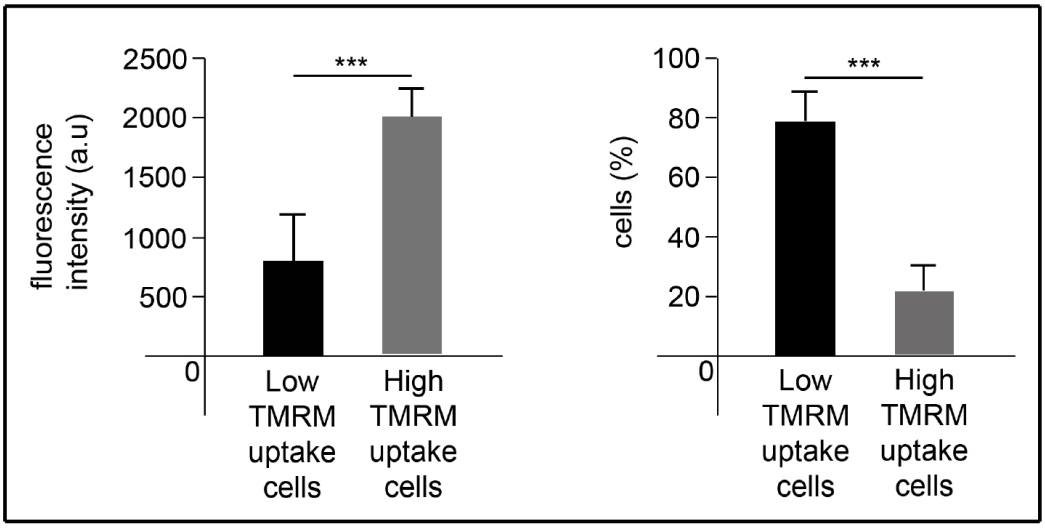

Figure 17. Measurement of mitochondrial membrane potential ($\Delta\Psi_m$) on freshly isolated SCs, immediately after adhesion. The diagram on the left shows that there was a threshold in fluorescence intensity (a.u.=arbitrary units), that allowed to divide SCs on the basis of low or high TMRM uptake. Diagram on the right shows the relative proportions of SCs distinguished on the basis of the TMRM uptake.

Once dissociated from their parental myofibers, LPC and HPC SCs revealed also a distinct differentiation potential. When cultured in myogenic medium, LPC exhibited a normal myogenic differentiation with formation of abundant myotubes (Fig. 18, top) expressing desmin (Fig. 18, bottom).

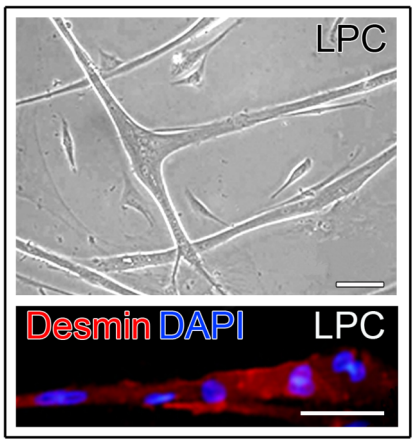

Figure 18. Spontaneous differentiation potential of LPC and HPC in high serum medium: LPC give rise to mature myotubes (top), as visible through phase contrast microscopy, that were positively immunostained for desmin (bottom, bar=100 μm).

Instead, in the same culture conditions, HPC spontaneously formed a large number of multi- and paucilocular adipocytes (Fig. 19, top left) while generating

only rare myotubes (Fig. 19, bottom left). Adipogenic differentiation was documented through characteristic assays: first of all they were stained with Oil-Red-O dye for lipid droplets (Fig. 19, top center), then perilipin, an adipocyte-specific protein coating lipid droplets was stained through immunofluorescence (Fig. 19, top right). In addition, 97±2.8% cells in HPC were positive for leptin, also before differentiation in preadipocytes (Fig. 19, bottom center), whereas LPC cells were all negative. Mitochondrial uncoupler protein 1 (UCP-1), a marker of brown adipose tissue (BAT), was not detected by quantitative real time PCR in either LPC or HPC (Fig. 19, bottom right).

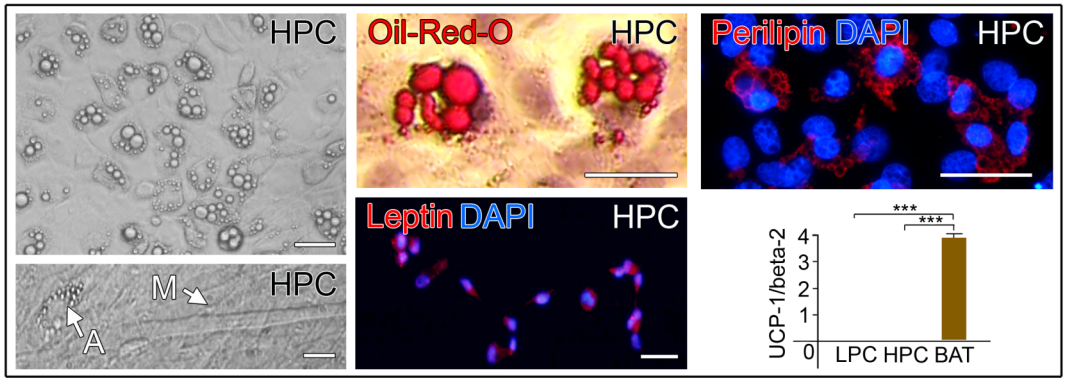

Figure 19. HPC give spontaneously rise to adipocytes, well visible through phase contrast microscopy (top left), and a small amount of myotubes (bottom left). Lipid droplets are marked through Oil-Red-O staining (top center) and immunostaining for perilipin (top right) (bar=100 µm). Immunostaining for leptin on HPC (bottom center). Real-time PCR for mitochondrial uncoupler protein UCP-1 on LPC and HPC, compared with brown adipose tissue (BAT) (***p<0.001; bottom right).

Previous studies have demonstrated that SCs can give rise to adipocytes, osteocytes and smooth-muscle cells, other than myotubes, if cultured in conditioned media containing tissue-specific differentiation factors (De Coppi et al., 2006b; Singh et al., 2007). This was believed to be a stochastic phenomenon driven by the MAD pathway (Shefer et al., 2004). Interestingly, this property seems to be confined to a fixed proportion of SCs, defined HPC as demonstrated by leptin and perilipin expression and Oil-Red-O staining. Whilst Oil-Red-O is not strictly specific for adipose cells (Kinkel et al., 2004), leptin and perilipin expression cannot be found in myogenic cells. Moreover, the type of adipose tissue that was produced from SCs transdifferentiation was investigated: differently to what previously demonstrated (Seale et al., 2008), the lipid droplets

inside the cytoplasm tended to fuse giving rise to unilocular cells with the morphological features of the white fat cell. This was in accordance with the absence of UCP-1 expression in the adipocytes formed by HPCs in these set of experiments as well as in previous studies carried out using both rodents and human SCs (Asakura et al., 2001; De Coppi et al., 2006b). Therefore, we believe that the adipogenic potential of SCs at clonal level is limited to a precise proportion of cells that is represented by a subset of those that downregulate MyoD after activation and retain great proliferative potential. Further studies however will be necessary to finally elucidate the fate of adipocytes derived from SCs. In this perspective, one limitation of our study was related to the fact that SCs were derived from one single muscle, but this choice was necessary to avoid the well described intermuscular variability (Shinin et al., 2006).

In order to investigate whether the remarkable differences of LPC and HPC cells *in vitro* were maintained *in vivo*, pools of 20.000 LPC cells or 20.000 HPC cells, derived from GFP-transgenic rats, were injected separately in regenerating wild-type rat muscles. To induce muscle regeneration, rat *tibialis anterioris* muscles were treated with bupivacaine (which causes muscle fiber necrosis followed by regeneration), injected with the cells 72 hours later and examined after 3 weeks. The contribution of donor cells to myonuclei, determined by the number of GFP positive fibers, was different between LPC and HPC. In particular, the number of GFP^+ muscle fibers was much higher in muscles injected with LPC cells (273±46 per section) than in muscles injected with HPC cells (52±12 per section) (Fig. 20).

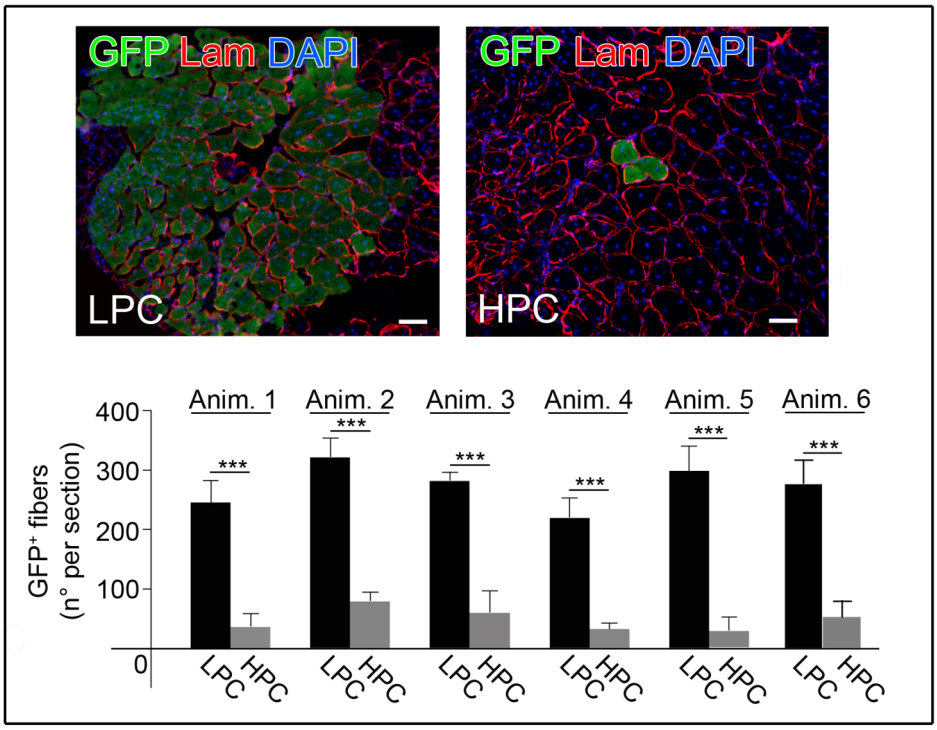

Figure 20. Epifluorescence analysis for GFP and immunostaining for laminin on muscle sections injected with LPC (left) and HPC (center). On the right is reported a diagram indicating for each of six animals treated the amount of GFP^+ fibers per section of muscle injected with LPC and HPC (mean ± s.d.,***$p<0.001$).

The engraftment of the implanted cells in SC niche has been also analized. Differently from the other experiment, there was no significative difference between LPC and HPC in contributing to SC pool. This has been determined both through co-staining between SC marker Pax7 and GFP, and analysing if the GFP^+ cells were in the canonical position of SCs under the basal lamina of myofibers, that was immunostained as well (Fig. 21).

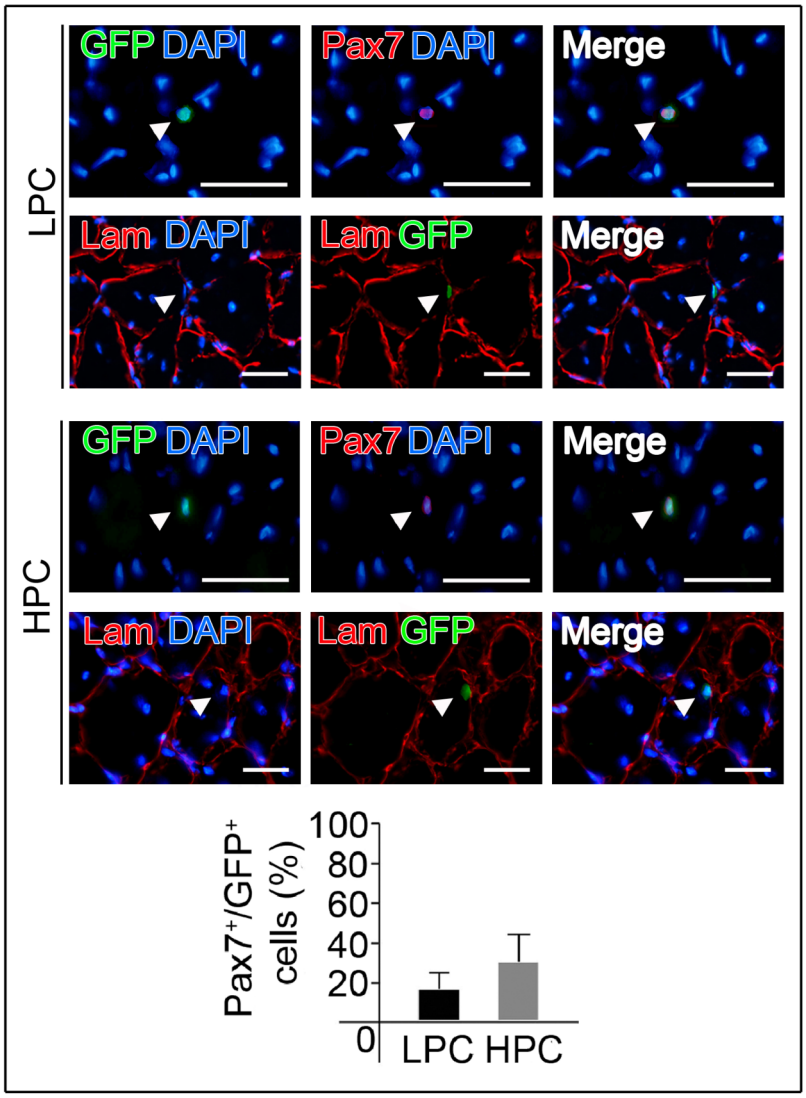

Figure 21. Immunofluorescence analysis for Pax7 and epifluorescence for GFP, merged with DAPI on sections of muscles treated with LPC (top panel, up) and HPC (middle panel, up). Epifluorescence for GFP and immunostaining for laminin, merged with DAPI, on sections of muscles treated with LPC (top panel, down) and HPC (middle panel, down) (bar=100 μm). When the number of $Pax7^{+}/GFP^{+}$ cells was evaluated after LPC and HPC injection we could not observe any significant difference as reported in the diagram (bottom, mean ± s.d.).

This could be due to the fact that HPC, which are less committed to myogenic lineages and subjected to high self-renewal, have more chance *in vivo* to engraft in the SC cell niche and could require longer or another cycle of muscle damage to act in myofibers formation. These results are in accordance to what previously reported about the potential of slow-cycling cells *in vitro* that showed a great proliferative potential *in vivo* (Beauchamp et al., 2000) and have been suggested also by the recent demonstration of a subset of satellite-side population cells

which *in vivo* preferentially contribute to the SC niche (Tanaka et al., 2009). Interestingly, in our setting the number of $Pax7^{+}GFP^{+}$ cells did not vary among the 2 different groups (Fig. 21, bottom). All these data together seem to indicate that while LPC may represent a transplantable population of committed progenitors, both LPC and HPC are functional to maintain SC niche. In our view this validates once more the high contribution to both muscle regeneration and self-renewal observed when different populations of SCs are transplanted either with their fiber (Collins et al., 2005) or as freshly isolated cells (Rossi et al., 2010).

An interesting point is that fat deposition within muscle tissue is not present in physiological conditions and adipocytes are rarely seen in standard SC cultures, suggesting that the propensity of HPC cells to undergo adipogenic differentiation is normally repressed and revealed only when HPC SCs are cultured in isolation. To determine whether this repression is influenced by the presence of LPC cells, we designed an experiment in which SCs clones derived from GFP-transgenic and wild type rats were co-cultured. Specifically, we added GFP^{+}-HPC to wild-type LPC or wild-type HPC to GFP^{+}-LPC, in an average proportion (HPC/LPC) of 26,5 (Fig. 22).

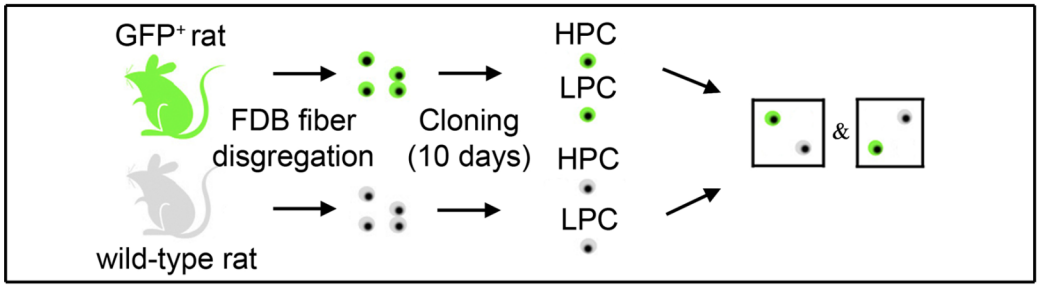

Figure 22. Scheme for co-cultures: SCs were derived from FDB muscles of both wild-type and GFP^{+} rats then cloned through limiting dilutions and after 10 days of culture HPC were seeded on LPC.

Under these conditions, none of the HPC observed gave rise to adipocytes, as determined by phase contrast microscopy, Oil-Red-O staining and immunostaining for perilipin and leptin. Instead, we observed an increased tendency of HPC to fuse and differentiate into myotubes (Fig. 23, top left). In particular, 20 days after culture 80±9 GFP^{+} myotubes were observed when GFP^{+}-HPC were co-cultured with LPC, compared to 3±1 myotubes formed when the

same number of HPC were clonally cultured for the same time (Fig. 23, top middle). The switch from adipogenic to myogenic program was not only induced by fusion of HPC with LPC cells, since also mononucleated HPC cells showed enhanced MyoD expression in the co-cultures. While only 4±2% of HPC cells expressed MyoD in control conditions, MyoD was present in 73±14% of HPC cells after 20 days in co-culture with LPC (Fig. 23, top right and bottom).

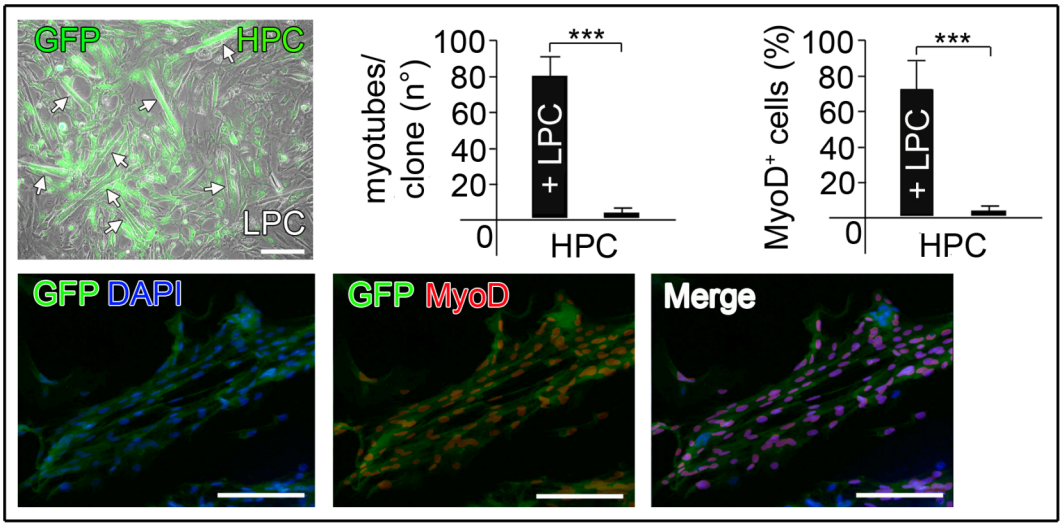

Figure 23. Increase in myotube formation derived from HPC. Epifluorescence for GFP^+ myotubes (indicated with white arrows, central panel left, bar=100 μm), and diagrams indicating number of myotubes per clone (central panel, center) and percentage of $MyoD^+$ cells (central panel, right) in co-cultures, compared to control HPC (mean values ± s.d., ***$p<0.001$). Immunostaining for MyoD and epifluorescence for GFP, merged with DAPI on co-cultures (bottom panel, bar=100 μm).

Similarly, when HPC were cultured in LPC-conditioned medium (Fig. 24) a much greater number of myotubes (43±8 vs. 3±1) was formed, and the expression of MyoD was present in 58±7% of HPC cells (Fig. 24, middle and bottom).

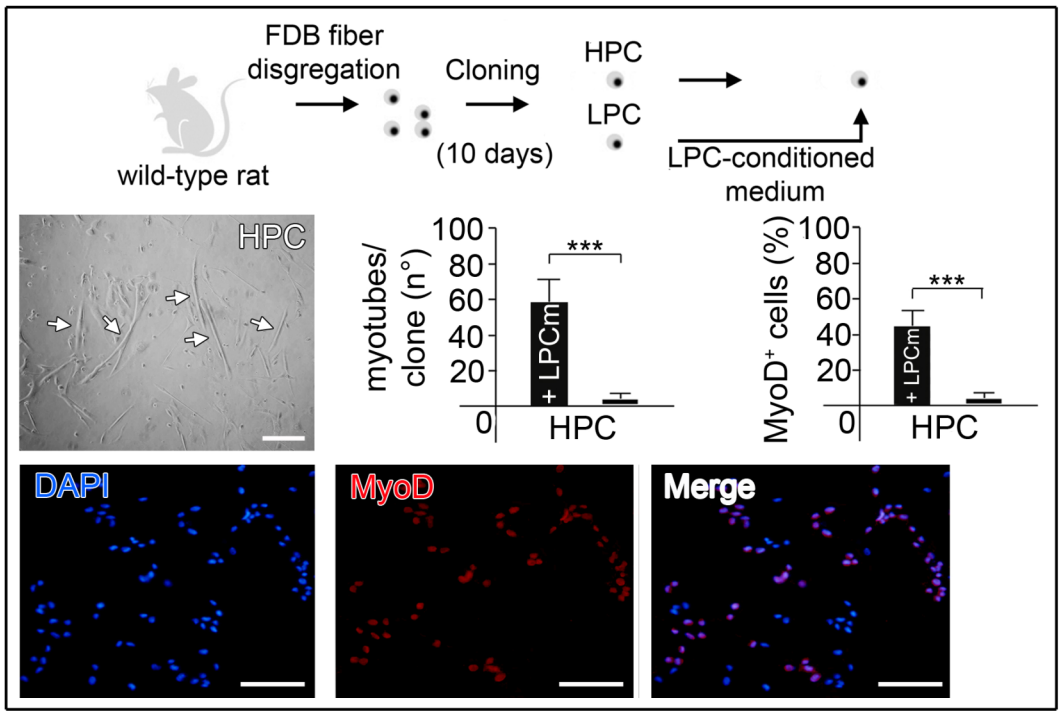

Figure 24. Scheme for culture in conditioned medium: SCs were derived from FDB muscles of wild-type rats then cloned through limiting dilutions. After 10 days of culture LPC-conditioned medium was transferred on HPC (top panel). Myotube formation (indicated with white arrows, central panel left, bar=100 μm), and diagrams indicating number of myotubes per clone (center) and percentage of $MyoD^+$ cells (right) in cultures with LPC-conditioned medium, compared to control HPC (mean values ± s.d., ***$p<0.001$; middle panel). Immunostaining for MyoD on HPC cells, subjected to LPC-conditioned medium, merged with DAPI (bottom panel, bar=100 μm).

While in physiological conditions, healthy muscle does not present intramuscular adipose tissue (IMAT), this is rather common in pathological conditions as in familiar partial lipodystrophy, obesity, type-2 diabetes and the metabolic syndrome (Gallagher et al., 2009). IMAT can be present in conditions characterized by an increase in muscle mass, such as in acromegaly, but it is particularly evident in conditions characterized by a primary decrease in the muscle mass as in myopaties, aging (Hilton et al., 2008), and sedentary young subjects. These changes in the regional body composition with an increase in the adipose tissue within muscle might also affect insulin sensitivity, glucose and lipid metabolism thus mimicking the normal-weight "metabolically obese" syndrome (Gauthier et al., 2008). In my experiments, SCs were derived from young healthy rats and it was unexpected to find such high proportion of cells that

in myogenic conditions were able to spontaneously generate mature adipocytes (Fig. 19). This phenomenon is originated only by a defined clonally expandable population of cells, namely HPC. By these means, we demonstrate that this regulation may also dependent on a cross-talk among distinct progenitors within the SC population similarly to what happens in other systems (Diamond, 1982).

Discussion

SCs and their heterogeneity have been widely investigated and various reports already described differences in their proliferative and myogenic potentials (Rantanen et al., 1995; Schultz, 1996; Molnar et al., 1996). Here, I confirmed such differences and showed for the first time that in rat myofibers there is a correlation between SCs proliferation and differentiation potential similarly to that previously reported for other stem cells. Using an innovative technique for single muscle fiber culture in suspension, adapted from embryoid-bodies cultures (Keller, 1995) I observed that not only SCs proliferate at different rates (McKenzie et al., 2006) but also that the ratio between clones with high (HPC) and low (LPC) proliferative rate was fixed at single fiber level. Moreover, after mechanical dissociation and cloning through limiting dilution, it was still possible to distinguish an identical ratio of LPC and HPC. Notably, differences in proliferation mirror differences in functional parameters such as mitochondrial membrane potential ($\Delta\Psi_m$), ATP balance and ROS generation. HPC compared to the LPC proved to have a more glycolytic phenotype characterized by increased $\Delta\Psi_m$, reduced mitochondrial generation of ATP and higher rate of ROS production. Abnormal rising of the $\Delta\Psi_m$ at resting conditions defines impairments in the H^+ transport through the Electron Respiratory Chain (ERC) thus acting as a parameter to assess mitochondrial activity (Campanella et al., 2008). Since this is normalized via pharmacological inhibition of the terminal enzyme of the ERC (the F_1Fo-ATPsynthase) (see Fig. 14), the oxidative phosphorylation of the HPC can be considered underperforming compared to that of the LPC. Therefore, the mitochondrial ATP generation is also reduced and addition of oligomycin able to promote a mild reduction of intracellular ATP in HPC compared to LPC (Fig. 15). Alternative efficiency of the mitochondrial coupling was not the only distinctive feature between the two populations since HPC presented also a remarkable higher level of ROS production compared to LPC. ROS is a signal associated to cell differentiation into adipocytes (Aguiari et al., 2008) and HPC which spontaneously differentiate into adipocytes (Fig. 19) show plausibly for this reason an increased rate of basal ROS production.

Taken these evidences together it may envisage that modifications in cell metabolism precede and possibly dictate the nature of the ultimate cellular differentiation. It has been already shown, although in alternative models, how environmental and nutritional conditions impinging on the animal metabolism may affect the number and the growth of muscle fibers (Maltby et al., 2004; Hammond et al., 2007), thus providing evidences for a bond between metabolism and quality of the muscle progenitors. The link between mitochondrial metabolism and stem cells has been previously proposed but an accurate evaluation of its entity and biological significance never performed despite its potential acknowledged (see Nesti et al., 2007 and references within). Here, we demonstrate that before the myogenic or adipogenic markers could be detectable, cells undergo remarkable modifications in their mitochondrial function. Future studies are needed to explore the real nature of these homeostatic modifications, however, to the best of our knowledge this as the entire clonal characterization here presented has never been described before and strongly suggests that proliferation and differentiation may be pre-determined and not stochastically activated among SCs (Shefer et al., 2004) whereas the metabolic features may act as early biological read-outs.

These innovative results pair with recent studies that described the presence of subsets of cells with stem cells characteristics within the SC compartment. HPC in fact fulfill the definition of multipotent stem cells, meaning they can retain their capacity to differentiate in alternative cell types although deriving from the same embryonic compartment (Jahagirdar & Verfaillie, 2005). Similarly to SP-satellite cells (Tanaka et al., 2009), skeletal muscle precursors-SMP (Cerletti et al., 2008) and muscle stem cells-MuSC (Sacco et al., 2008), HPC can contribute *in vivo* to the SC pool when injected after injury and may divide asymmetrically to produce LPC. However, in our experimental setting HPC, differently to SP-satellite cell, SMP and MuSC, are poorly myogenic when cultured clonally. Noteworthy, their myogenic potential is boosted when cultured in contact with conditioned LPC-media. When co-cultured together, distinguishing one or the other clone type *via* GFP expression, LPC were able to condition HPC and block their adipogenic conversion alongside an increase in the MyoD expression and myotubes formation. I verified that this conditioning was not due to cell-cell contact, but plausibly to released factors since the effects were obtained after 10 days of HPC

culture in LPC conditioned medium (Fig. 24). Further studies however are necessary to define which soluble factors (myokine) and signaling pathways are involved in such cross-talk. If it will be confirmed that HPC represent a source of adipogenic tissue within the skeletal muscle in pathological conditions, the ability of controlling their fate could lead to important implications for therapy. However, while this study deeply investigated *in vitro* the characteristics of LPC and HPC their physiological role *in vivo* remains partially unknown.

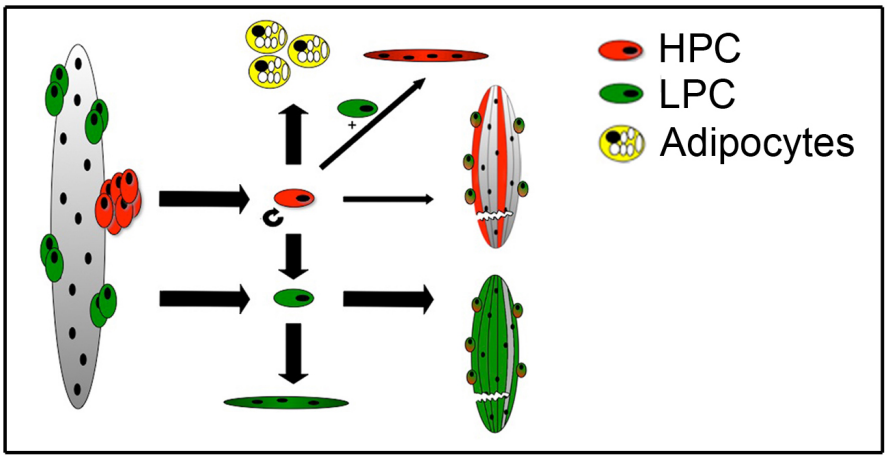

Figure 25. Cartoon of the current working model: pools of Satellite Cells can be isolated from the muscle fiber and cultured in vitro preserving their original diversities. HPC spontaneously differentiate into adipocytes whilst LPC into myoblasts. Notably, HPC may undergo myogenic pathway if cultured together with LPC. LPC and HPC in vitro diversities mirror differences in the capacity of regenerating damaged muscles tissues.

By these means, I was able to characterize an intrinsic potential of SCs able to give rise to high and low proliferative clones. The high proliferative spontaneously differentiated to adipocytes but they could still be conditioned towards a massive myogenic differentiation if co-cultured with LPC (Fig. 25). This is an insightful notion suggesting that a paracrine effect might occur and it would explain why spontaneous adipogenic generation/differentiation is not present in healthy muscles. Although future work is essential to understand the molecular factors conditioning the “choice” of SCs between LPC and HPC as well as the cross-talk existing between these two subpopulations, this study offers novel insights towards a new level of understanding of muscle regeneration, definition and prevention of fat deposition within the skeletal muscle.

REFERENCES

- Aguiari P, Leo S, Zavan B, Vindigni V, Rimessi A, Bianchi K, Franzin C, Cortivo R, Rossato M, Vettor R, Abatangelo G, Pozzan T, Pinton P & Rizzuto R. High glucose induces adipogenic differentiation of muscle-derived stem cells. *Proc Natl Acad Sci USA.* 105; 1226-1231 (2008)

- Appell HJ, Forsberg S & Hollmann W. Satellite cells activation in human skeletal muscle after training: evidence for muscle fiber neoformation. *Int J Sports Med.* 9; 297-299 (1988)

- Armand O, Boutineau AM, Mauger A, Pautou MP & Kieny M. Origin of satellite cells in avian skeletal muscle. *Arch Anat Microsc Morphol Exp.* 72(2); 163-181 (1983)

. Asakura A, Komaki M & Rudnicki M. Muscle satellite cells are multipotential stem cells that exhibit myogenic, osteogenic, and adipogenic differentiation. *Differentiation.* 68; 245-253 (2001)

- Austin L, Bower J, Kurek J & Vakakis N. Effects of leukaemia inhibitory factor and other cytokines on murine and human myoblast proliferation. *J Neurol Sci.* 112; 185-191 (1992)

- Bach AD, Stern-Straeter J, Beier JP, Bannasch H & Stark JB. Engineering of muscle tissue. *Clin Plast Surg.* 30; 589-599 (2003)

- Bach AD, Beier JP, Stern- Straeter J, Horch RE. Skeletal muscle tissue engineering. *J Cell Mol Med.* 8(4); 413-422 (2004)

- Barker N, van Es JH, Kuipers J, Kujala P, van den Born M, Cozijnsen M, Haegebarth A, Korving J, Begthel H, Peters PJ & Clevers H. Identification of stem cells in small intestine and colon by marker gene Lgr5. *Nature.* 449; 1003-1007 (2007)

- Barr E & Leiden JM. Systemic delivery of recombinant proteins by genetically modified myoblasts. *Science.* 254; 1507-1509 (1991)

- Beauchamp JR, Heslop L, Yu DS, Tajbakhsh S, Kelly RG, Wernig A, Buckingham ME, Partridge TA & Zammit PS. Expression of CD34 and Myf5 defines the majority of quiescent adult skeletal muscle satellite cells. *J Cell Biol.* 151; 1221-1234 (2000)

- Bindokas VP, Jordan J, Lee CC, Miller RJ. Superoxide production in rat hippocampal neurons: selective imaging with hydroethidine. *J Neurosci*. 16: 1324-1336 (1996)

- Bischoff R & Holtzer H. Inhibition of myoblast fusion after one round of DNA synthesis in 5-bromodeoxyuridine. *J Cell Biol.* 44; 134-150 (1970)

- Bischoff R. Interaction between satellite cells and skeletal muscle fibers. *Development* 109(4); 943-952 (1990)

- Bischoff R. The satellite cell and muscle regeneration. *In: Myogenesis, Mc Graw-Hill, New York.* 97-118 (1994)

- Bischoff R & Heintz C. Enhancement of skeletal muscle regeneration. *Dev Dyn.* 201; 41-54 (1994)

- Bittner RE, Schofer C, Weipoltshammer K, Ivanova S, Hauser E, Freilinger M, Hoger A, Elbe-Burger A & Wachtler F. Recruitment of bone-marrow-derived cells by skeletal and cardiac muscle in adult dystrophic mdx mice. *Anat Embryol.* 199; 391-396 (1999)

- Blaauw B, Mammucari C, Toniolo L, Agatea L, Abraham R, Sandri M, Reggiani C & Schiaffino S. Akt activation prevents the force drop induced by eccentric contractions in dystrophin-deficient skeletal muscle. *Hum Mol Genet.* 17(23); 3686-3696 (2008)

- Boldrin L, Elvassore N, Malerba A, Flaibani M, Cimetta E, Piccoli M, Baroni MD, Gazzola MV, Messina C, Gamba P, Vitiello L & De Coppi P. Satellite cells delivered by micro-patterned scaffolds: a new strategy for cell transplantation in muscle diseases. *Tissue Eng.* 13(2); 253-262 (2007)

- Bonassar LJ & Vacanti CA. Tissue engineering: the first decade and beyond. *J Cell Biochem Suppl.* 30; 297-303 (1998)

- Borselli C, Storrie H, Benesch-Lee F, Shvartsman D, Cezar C, Lichtman JW, Vandenburgh HH & Mooney DJ. Functional muscle regeneration with combined delivery of angiogenesis and myogenesis factors. *Proc Natl Acad Sci USA*. In press (2009)

- Brack AS, Conboy MJ, Roy S, Lee M, Kuo CJ, Keller C & Rando TA. Increased Wnt signaling during aging alters muscle stem cell fate and increases fibrosis. *Science.* 317; 807-810 (2007)

- Brack AS, Conboy IM, Conboy MJ, Shen J & Rando TA. A temporal switch from Notch to Wnt signaling in muscle stem cells is necessary for normal adult myogenesis. *Cell Stem Cell.* 2; 50-59 (2008)
- Bulfield G, Siller WG, Wight PA & Moore KJ. X chromosome-linked muscular dystrophy (mdx) in the mouse. *Proc Natl Acad Sci USA*. 81; 1189-1192 (1984)
- Cairns J. Mutation selection and the natural hystory of cancer. *Nature.* 255; 197-200 (1975)
- Campanella M, Casswell E, Chong S, Farah Z, Wieckowski MR, Abramov AY, Tinker A & Duchen MR. Regulation of the mitochondrial structure and function by the F_1F_0-ATPase inhibitor protein, IF1. *Cell Metab*. 8: 13-25 (2008)
- Campanella M, Seraphim A, Abeti R, Casswell E, Echave P & Duchen MR. IF1, the endogenous regulator of the F_1F_0-ATP synthase, defines mitochondrial volume fraction in HeLa cells by regulating autophagy. *Biochim Biophys Acta.* 1787; 393-401 (2009)
- Cantini M & Carraro U. Macrophage-released factor stimulates selectively myogenic cells in primary muscle culture. *J Neuropathol Exp Neurol.* 54; 121-128 (1995)
- Carlson BM & Faulkner JA. Muscle transplantation between young and old rats: age of host determines recovery. *Am J Physiol.* 256; C1262-C1266 (1989)
- Cerletti M, Jurga S, Witczak CA, Hirshman MF, Shadrach JL, Goodyear LJ, Wagers AJ. Highly efficient, functional engraftment of skeletal muscle stem cells in dystrophic muscle. *Cell.* 134: 37-47 (2008)
- Charge SB & Rudnicki MA. Cellular and molecular regulation of muscle regeneration. *Physiol Rev.* 84; 209-238 (2004)
- Christov C, Chretien F, Abou-Khalil R, Bassez G, Vallet G, Authier FJ, Bassaglia Y, Shinin V, Tajbakhsh S, Chazaud B & Gherardi RK. Muscle satellite cells and endothelial cells: close neighbours and privileged partners. *Mol Biol Cell.* 18(4); 1397-1409 (2007)
- Clayton E, Doupe DP, Klein AM, Winton DJ, Simons BD & Jones PH. A single type of progenitor maintains normal epidermis. *Nature.* 446; 185-189 (2007)
- Cleland RL & Wang JL. Ionic polysaccharides. 3. Dilute solution properties of hyaluronic acid fractions. *Biopolymers.* 9(7); 799-810 (1970)

- Collins CA, Olsen I, Zammit PS, Heslop L, Petrie A, Partridge TA & Morgan JE. Stem cell function, self-renewal, and behavioural heterogeneity of cells from the adult muscle satellite cell niche. *Cell.* 122; 289-301 (2005)
- Conboy IM, Conboy MJ, Smythe GM & Rando TA. Notch-mediated restoration of regenerative potential to aged muscle. *Science.* 302; 1575-1577 (2003)
- Conboy IM, Conboy MJ, Wagers AJ, Girma ER, Weissman IL & Rando TA. Rejuvenation of aged progenitor cells by exposure to a young systemic environment. *Nature.* 433; 760-764 (2005)
- Conboy MJ, Karasov AO & Rando TA. High incidence of non-random template strand segregation and asymmetric fate determination in dividing stem cells and their progeny. *PLoS Biol.* 5; e102 (2007)
- Cornelison DD & Wold BJ. Single-cell analysis of regulatory gene expression in quiescent and activated mouse skeletal muscle satellite cells. *Dev Biol.* 191; 270-283 (1997)
- Cornelison DD, Filla MS, Stanley, HM, Rapraeger AC & Olwin BB. Syndecan-3 and syndecan-4 specifically mark skeletal muscle satellite cells and are implicated in satellite cell maintenance and muscle regeneration. *Dev Biol.* 239; 79-94 (2001)
- Cornelison DD, Wilcox-Adelman SA, Goetlinck PF, Rauvala H, Papraeger AC & Olwin BB. Essential and separable roles for Syndecan-3 and Syndecan-4 in skeletal muscle development and regeneration. *Genes Dev.* 18; 2231-2236 (2004)
- Cossu G, Cicinelli C, Fieri M, Coletta M & Molinaro M. Emergence of TPA-resistant 'satellite' cells during muscle histogenesis of human limb. *Exp Cell Res.* 160; 403-411 (1985)
- Daley WP, Peters SB & Larsen M. Extracellular matrix dynamics in development and regenerative medicine. *J Cell Sci.* 121; 255-264 (2008)
- Darr KC & Schultz E. Exercise-induced satellite cell activation in growing and mature skeletal muscle. *J Appl Physiol.* 63; 1816-1821 (1987)
- Day K, Shefer G, Richardson JB, Enikolopov G & Yablonka-Reuveni Z. Nestin-GFP reporter expression defines the quiescent state of skeletal muscle satellite cells. *Dev Biol.* 304; 246-259 (2007)
- De Coppi P, Delo D, Farrugia L, Udompanyanan K, Yoo JJ, Nomi M, Atala A & Soker S. Angiogenic gene-modified muscle cells for enhancement of tissue formation. *Tissue Eng.* 11(7-8); 1034-1044 (2005)

- De Coppi P, Bellini S, Conconi MT, Sabatti M, Simonato E, Gamba PG, Nussdorfer GG & Parnigotto PP. Myoblast-acellular skeletal muscle matrix constructs guarantee a long-term repair of experimental full-thickness abdominal wall defects. *Tissue Eng.* 12(7); 1929-1936 (2006a)
- De Coppi P, Milan G, Scarda A, Boldrin L, Centobene C, Piccoli M, Pozzobon M, Pilon C, Pagano C, Gamba PG & Vettor R. Rosiglitazone modifies the adipogenic potential of human muscle satellite cells. 49(8); 1962-1973 (2006b)
- De Coppi P, Bartsch G, Siddiqui MM, Xu T, Santos CC, Perin L, Mostoslavsky G, Serre AC, Snyder E, Yoo JJ, Furth ME, Soker S & Atala A. Isolation of amniotic fluid stem cell lines with potential for therapy. *Nat Biotechnol.* 25; 100-106 (2007)
- Del Pozo MA, Balasubramanian N, Alderson NB, Kiosses WB, Grande-Garcia A, Anderson RG & Schwartz MA. Phospho-caveolin-1 mediates integrin-regulated membrane domain internalization. *Nat Cell Biol.* 7; 901-908 (2005)
- Diamond JM. Transcellular cross-talk between epithelial cell membranes. *Nature* 300; 683-685 (1982)
- Duchen MR, Surin A, Jacobson J. Imaging mitochondrial function in intact cells. *Methods Enzymol*. 361: 353-389 (2003)
- Elisseeff J. Hydrogels: structure starts to gel. *Nat Mater.* 7; 271-273 (2008)
- Emery E. The muscular dystrophies. *BMJ.* 317; 991-995 (1998)
- Feldman JL & Stockdale FE. Skeletal muscle cell diversity: satellite cells form fibers of different types in cell culture. *Dev Biol.* 143; 320-334 (1991)
- Ferrari G, Cusella-De Angelis G, Coletta M, Paolucci E, Stornaiuolo A, Cossu G & Mavilio F. Muscle regeneration by bone marrow-derived myogenic progenitors. *Science* 279; 1528-1530 (1998)
- Freed LE, Vunjak-Novakovic G, Biron RJ, Eagles DB, Lesnoy DC, Barlow SK & Langer R. Biodegradable polymer scaffolds for tissue engineering. *Biotechnology (NY).* 12(7); 689-693 (1994)
- Fuchs E, Tumbar T & Guasch G. Socializing with the neighbours: stem cells and their niche. *Cell.* 116; 769-778 (2004)
- Fukada S, Uezumi A, Ikemoto M, Masuda S, Segawa M, Tanimura N, Yamamoto H, Miyagoe-Suzuki Y & Takeda S. Molecular signature of quiescent satellite cells in adult skeletal muscle. *Stem Cells.* 25; 2448-2459 (2007)

- Gallagher D, Kelley DE, Yim JE, Spence N, Albu J, Boxt L, Pi-Sunyer FX, Heshka S, MRI Ancillary Study Group of the Look AHEAD Research Group. Adipose tissue distribution is different in type 2 diabetes. *Am J Clin Nutr.* 89; 807-814 (2009)

- Gauthier MS, Miyoshi H, Souza SC, Cacicedo JM, Saha AK, Greenberg AS & Ruderman NB. AMP-activated protein kinase is activated as a consequence of lipolysis in the adipocyte: potential mechanism and physiological relevance. *J Biol Chem.* 283; 16514-16524 (2008)

- Gibson MC & Schultz E. Age related differences in absolute numbers of skeletal muscle satellite cells. *Muscle Nerve.* 6(8); 574-580 (1983)

- Gordon MD & Nusse R. Wnt signaling: multiple pathways, multiple receptors, and multiple transcription factors. *J Biol Chem.* 281; 22429-22433 (2006)

- Grounds MD & Yablonka-Reuveni Z. Molecular and cell biology of skeletal muscle regeneration. *Mol Cell Biol Hum Dis Ser.* 3; 210-256 (1993)

- Grounds MD. Age-associated changes in the response of skeletal muscle cells to exercise and regeneration. *Ann NY Acad Sci.* 854; 78-91 (1998)

- Guettier-Sigrist S, Coupin G, Braun S, Warter JM & Poindron P. Muscle could be therapeutic target in SMA treatment. *J Neurosci Res.* 53; 663-669 (1998)

- Gussoni E, Soneoka Y, Strickland CD, Buzney EA, Khan MK, Flint AF, Kunkel LM & Mulligan RC. Dystrophin expression in the mdx mouse restored by stem cell transplantation. *Nature.* 401; 390-394 (1999)

- Hall-Craggs EC. Rapid degeneration and regeneration of a whole skeletal muscle following treatment with bupivacaine (Marcain). *Exp Neurol.* 43; 349-358 (1974)

- Hammond CL, Simbi BH, Stickland NC. In ovo temperature manipulation influences embryonic motility and growth of limb tissues in the chick (Gallus gallus). *J Exp Biol*. 210; 2667-2675 (2007)

- Hartley RS, Bandman E & Yablonka-Reuveni Z. Skeletal muscle satellite cells appear during late chicken embryogenesis. *Dev Biol.* 153; 206-216 (1992)

- Hathcock JJ, Hall CL & Turitto VT. Active tissue factor shed from human smooth skeletal muscle adheres to artificial surfaces. *J Biomater Sci Polym Ed.* 11(11); 1211-1225 (2000)

- Heslop L, Morgan JE, Partridge TA. Evidence for a myogenic stem cell that is exhausted in dystrophic muscle. *J Cell Sci.* 113: 2299-2308 (2000)
- Hilton TN, Tuttle LJ, Bohnert KL, Mueller MJ, Sinacore DR. Excessive adipose tissue infiltration in skeletal muscle in individuals with obesity, diabetes mellitus, and peripheral neuropathy: association with performance and function. Phys Ther 88: 1336-1344 (2008)
- Hoh JF & Hughes S. Expression of superfast myosin in aneural regenerates of cat jaw muscle. *Muscle Nerve.* 14; 316-325 (1991)
- Horch RE, Debus M, Wagner G & Stark GB. Cultured human keratinocytes on type I collagen membranes to reconstitute the epidermis. *Tissue Eng.* 6; 53-67 (2000)
- Huang LK, Metha RC & DeLuca PP. Evaluation of a statistical model for the formation of poly [acryloil hydroxyethyl starch] microspheres. *Pharm Res.* 14(4); 475-482 (1997)
- Hwang NS, Varghese S, Zhang Z & Elisseeff J. Chondrogenic differentiation of human embryonic stem cell-derived cells in arginine-glycine-aspartate-modified hydrogel. *Tissue Eng.* 12; 2659-2706 (2006)
- Irintchev A, Zeschnigk M, Starzinski-Powitz A & Wernig A. Expression pattern of M-cadherin in normal, denervated, and regenerating mouse muscles. *Dev Dyn.* 199; 326-337 (1994)
- Jahagirdar BN, Verfaillie CM. Multipotent adult progenitor cell and stem cell plasticity. *Stem Cell Rev.* 1; 53-59 (2005)
- Jenniskens GJ, Veerkamp JH & van Kuppevelt TH. Heparan sulfates in skeletal muscle development and physiology. *J Cell Physiol.* 206, 283-294 (2006)
- Jesse TL, LaChance R, Iademarco MF & Dean DC. Interferon regulatory factor-2 is a transcriptional activator in muscle where it regulates expression of vascular cell adhesion molecule-1. *J Cell Biol.* 140; 1265-1276 (1998)
- Jouaville LS, Pinton P, Bastianutto C, Rutter GA, Rizzuto R. Regulation of mitochondrial ATP synthesis by calcium: evidence for a long-term metabolic priming. *Proc Natl Acad Sci USA*. 96; 13807-13812 (1999)
- Jones NC, Tyner KJ, Nibarger L, Stanley HM, Cornelison DD, Fedorov YV & Olwin BB. The p38alpha/beta MAPK functions as a molecular switch to activate the quiescent satellite cell. *J Cell Biol.* 169; 105-116 (2005)

- Kaufmann U, Martin B, Link D, Witt K, Zeitler S, Reinhard S &Starzinski-Powitz A. M-cadherin and its sisters in development of striated muscle. *Cell Tissue Res.* 296; 191-198 (1999)
- Keller GM. In vitro differentiation of embryonic stem cells. *Curr Opin Cell Biol*. 7; 862-869 (1995)
- Keren A, Bengal E & Frank D. p38 MAP kinase regulates the expression of XMyf5 and affects distinct myogenic programs during Xenopus development. *Dev Biol.* 288; 73-86 (2005)
- Khodabukus A, Paxton JZ, Donnelly K & Baar K. Engineered muscle: a tool for studying muscle physiology and function. *Exerc Sport Sci Rev.* 35; 186-191 (2007)
- Kinkel AD, Fernyhough Me, Helterline DL, Vierck JL, Oberg KS, Vance TJ, Hausman GJ, Hill RA & Dodson MV. Oil-red-O stains non-adipogenic cells: a precautionary note. *Cytotechnology* 46; 49-56 (2004)
- Kopp J, Jeschke MG, Bach AD, Kneser U & Horch RE. Applied tissue engineering in the closure of severe burns and chronic wounds using cultured human autologous keratinocytes in a natural fibrin matrix. *Cell Tissue Bank.* 5; 81-96 (2004)
- Kuang S, Kuroda K, Le Grand F & Rudnicki MA. Asymmetric self-renewal and commitment of satellite stem cells in muscle. *Cell.* 129; 999-1010 (2007)
- Kurek JB, Nouri S, Kannourakis G, Murphy M & Austin L. Leukemia inhibitory factor and interleukin-6 are produced by diseased and regenerating skeletal muscle. *Muscle Nerve.* 19; 1291-1301 (1996)
- Lansdorp PM. Immortal strands? Give me a break. *Cell.* 129; 1244-1247 (2007)
- Langsdorf A, Do AT, Kusche-Gullberg M, Emerson CP & Ai X. Sulfs are regulators of growth factor signaling for satellite cell differentiation and muscle regeneration. *Dev Biol.* 311; 464-477 (2007)
- Law PK, Goodwin TG, Fang Q, Deering MB, Duggirala V, Larkin C, Florendo JA, Kirby DS, Li HJ & Chen M. Cell transplantation as an experimental treatment for Duchenne muscular dystrophy. *Cell Transpl.* 2; 485-505 (1993)
- Lee HJ, Lee JS, Chansakul T, Yu C, Elisseeff JH & Yu SM. Collagen mimetic peptide-conjugated photopolymerizable PEG hydrogel. *Biomaterials.* 27; 5268-5276 (2006)

- Lee HJ, Yu C, Chansakul T, Hwang NS, Varghese S, Yu SM & Elisseeff JH. Enhanced chondrogenesis of mesenchymal stem cells in collagen mimetic peptide-mediated microenvironment. *Tissue Eng Part A*. 14; 1843-1851 (2008)
- Leyssens A, Nowicky AV, Patterson L, Crompton M, Duchen MR. The relationship between mitochondrial state, ATP hydrolysis, $[Mg^{2+}]i$ and $[Ca^{2+}]i$ studied in isolated cardiomyocytes. *J Physiol*. 496; 111-128 (1996)
- Lescaudron L, Peltekian E, Fontaine-Perus J, Paulin D, Zampieri M, Garcia L & Parrish E. Blood borne macrophages are essential for the triggering of muscle regeneration following muscle transplant. *Neuromuscul Disord.* 9; 72-80 (1999)
- Liu ZJ, Zhuge Y & Velasquez OC. Trafficking and differentiation of mesenchymal stem cells. *J Cell Biochem.* 106; 984-991 (2009)
- Lutolf MP & Hubbell JA. Synthetic byopolymers as instructive extracellular microenvironments for morphogenesis in tissue engineering. *Nat Biotechnol.* 23; 47-55 (2005)
- Malm C. Exercise-induced muscle damage and inflammation: fact or fiction?. *Acta Physiol Scand.* 171(3); 233-239 (2001)
- Maltby V, Somaiya A, French NA, Stickland NC. In ovo temperature manipulation influences post-hatch muscle growth in the turkey. *Br Poult Sci.* 45; 491-498 (2004)
- Matsuda R, Spector DH & Strohman RC. Regenerating adult chicken skeletal muscle and satellite cell cultures express embryonic patterns of myosin and tropomyosin isoforms. *Dev Biol.* 100; 478-488 (1983)
- Mauro A. Satellite cells of skeletal muscle fibers. *J Biophys Biochem Cytol.* 9; 493-495 (1961)
- McCroskery S, Thomas M, Maxwell L, Sharma M & Kambadur R. Myostatin negatively regulates satellite cell activation and self-renewal. *J Cell Biol.* 162; 1135-1147 (2003)
- McKenzie JL, Gan OI, Doedens M, Wang JC, Dick JE. Individual stem cells with highly variable proliferation and self-renewal properties comprise the human hematopoietic stem cell compartment. *Nat Immunol.* 7; 1225-1233 (2006)
- Megeney LA & Rudnicki MA. Determination versus differentiation and the MyoD family of transcription factors. *Biochem Cell Biol.* 73; 723-732 (1995)

- Milan G, Dalla Nora E, Pilon C, Pagano C, Granzotto M, Manco M, Mingrone G & Vettor R. Changes in muscle myostatin expression in obese subjects after weight loss. *J Clin Endocrin Metab.* 89; 2724-2727 (2004)
- Molnar G, Ho ML & Schroedl NA. Evidence for multiple satellite cell populations and non-myogenic cell type that is regulated differently in regenerating and growing skeletal muscle. *Tissue Cell.* 28; 547-556 (1996)
- Mooney DJ & Mikos AG. Growing new organs. *Sci Am.* 280; 60 (1999)
- Morlet K, Grounds MD & McGeachie JK. Muscle precursor replication after repeated regeneration of skeletal muscle in mice. *Anat Embryol (Berl).* 180; 471-478 (1989)
- Mothe AJ, Kulbatski I, van Bendegem RL, Lee L, Kobayashi E, Keating A & Tator CH. Analysis of green fluorescent protein expression in transgenic rats for tracking transplanted neural stem/progenitor cells. *J Histochem Cytochem*. 53: 1215-1226 (2005)
- Mueller MB & Tuan RS. Functional characterization of hypertrophy in chondrogenesis of human mesenchymal stem cells. *Arthritis Rheum.* 58; 1377-1388 (2008)
- Nagata Y, Partridge TA, Matsuda R & Zammit PS. Entry of muscle satellite cells into the cell cycle requires sphingolipid signaling. *J Cell Biol.* 174; 245-253 (2006)
- Nehrer S, Breinan HA, Ramappa A, Young G, Shortkroff S, Louie LK, Sledge CB, Yannas IV & Spector M. Matrix collagen type and pore size influence behaviour of seeded canine chondrocytes. *Biomaterials.* 18; 769-776 (1997)
- Nesti C, Pasquali L, Vaglini F, Siciliano G, Murri L. The role of mitochondria in stem cell biology. *Biosci Rep*. 27: 165-171 (2007)
- Nuttelman CR, Tripodi MC & Anseth KS. In vitro osteogenic differentiation of human mesenchymal stem cells photoencapsulated in PEG hydrogels. *J Biomed Mater Res A.* 68; 773-782 (2004)
- Ogino H, Satou W, Fujii M, Suzuki T, He Y, Michishita E & Ayusawa D. The human MYOD1 transgene is suppressed by 5-bromodeoxyuridine in mouse myoblasts. *J Biochem.* 132; 953-959 (2002)
- Olwin BB & Rapraeger A. Repression of myogenic differentiation by aFGF, bFGF, and K-FGF is dependent on cellular heparan sulfate. *J Cell Biol.* 118; 631-639 (1992)

- Orimo S, Hiyamuta E, Arahata K & Sugita H. Analysis of inflammatory cells and complement C3 in bupicavaine-induced myonecrosis. *Muscle Nerve.* 14; 515-520 (1991)
- Palacios D & Puri PL. The epigenetic network regulating muscle development and regeneration. *J Cell Physiol.* 207; 1-11 (2006)
- Pelicano H, Carney D, Huang P. ROS stress in cancer cells and therapeutic applications. *Drug Resist Updat*. 7; 97-110 (2008)
- Pittenger MF, Mackay AM, Beck SC, Jaiswal RK, Douglas R, Mosca JD, Moorman MA, Simonetti DW, Craig S & Marshak DR. Multilineage potential of adult human mesenchymal stem cells. *Science.* 284; 143-147 (1999)
- Polesskaya A, Seale P & Rudnicki MA. Wnt signaling induces the myogenic specification of resident CD45+ adult stem cells during muscle regeneration. *Cell.* 113; 841-852 (2003)
- Powell C, Shansky J, Del Tatto M, Forman DE, Hennessey J, Sullivan K, Zielinski BA & Vandenburgh HH. Tissue-engineered human bioartificial muscles expressing a foreign recombinant protein for gene therapy. *Hum Gene Ther.* 10; 565-577 (1999)
- Radice M, Brun P, Cortivo R, Scapinelli R, Battaliard C & Abatangelo G. Hyaluronan-based biopolymers as delivery vehicles for bone-marrow-derived mesenchymal progenitors. *J Biomed Mater Res.* 50; 101-109 (2000)
- Ramirez-Zacarias JL, Castros Munozledo F, Kuri-Harcuch W. Quantitation of adipose conversion and triglycerides by staining intracytoplasmic lipids. *Hystochemistry.* 97; 493-497 (1992)
- Rantanen J, Hurme T, Lukka R, Heino J & Kalimo H. Satellite cell proliferation and the expression of myogenin and desmin in regenerating skeletal muscle: evidence for two different populations of satellite cells. *Lab Invest.* 72; 341-347 (1995)
- Relaix F, Montarras D, Zaffran S, Gayraud-Morel B, Rocancourt D, Tajbakhsh S, Mansouri A, Cumano A & Buckingham M. Pax3 and Pax7 have distinct and overlapping functions in adult muscle progenitor cells. *J Cell Biol.* 172; 91-102 (2006)
- Revell PA, Damien E, Di Silvio L, Gurav N, Longinotti C & Ambrosio L. Tissue engineered intervertebral disc repair in the pig using injectable polymers. *J Mater Sci Mater Med.* 18(2); 303-308 (2007)

- Rosen GD, Sanes JR, LaChance R, Cunningham JM, Roman J & Dean DC. Roles for the integrin VLA-4 and its counter receptor VCAM-1 in myogenesis. *Cell.* 69; 1107-1119 (1992)
- Rosenblatt JD, Yong D & Parry DJ. Satellite cell activity is required for hypertrophy of overloaded adult rat muscle. *Muscle Nerve.* 17; 608-613 (1994)
- Rosenblatt JD, Lunt AI, Parry DJ & Partridge TA. Culturing satellite cells from living single muscle fiber explants. *In Vitro Cell Dev Biol Anim.* 31(10); 773-779 (1995)
- Rosenblatt JD, Parry DJ & Partridge TA. Phenotype of adult mouse muscle myoblasts reflects their fiber type of origin. *Differentiation* 60; 39-45 (1996)
- Rossi CA, Pozzobon M, Ditadi A, Archacka K, Gastaldello A, Sanna M, Franzin C, Malerba A, Milan G, Cananzi M, Schiaffino S, Campanella M, Vettor R & De Coppi P. Clonal characterization of rat muscle satellite cells: proliferation, metabolism and differentiation define an intrinsic heterogeneity. *PLoS ONE.* 5(1); e8523 (2010)
- Rouger K, Brault M, Daval N, Leroux I, Guigand L, Lesoeur J, Fernandez B & Cherel Y. Muscle satellite cell heterogeneity: in vitro and in vivo evidences for populations that fuse differently. *Cell Tissue Res*. 317; 319-326 (2004)
- Salinas CN & Anseth KS. The influence of the RGD peptide motif and its contextual presentation in PEG gels on human mesenchymal stem cell viability. *J Tissue Eng Regen Med.* 12; 296-304 (2008)
- Rumsey JW, Das M, Kang JF, Wagner R, Molnar P & Hickman JJ. Tissue engineering intrafusal fibers: dose- and time-dependent differentiation of nuclear bag fibers in a defined in vitro system using neuregulin 1-beta-1. *Biomaterials.* 29(8); 994-1004 (2008)
- Sacco A, Doyonnas R, Kraft P, Vitorovic S & Blau HM. Self-renewal and expansion of single transplanted muscle stem cells. *Nature.* 456; 502-506 (2008)
- Salic A & Mitchison TJ. A chemical method for fast and sensitive detection of DNA synthesis in vivo. *Proc Natl Acad Sci USA.* 105(7); 2415-2420 (2008)
- Schiaffino S, Gorza L, Sartore S, Saggin L & Carli M. Embryonic myosin heavy chain as a differentiation marker of developing human skeletal muscle and rhabdomyosarcoma. A monoclonal antibody study. *Exp Cell Res.* 163(1); 211-220 (1986)

- Schultz E. Fine structure of satellite cells in growing skeletal muscle. *Am J Anat.* 147(1); 49-70 (1976)
- Schultz E & Lipton BH. Skeletal muscle satellite cells: changes in proliferation potential as function of age. *Mech Ageing Dev.* 20; 377-383 (1982)
- Schultz E & Jariszak DL. Effects of skeletal muscle regeneration on the proliferation potential of satellite cells. *Mech Ageing Dev.* 30; 63-72 (1985)
- Schultz E. Satellite cell behaviour during skeletal muscle growth and regeneration. *Med Sci Sports Exerc.* 21(5); S181-S186 (1989)
- Schultz E. Satellite cell proliferative compartments in growing skeletal muscles. *Dev Biol.* 175; 84-94 (1996)
- Schuster-Gossler K, Cordes R & Gossler A. Premature myogenic differentiation and depletion of progenitor cells cause severe muscle hypotrophy in Delta1 mutants. *Proc Natl Acad Sci USA.* 104; 537-542 (2007)
- Seale P & Rudnicki MA. A new look at the origin, function, and "stem-cell" status of muscle satellite cells. *Dev Biol.* 218(2); 115-124 (2001)
- Seale P, Bjork B, Yang W, Kajimura S, Chin S, Kuang S, Scimè A, Devarakonda S, Conroe HM, Erdjument-Bromage H, Tempst P, Rudnicki MA, Beier DR & Spiegelman BM. PRDM16 controls a brown fat/skeletal muscle switch. *Nature* 454; 961-967 (2008)
- Sekiya I, Vuoristo JT, Larson BL & Prockop DJ. In vitro cartilage formation by human adult stem cells from bone marrow stroma defines the sequence of cellular and molecular events during chondrogenesis. *Proc Natl Acad Sci USA.* 99; 4397-4402 (2002)
- Shefer G, Wleklinski-Lee M, Yablonka–Reuveni Z. Skeletal muscle satellite cells can spontaneously enter an alternative mesenchymal pathway. *J Cell Sci.* 117: 5393-5404 (2004)
- Shefer G, Van de Mark DP, Richardson JB & Yablonka-Reuveni Z. Satellite-cell pool size does matter: defining the myogenic potency of aging skeletal muscle. *Dev Biol.* 294; 50-66 (2006)
- Sherwood RI, Christensen JL, Conboy IM, Conboy MJ, Rando TA, Weissman IL & Wagers AJ. Isolation of adult mouse myogenic progenitors: functional heterogeneity of cells within and engrafting skeletal muscle. *Cell.* 119; 543-554 (2004)

- Shinin V, Gayraud-Morel B, Gomes D & Tajbakhsh S. Asymmetric division and cosegregation of template DNA strands in adult muscle satellite cells. *Nat Cell Biol.* 8; 677-687 (2006)
- Singh NK, Chae HS, Hwang IH, Yoo IM, Ahn CN, Lee SH, Lee HJ, Park HJ & Chung HY. Transdifferentiation of porcine satellite cells to adipoblasts with ciglitizone. *J Anim Sci.* 85; 1126-1135 (2007)
- Smith CK, Janney MJ & Allen RE. Temporal expression of myogenic regulatory genes during activation, proliferation, and differentiation of rat skeletal muscle satellite cells. *J Cell Physiol.* 159; 379-385 (1994)
- Tanaka KK, Hall JK, Troy AA, Cornelison DD, Majka SM & Olwin BB. Syndecan-4-expressing muscle progenitor cells in the SP engraft as satellite cells during muscle regeneration. *Cell Stem Cell* 4: 217-225 (2009)
- Tatsumi R, Liu X, Pulido A, Morales M, Sakata T, Dial S, Hattori A, Ikeuchi Y & Allen RE. Satellite cell activation in stretched skeletal muscle and the role of nitric oxide and hepatocyte growth factor. *Am J Physiol Cell Physiol.* 290; C1487-C1494 (2006)
- Thomson JA, Itskovitz-Eldor J, Shapiro SS, Waknitz MA, Swiergel JJ, Marshal VS & Jones JM. Embryonic stem cell lines derived from human blastocysts. *Science.* 282; 1145-1147 (1998)
- Tidball JG. Inflammatory cell response to acute muscle injury. *Med Sci Sports Exerc.* 27; 1022-1032 (1995)
- Vandenburgh HH. Functional assessment and tissue design of skeletal muscle. *Ann NY Acad Sci.* 961; 201-202 (2002)
- Vangsness CT, Kurzweil PR & Lieberman JR. Restoring articular cartilage in the knee. *Am J Orthop.* 33; 29-34 (2004)
- Vasjutina E, Lenhard DC, Wende H, Erdmann B, Epstein JA & Birchmeier C. RBP-J (Rbpsuh) is essential to maintain muscle progenitor cells and to generate satellite cells. *Proc Natl Acad Sci USA.* 104; 4443-4448 (2007)
- Volonte D, Liu Y & Galbiati F. The modulation of caveolin-1 expression controls satellite cell activation during muscle repair. *FASEB J.* 19; 237-239 (2005)
- Waghmare SK, Bansal R, Lee J, Zhang YV, McDermott DJ & Tumbar T. Quantitative proliferation dynamics and random chromosome segregation of hair follicle stem cells. *EMBO J.* 27; 1309-1320 (2008)

- Webster C & Blau HM. Accelerated age-related decline in replicative life-span of Duchenne muscular dystrophy myoblasts: implications for cell and gene therapy. *Somatic Cell Mol Genet.* 164; 557-565 (1990)
- Wong DJ, Liu H, Ridky TW, Cassarino D, Segal E & Chang HY. Module map of stem cell genes guides creation of epithelial cancer stem cells. *Cell Stem Cell.* 2; 333-344 (2008)
- Wozniak AC & Anderson JE. Nitric oxide-dependence of satellite stem cell activation and quiescence on normal skeletal muscle fibers. *Dev Dyn.* 236; 240-250 (2007)
- Yablonka-Reuveni Z & Rivera AJ. Temporal expression of regulatory and structural muscle proteins during myogenesis of satellite cells on isolated adult rat fibers. *Dev Biol.* 164; 588-603 (1994)
- Yan W, George S, Fotadar U, Tyhovych N, Kamer A, Yost MJ, Price RL, Haggart CR, Holmes JW, Terracio L. Tissue engineering of skeletal muscle. *Tissue Eng.* 13(11); 2781-2790 (2007)
- Zammit PS, Heslop L, Hudon V, Rosenblatt JD, Tajbakhsh S, Buckingham ME, Beauchamp JR, Partridge TA. Kinetics of myoblast proliferation show that resident satellite cells are competent to fully regenerate skeletal muscle fibers. *Exp Cell Res.* 281; 39-49 (2002)
- Zammit PS, Golding JP, Nagata Y, Hudon V, Partridge TA & Beauchamp JR. Muscle satellite cells adopt divergent fates: a mechanism for self-renewal? *J Cell Biol.* 166; 347-357 (2004)
- Zeschnigk M, Kozian D, Kuch C, Schmoll M & Stanzinski-Powitz A. Involvement of M-cadherin in terminal differentiation of skeletal muscle cells. *J Cell Sci.* 108; 2973-2981 (1995)
- Zhivotovsky B & Orrenius S. The Warburg effect returns to a cancer stage. *Semin Cancer Biol.* 19; 1-3 (2009)